$CD8^+$ T cells in the bone marrow and their impact on the differentiation of dendritic cells during polymicrobial sepsis

Inaugural Dissertation
for
the doctoral degree of
Dr. rer. nat.

from the Faculty of Biology
University of Duisburg-Essen
Germany

Submitted by
Anne-Charlotte Antoni
Born in Hildesheim

June 2021

The experiments underlying the present work were conducted in the laboratory of Prof. Dr. rer. nat. Stefanie Flohé, Department of Orthopedics and Trauma Surgery, Essen University Hospital, University of Duisburg-Essen.

1. Examiner: Prof. Dr. Stefanie Flohé
2. Examiner: PD Dr. Kathrin Sutter
Chair of the Board of Examiners: Prof. Dr. Astrid Westendorf

Date of the oral examination: 06.10.2021

DOI: 10.17185/duepublico/74888
URN: urn:nbn:de:hbz:465-20221011-112852-7

So eine Arbeit wird eigentlich nie fertig, man muss sie für fertig erklären,
wenn man nach Zeit und Umständen das Mögliche getan hat.

- Johann Wolfgang von Goethe -

I. Graphical Abstract

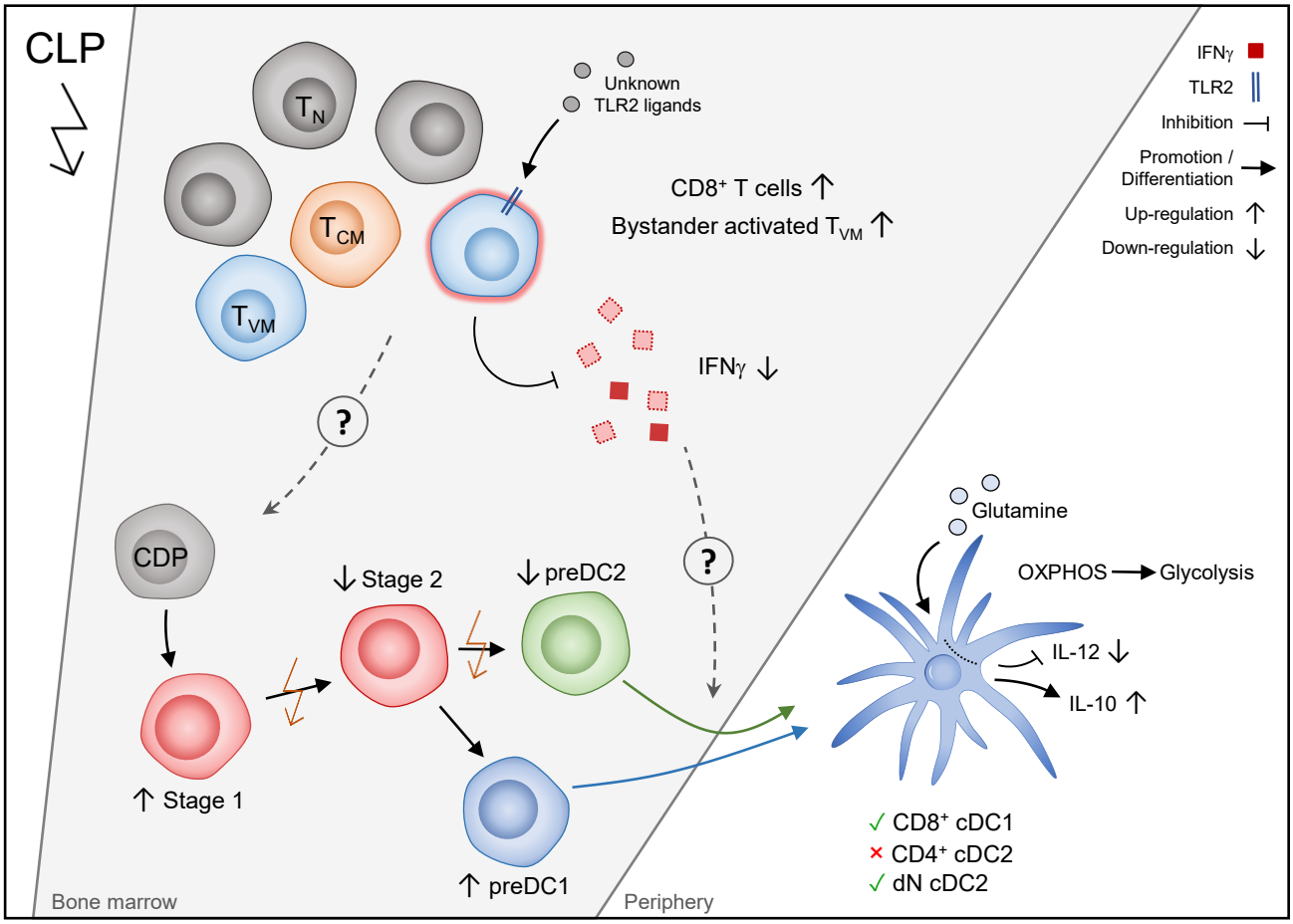

II. Abstract

Polymicrobial sepsis, a systemic bacterial infection, not only causes initial hyperinflammation but also induces a state of immunosuppression in the later course of disease. Thereby, susceptibility to secondary infections is increased, which has been attributed to a reprogramming of myeloid cells like DCs. These differentiate inside of the bone marrow dependent on the cytokine microenvironment, which is precisely regulated by the composition and activity of bone marrow cells. The mouse model of cecal ligation and puncture (CLP) was used to investigate post-septic immunosuppression.

In contrast to sepsis-induced T cell apoptosis in the spleen, T cells accumulated within 12 to 24 hours after the onset of sepsis in the bone marrow. The number of $CD8^+$ T_N, T_{CM} and T_{VM} but not $T_{E/EM}$ significantly increased in the bone marrow. Thereby, T_{VM} were particularly activated, which was proven to be antigen-independent bystander activation. Furthermore, $CD8^+$ T cells had an impaired ability to produce Interferon (IFN)γ in wild-type but not in TLR2 knockout (ko) mice. Transfer of TLR2ko $CD8^+$ T cells narrowed down the TLR2-dependence to a T cell intrinsic effect. Here, in the naïve *in vitro* model, prestimulation of the TLR2 signaling pathway led to the formation of T cells with reduced capacity to produce IFNγ. Thus, TLR2 induction can alter the cytokine secretion pattern of $CD8^+$ T cells. However, the TLR2 ligands during sepsis still have to be identified in future studies. Transfer of TLR2ko $CD8^+$ T cells further demonstrated that these cells were able to influence the overall RNA expression of bone marrow cells towards enhanced IFNγ signaling. By altering cytokine production, these cells could interfere with the bone marrow cytokine milieu and thereby influence cell development.

In addition to the loss of DCs in the spleen, there is sepsis-induced loss of dendritic progenitor cells (preDCs) in the bone marrow. The still existing preDCs shift their composition towards $Ly6c^-$ preDCs. This might be caused by a dysregulation of preDC formation from stage 1 to stage 2. At the same time, a preferential commitment of preDCs toward the cDC1-committed preDC1 subtype seems to take place. Underlying mechanisms need to be elucidated in further studies. In this context, $CD8^+$ T cells did not affect the composition but the preDC count, as depletion of $CD8^+$ T cells led to a further reduced number of preDCs.

A correlation between IFNγ production by $CD8^+$ T cells and the function of splenic DCs as well as *de novo* generated BMDCs was demonstrated. Here, the transfer of TLR2ko $CD8^+$ T cells led to a clear shift to a decreased IL-12p70/IL10 ratio after LPS stimulation compared to CLP. An experiment with bone marrow-derived DC (BMDC) cultures from wild-type or IFNγko mice had similar results, in which the presence of IFNγ during DC differentiation led to a reduced IL-12p70/IL10 ratio.

A possible explanation for different cytokine production of BMDC after CLP might be sepsis-induced altered metabolism of the cells. In this regard, glycolysis and the glutamine synthesis increased in DCs after sepsis. The specific and opposite regulation of IL-10 as well as IL-12p70 production after manipulation of the glutamine metabolism provides the opportunity to precisely regulate cytokine production by DCs. The extent to which $CD8^+$ T cells interfere with metabolic processes needs to be investigated in further studies.

All in all, sepsis-induced dysfunctional DC differentiation is already evident by restructuring of the preDC compartment in the bone marrow, as well as DCs exhibit an altered metabolic profile. Thereby, the parallel increase of bystander activated $CD8^+$ T cells is striking. In addition to other possible factors, these cells could mediate the cytokine milieu via TLR2-dependent altered IFNγ production and thus alter DC differentiation. In this context, an interfering in the metabolism might be a possible factor since glutamine metabolism can specifically regulate cytokine production by DCs.

III. Zusammenfassung

Bei einer polymikrobiellen Sepsis, einer systemischen bakteriellen Infektion, kommt es nicht nur zu einer initialen Entzündungsreaktion, sondern im späteren Krankheitsverlauf zu einem Zustand der Immunsuppression. Dadurch wird die Anfälligkeit für Sekundärinfektionen erhöht, was auf eine Umprogrammierung von myeloischen Zellen wie dendritischen Zellen (DCs) zurückgeführt werden kann. Diese differenzieren sich innerhalb des Knochenmarks in Abhängigkeit von der Zytokin-Mikroumgebung, welche durch die Zusammensetzung und Aktivität der Knochenmarkzellen bedingt ist, aus. Um die postseptische Immunsuppression zu untersuchen, wurde das Mausmodell der zökalen Ligation und Punktion (*cecal ligation and puncture* / CLP) verwendet.

Im Gegensatz zur Sepsis-induzierten T-Zell-Apoptose in der Milz, reicherten sich T-Zellen innerhalb von 12 bis 24 Stunden nach Beginn der Sepsis im Knochenmark an. Innerhalb der $CD8^+$ T-Zellen im Knochenmark war die Anzahl der naiven T-Zellen, zentralen T-Gedächtniszellen und virtuellen T-Gedächtniszellen (T_{VM}), aber nicht der Effektor und Effektor T-Gedächtniszellen, signifikant erhöht. Dabei waren insbesondere T_{VM} aktiviert, welches als antigen-unabhängige Bystander-Aktivierung identifiziert werden konnte.

Darüber hinaus hatten $CD8^+$ T-Zellen in Wildtyp Mäusen eine verminderte Fähigkeit Interferon (IFN) γ zu produzieren, welches in Toll-like Rezeptor 2 knockout (TLR2ko) Mäusen nicht auftrat. Der Transfer von TLR2ko $CD8^+$ T-Zellen konnte die TLR2-Abhängigkeit auf einen T-Zell-intrinsischen Effekt eingrenzen. Hier führte auch im naiven *in vitro* Modell eine Vorstimulation des TLR2-Signalweges zu einer Bildung von T-Zellen mit reduzierter IFN-Produktion. Somit kann die TLR2-Induktion das Zytokin-Sekretionsmuster von $CD8^+$ T-Zellen verändern. Die TLR2-Liganden während der Sepsis müssen jedoch in zukünftigen Studien identifiziert werden. Der Transfer von TLR2ko $CD8^+$ T-Zellen zeigte weiterhin, dass diese Zellen in der Lage sind die Gesamt-RNA-Expression der Knochenmarkzellen in Richtung einer verstärkten IFNγ-Signalisierung zu beeinflussen. Durch die Veränderung der Zytokinproduktion könnten diese Zellen in das Zytokin Milieu des Knochenmarks eingreifen und die Zellentwicklung beeinflussen.

Zusätzlich zum Verlust von DCs in der Milz kommt es zu einem Sepsis-induzierten Verlust von dendritischen Vorläuferzellen (preDCs) im Knochenmark. Die noch vorhandenen preDCs verschieben dabei ihre Zusammensetzung in Richtung $Ly6c^-$ preDCs. Dies

könnte durch eine Dysregulation der preDC-Bildung von Stadium 1 zu Stadium 2 verursacht werden. Gleichzeitig scheint eine präferentielle Bildung der preDCs in Richtung des preDC1-Subtyps stattzufinden, welche sich in der weiteren Entwicklung in konventionelle DCs typ 1 (cDC1) ausbilden. Die zugrunde liegenden Mechanismen müssen in weiteren Studien aufgeklärt werden. In diesem Zusammenhang beeinflussten $CD8^+$ T-Zellen nicht die Zusammensetzung, sondern die Anzahl der preDCs, da eine Depletion von $CD8^+$ T-Zellen zu einer noch mehr reduzierten Anzahl von preDCs führte.
Eine Korrelation zwischen der IFNγ-Produktion durch $CD8^+$ T-Zellen und der Funktion der Milz-DCs sowie der *de novo* generierten BMDCs konnte nachgewiesen werden. Hier führte der Transfer von TLR2ko $CD8^+$ T-Zellen im Vergleich zu CLP zu einem deutlich verringerten Interleukin (IL)-12p70/IL-10-Verhältnis nach LPS-Stimulation. Ein Experiment mit *de novo* differenzierten dendritischen Knochenmarkszellen (*Bone marrow-derived DCs*, BMDCs) von Wildtyp- oder IFNγko-Mäusen zeigte ähnliche Ergebnisse, bei denen die Anwesenheit von IFNγ während der DC-Differenzierung zu einem reduzierten IL-12p70/IL-10-Verhältnis führte.
Eine mögliche Erklärung für die unterschiedliche Zytokinproduktion von BMDC nach CLP könnte der durch die Sepsis veränderte Metabolismus der Zellen sein. Diesbezüglich waren die Glykolyse und die Glutamin Synthese in DCs nach Sepsis erhöht. Die spezifische und gegenläufige Regulation der IL-10- sowie IL-12p70-Produktion nach Eingriff in den Glutamin-Stoffwechsel eröffnet die Möglichkeit, die Zytokinproduktion der DCs spezifisch zu regulieren. Inwieweit $CD8^+$ T-Zellen Zellen in die Stoffwechselprozesse eingreifen, muss in weiteren Studien untersucht werden.
Insgesamt zeigt sich die Sepsis-induzierte dysfunktionale DC-Differenzierung bereits durch eine Restrukturierung des preDC-Kompartiments im Knochenmark sowie in einem veränderten metabolischen Profil der DCs. Auffällig ist dabei der zeitgleiche Anstieg von „Bystander“ aktivierten $CD8^+$ T-Zellen. Neben anderen möglichen Faktoren könnten diese Zellen über eine TLR2-abhängige veränderte IFNγ-Produktion das Zytokin-Milieu verändern und damit die DC-Differenzierung vermitteln. In diesem Zusammenhang könnte eine Störung des Stoffwechsels ein möglicher Faktor sein, da der Glutamin-Stoffwechsel die Zytokinproduktion von DCs spezifisch regulieren kann.

IV. Publications

In the context of this work, the following articles were published or are in preparation:

1. Smirnov, A. et al. (2017). Sphingosine 1-phosphate- and C-C chemokine receptor 2-dependent activation of $CD4^+$ plasmacytoid dendritic cells in the Bone marrow contributes to signs of sepsis-induced immunosuppression. *Frontiers in Immunology*, 8(Nov):1–15. [210]
2. Antoni, AC. et al. (in preparation). $CD8^+$ T cells in the bone marrow and their impact on the differentiation of dendritic cells during polymicrobial sepsis (working title).

Furthermore, the following abstracts were accepted to various conferences:

1. Antoni, AC., Dudda, M., Flohé, S.B. (2018). Characterization of antigen-independent activation of memory T cells in the bone marrow during polymicrobial sepsis. *17th Day of Research, Essen University Hospital, Germany* (7. December 2018)

2. Antoni, AC., Wienhöfer, L., Bak, M., Frisch, M., Dudda, M., Flohé, S.B. (2019). Characterization of effector and memory T cells and their antigen-independent activation in the bone marrow during polymicrobial sepsis. *23rd Symposium "Infection and Immunity", Rothenfels, Germany* (27. - 29. March 2019)

3. Antoni, AC., Dudda, M., Flohé, S.B. (2019). Identification of bystander activated $CD8^+$ T cells in the bone marrow during polymicrobial sepsis. *II. Joint Meeting of DGfI and SIICA, Munich, Germany* (10.-13. September 2019)

4. Antoni, AC., Dudda, M., Flohé, S.B. (2019). Characterization of $CD8^+$ T cells and their antigen-independent activation in the bone marrow during polymicrobial sepsis. *Deutscher Kongress für Orthopädie und Unfallchirurgie (DKOU), Berlin, Germany.* (22. - 25. October 2019)

5. Antoni, AC., Dudda, M., Flohé, S.B. (2019) Characterization of bystander activated CD8+ T cells in the bone marrow during polymicrobial sepsis. *18th Day of Research, Essen University Hospital, Germany* (22. November 2019)

V. Table of contents

1. Introduction

1.1 The immune system – innate and adaptive immunity

The immune system is the biological defense system of organisms against various pathogens and infectious agents. All organisms are constantly exposed to the potentially harmful influences of the living environment including bacteria, viruses, fungi, and parasites. Even damaged endogenous cells, which are not adequately degraded, can be a major problem. To ensure defense against these potential threats, all organisms have protective functions that consist of molecules like enzymes and proteins up to various effector cells able to identify and combat infections. Simple organisms like plants, fungi, insects, and primitive multicellular organisms possess such defense mechanisms in the form of an innate immune system, which originated very early in the evolutionary history of living organisms and is largely conserved [7,85]. The main task of this protective system is to recognize conserved patterns on different pathogens via generic receptors resulting in an inflammatory response [3,96]. The development of vertebrates was accompanied by the emergence of the more specific adaptive immune system, also known as the acquired immune system [20,45]. This enabled the possibilities to selectively recognize and eliminate pathogens as well as generate an antigen-specific immunological memory, which is associated with a more rapid and specific secondary immune response. The highly sophisticated human immune system is divided into these two functional parts: innate and adaptive immunity [157]. Both subsystems use humoral and cell-mediated immunity to perform their functions.

The first line against non-self-pathogens is the innate immune response. It consists of physical, chemical, and cellular defense mechanisms able to prevent the spread and movement of foreign pathogens. Epithelial surfaces of the body act as a physical barrier. These include not only the skin but also the surface of the gastrointestinal, respiratory, and urogenital tracts that are constitutively colonized by endogenous beneficial microbiota [147]. Commensal microorganisms are important for the supply of essential nutrients and protect against invading pathogens by competing for nutrients and epithelial binding sites [86,157]. If a pathogen colonizes or crosses these barriers, an infection occurs. Subsequently, a broad range of pathogens is detected and destroyed within minutes or

hours by efficient mechanisms of the innate immune system. Cellular components are different leukocytes (white blood cells) that include phagocytes such as macrophages, granulocytes, dendritic cells[1], and natural killer (NK) cells (Figure 1). Besides, humoral immunity in the form of complement proteins plays an important role [96]. The innate immune response is rapid but rather unspecific.

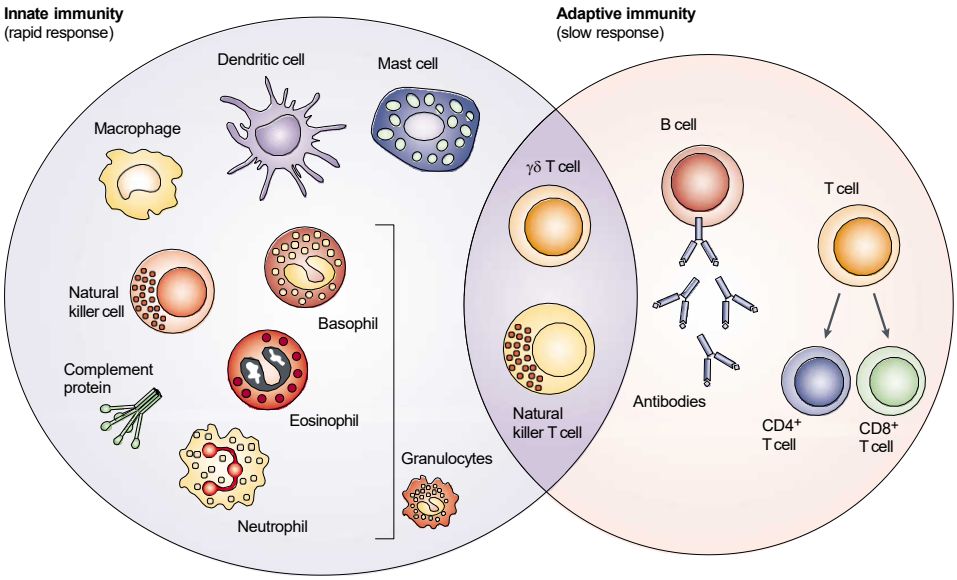

Figure 1 Cellular and humoral factors of the innate and adaptive immunity. The innate immune response acts as the first line of defense against infections. It consists of both soluble factors (e.g. complement proteins) and various cellular components (e.g. granulocytes, mast cells, macrophages, dendritic cells, and natural killer cells). The adaptive immune response develops slowly but is much more specific and can result in immunological memory. It consists of antibodies, B cells, and various T cells. Natural killer T cells and γδT cells are found as the interface between innate and adaptive immunity in their role as cytotoxic lymphocytes. Figure taken from [56].

The adaptive immune response is induced when a pathogen was able to overcome innate immunity. B lymphocytes (B cells) and T lymphocytes[2] (T cells) are the two main cellular components. Additionally, innate-like lymphocytes like natural-killer T cells and γδ T cells are involved in adaptive immunity [147]. A particular strength of the adaptive immune system is the clonal expansion of lymphocytes, where T and B cells rapidly increase from one to a million. Further, cell-mediated immunity is carried out by T cells, whereas antibodies against a specific pathogen or its product produced by B cells are part of the

[1] Further described in section 1.2 (p. 3)
[2] Further described in section 1.3 (p. 7)

humoral adaptive immunity [157]. The adaptive immune response develops throughout life in response to infections with a specific pathogen. Consequently, the body builds up an immunological memory that creates a lifelong protective immunity against reinfections [157]. Effective immune protection can be distinguished into four main tasks: immunological recognition, immune effector functions, immune regulation, and immunological memory. The innate immune system is crucially involved in the first three of these tasks, whereas the immunological memory is a specific feature of adaptive immunity.

1.2 Dendritic cells

The complexity of the immune system not only allows for improved immune responses against a wide variety of pathogens, but thereby also increases the amount of control needed to prevent harmful immune reactions that damage the host. In this context, dendritic cells (DCs) play an important regulatory role, as they are not only responsible for the detection of pathogens but also for the specific activation of the required composition of various effector cells.

Paul Langerhans first found DCs in human skin in 1868, where they were thought to be cutaneous nerve cells [112]. Later, they were identified and characterized as DCs by Ralph M. Steinman and Zanvil A. Cohn in 1973 and named for their “tree-like” and dendritic shapes [213]. These cytoplasmic extensions form during the maturation process of DCs and enhance functions such as T cell activation by increasing the surface area of the cell [113]. Mature DCs are identified by their high expression of the integrin-α chain (Cluster of Differentiation (CD)11c), moderate to high levels of Major Histocompatibility Complex (MHC) expression and costimulatory molecules like CD80, CD86 and CD40. The phagocytosis, processing and presentation of antigens on their surface by using the MHC I or II is the primary task of DCs. Thus, they belong to the professional antigen-presenting cells (APCs) as well as monocytes, macrophages, and B cells and thereby are crucially involved in immunological recognition. In addition to antigen presentation, the production of various mediators such as cytokines and chemokines plays a major role in the regulation of the immune response. As soon as DCs encounter antigens from invading pathogens, they migrate to the draining lymphoid organ and initiate the primary immune

response [13]. Thus, they have a strong influence on T cell formation, differentiation, and function during the initial immune phase. This further leads to the fact that DCs are very important in regulating the balance between immunity and tolerance by inhibiting T cell functions, mediating T cell apoptosis or inducing the generation of regulatory T cells [71,237]. Thereby, several factors such as maturational state, DC subset, cytokine microenvironment, and tissue localization play important roles.

1.2.1 Immunological recognition and antigen presentation

Immunological recognition and the regulation of responding or not responding to a specific ligand is mainly carried out by genome-encoded innate immune system receptors [96]. A variety of these pattern recognition receptors (PRRs) are known. These enable the discrimination between host cells and pathogens via pathogen-associated molecular patterns (PAMPs), which manage an initial immune response and trigger adaptive immunity [157]. PAMPs are present on many microorganisms and are often essential molecules in microbial physiology like lipopolysaccharides (LPS) or bacterial CpG DNA. Besides, the activation of many PRRs can occur through damage-associated molecular patterns (DAMPs) that are actively or passively released by cells in response to injury or life-threatening stress [157,230]. PRRs are expressed by all cells that are likely to encounter pathogens like macrophages, neutrophils, and DCs. Hereby, PRRs are present in different cellular locations and may be membrane-bound, in intracellular compartments [93], or even in a secreted form, where they are highly important during the acute phase response at early stages of infection [43,199]. PRRs on macrophages mostly regulate phagocytosis of microorganisms like the macrophage mannose receptor (MMR) that interacts with gram-positive and gram-negative bacteria as well as fungal pathogens [68]. A close relative of MMR is DEC205, a receptor mostly expressed on DCs [96], which is important for the internalization of proteins and antigen processing [99]. Intracellular recognition of viruses or bacterial pathogens can be done by the protein kinase PKR [44] or NOD proteins [92,161]. The evolutionary conserved Toll-like receptors (TLRs) are the PRRs best described, which can be expressed on the cell surface as well as in intracellular compartments and are able to recognize a wide range of microbial components [3]. Ten different TLRs have been described in humans and 12 in mice. TLR1, 2, 4, 5, 6, and 10

are extracellularly while TLR3, 7, 8, and 9 are intracellularly located. Within these receptors, TLR4 was first described in its function as PRR [148] and is primarily known for its essential ability to recognize LPS, a major component of gram-negative bacteria [87]. TLR2 identifies a variety of ligands and is therefore considered the most variable PRR. In most of these cases, TLR2 forms heterodimers with either TLR1 or TLR6 [166,219], which opens up the opportunity of a highly increased repertoire of ligand specificities. TLR2 is expressed on various immune cells, like macrophages, DCs, and granulocytes [157,258] but also activated T cells [107], indicating a high variety of roles and functions for TLR2. Upon pathogen recognition, DCs migrate to the draining lymph nodes and activate immune cells like T cells by antigen presentation[3].

1.2.2 Heterogeneity and origin of dendritic cells

DCs are a heterogeneous group of cells, each of which has specific functional properties. The phenotypic marker expression can be used to distinguish between different DC subsets. The first distinction can be made between conventional DCs (cDCs), firstly discovered in their function as APCs [160,213,214], and the potent Interferon (IFN)α producing plasmacytoid DCs (pDCs) with their spherical shape [36,125].

While pDCs express low levels of MHC II and the integrin CD11c under steady state, cDCs typically express high levels of MHC II and CD11c. Further separation of cDCs can be done via their expression pattern of the coreceptor CD8α or CD4 into $CD4^-$ $CD8\alpha^+$ $CD103^+$ cDCs, also referred to as cDC1, and $CD4^+$ $CD8\alpha^-$ $CD11b^+$ cDCs as well as $CD4^-$ $CD8\alpha^-$ $CD11b^+$ cDCs, also referred to as cDC2. The cDC line cDC1 is specialized for antigen cross-presentation, polarization towards T helper cells type 1 (Th1) and TLR3-induced secretion of IFN-λ [197]. Thus, this DC subtype is particularly important in targeting intracellular pathogens. In contrast, $CD4^+$ and $CD11b^+$ cDC2 are specialized for antigen presentation to $CD4^+$ T cells, which results in increased Th2- and Th17-mediated immune responses. Thus, cDC2 are specialized to combat extracellular pathogens.

Like all other leukocytes, DCs develop from hematopoietic stem cells in the bone marrow. The cell differentiation in the bone marrow distinguishes very early between the myeloid

[3] Further described in section 1.3.1 (p. 9)

and lymphoid lineage. The common myeloid progenitor develops into monocytes, macrophages, granulocytes, megakaryocytes, and erythrocytes, while the common lymphoid progenitor generates B cells, T cells, and NK cells [2,66,108]. Independently of inflammation, DCs are continuously replaced within 10 to 14 days by dendritic progenitor cells (preDCs) generated *de novo* from the bone marrow [120]. In this context, the developmental origin of DCs is still under debate. Beside a lymphoid origin of $CD8^+$ $DEC205^+$ DCs [252–254], a myeloid origin was shown for most DCs [2,66,134]. Further, inflammatory DCs can arise from monocytes that exit the bone marrow during infection [185,202]. These monocyte-derived DCs are as effective as cDCs in antigen-presenting functions [40,115].

An important factor during cell differentiation is the cytokine microenvironment. This in turn depends on the composition and activity of the bone marrow cells. Thereby, for example, IL-10 is able to induce differentiation of tolerogenic DCs [238]. Also, IFNγ has been identified as a master checkpoint regulator for many cytokines with various influences on developmental processes in the bone marrow [183,260]. Moreover, flt3 ligand (FL) has a particular relevance on the formation of functionally mature DCs [216]. This is underlined by the fact of reduced formation of DCs in mice lacking FL [146] and, in turn, by the numerical increase after daily injection of FL [135]. A major source of this protein are bone marrow stromal cells and T cells [145].

According to the classical model of DC development in the bone marrow, the monocyte-DC progenitor (MDP) give rise to the common DC progenitor (CDP), which is able to generate DC subsets including pDCs [158,165] (Figure 2). Afterwards, CDP further differentiate into the cDC exclusive preDC stage, which then migrate into the tissue and can differentiate into cDC1 as well as cDC2 [121]. However, there are groups providing evidence that the preDC population in the bone marrow distinguishes between progenitor cells to develop into different DC populations. On the one hand, Grajales-Reyes et al. proposed the preDC compartment to consist of clonogenic precursors for the cDC1 and cDC2 subset, whereas the cDC1 commitment is regulated by an auto-activation loop of IRF8 expression via IRF8 itself and Batf3 [76]. On the other hand, Schlitzer et al. introduced the separation of four different subtypes within the preDC population in the bone marrow [196]. Such commitment of preDCs has recently been described in human

[201]. To interpret the data in this study, the model from Schlitzer et al. was used. After gating for preDCs, the different subtypes are distinguished based on the expression of Ly6c and Siglec-H. Thereby, the preDC stage 1 (Siglec-H$^+$Ly6C$^-$), still able to differentiate into pDCs, further develops into preDC stage 2 (Siglec-H$^+$Ly6C$^+$) and finally into committed preDC1 (preDC1 / Siglec-H$^-$Ly6C$^-$) and preDC2 (preDC2 / Siglec-H$^-$Ly6C$^+$).

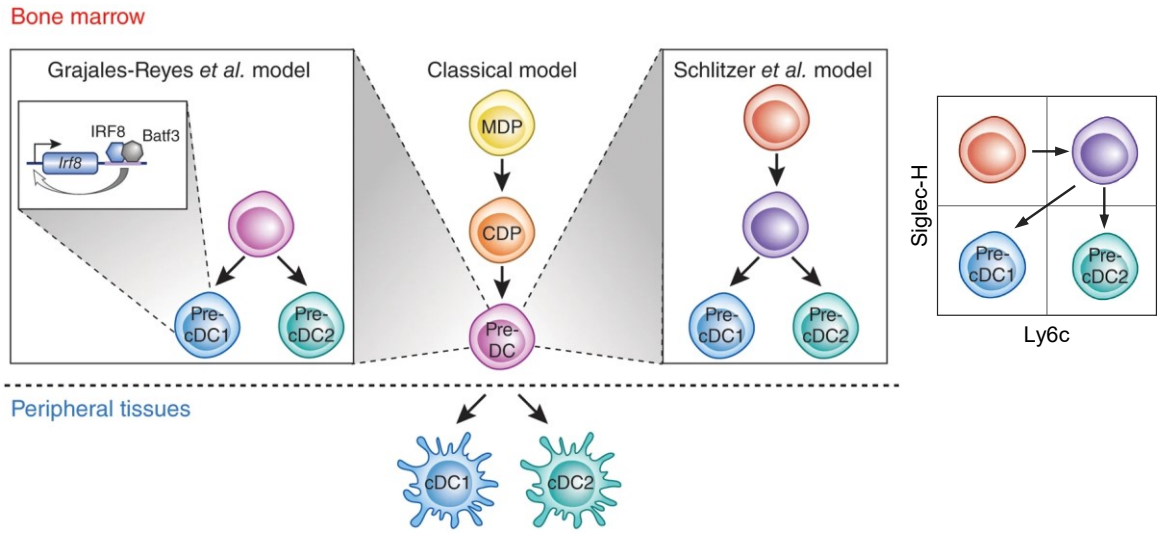

Figure 2 Different models proposed for DC development. A schematic representation of the long-accepted classical model of DC development (center) is compared here with two different and more recent models. On the left side, the model of Grajales-Reyes et al. can be seen, in which the preDCs in the bone marrow are comprised of clonogenic precursors for the cDC1 and cDC2 subset. On the right side, one can see the model of Schlitzer et al., in which four different DC progenitor subsets can be distinguished by gating for Siglec-H and Ly6c Expression. Figure adapted from Winter and Amit (2015) [250] MDP = monocyte- DC progenitor; CDP = common DC progenitor

1.3 CD8$^+$ T cells

T cells are an important component of an effective adaptive immune response. They originate from the bone marrow, which, besides the thymus, belongs to the primary lymphoid organs. T cell precursors leave the bone marrow and migrate into the thymus to mature. After successful maturation, T cells circulate as mature naïve T cells in the blood and peripheral lymphoid tissues consisting of lymph nodes, spleen and the mucosal lymphoid tissues [157]. T cells can be divided into different subpopulations by the expression of the glycoproteins CD4 and CD8, which serve as coreceptors for the MHC I or II molecule. Within the CD4$^+$ and CD8$^+$ T cells there are further subtypes that perform distinct functions to ensure a proper immune response.

For example, $CD4^+$ T cells can differentiate into different Th subpopulations, which depends on the secreted cytokine profile of DCs. These in turn differ in their cytokine expression pattern and thus have different influences on the immune response. While IL-12 conditions Th1-differentiation characterized by IFNγ and IL-2 secretion [84,133], IL-10 leads to altered DC maturation that results in a polarization towards a Th2 response in which T cells produce increased IL-4, IL-5, and IL-10 [122,209].

$CD8^+$ T cells are particularly well known as cytotoxic T lymphocytes for their role in the immune response against viruses or other intracellular pathogens and tumors [106,127,153,204,225]. The CD8 receptor consists of one CD8α and one CD8β domain and can recognize peptides presented by MHC I molecules. This receptor is found on all nucleated cells and therefore facilitates the cytotoxic function of $CD8^+$ T cells to kill infected cells [157].

The naïve $CD8^+$ T cells (T_N) mentioned above can be identified by expression of L-selection (CD62L), which guides the cells from the blood into peripheral tissues [157], and by low expression of CD44. Further, effector and memory T cell types can be distinguished. The effector $CD8^+$ T cells are mostly found in peripheral tissues. Their initial activation results in the up-regulation of CD44 and in the down-regulation of CD62L. Markers like the killer cell lectin-like receptor G1 or IL-7 receptor subunit-α would be needed to further distinguish between effector and effector memory T cells [101,153]. In this study, however, only the expression pattern $CD44^{hi}$ $CD62L^{lo}$ is used, which thus includes the effector and effector memory population as well, termed effector/effector memory $CD8^+$ T cells ($T_{E/EM}$). The differentiation into memory cells is important to assure long-lasting immunity to respond more efficiently to reinfection with the same pathogen, an important feature of adaptive immunity [101,207]. In this context, IL-7 and IL-15 are known to maintain T cell memory by promoting survival and self-renewal [218]. In addition to the effector memory population described above, there are antigen experienced central memory $CD8^+$ T cells (T_{CM}), which can be identified via the expression pattern of $CD62L^+$ $CD44^+$. Among other things, T_{CM} differ from effector memory T cells by the expression of CC-motif receptor (CCR)7, which enables a circulation similar to that of naïve T cells [31,67]. Thus, T_{CM} can migrate to peripheral lymphatic tissue and are enriched in lymph nodes and tonsils.

1.3.1 T cell immunity and activation

A characteristic component of all T cells is the expression of the immunoglobulin related T cell receptor (TCR/CD3 complex), which is crucial for differentiation, survival, and diverse functions of T cells [30]. The functions of the immune response of $CD8^+$ T cells are divided into cytolytic and non-cytolytic mechanisms. The production and fast release of cytotoxic granules like perforin and granzymes, also found on NK cells, and Fas/Fas ligand interaction are important during cytolytic elimination of infected target cells, which subsequently undergo a caspase cascade-induced apoptosis [80]. Using those mechanisms, $CD8^+$ T cells eliminate immune effector cells at the end of an immune response and are able to kill each other. Non-cytolytic antitumor and antimicrobial effects can be achieved by secretion of primarily tumor necrosis factor (TNF) α and IFNγ. Besides their role in killing infected immune cells, they have regulatory properties. Through the production of chemokines, $CD8^+$ T cells can initiate immune cell recruitment as well as activate other effector cells [79]. However, their increased cytokine production can result in pathologic processes like autoimmune or allergic disorder [91,103,221].

The best described and longest known form of T cell activation is via the TCR receptor in response to a presented antigen (Figure 3A). For this purpose, DCs migrate via the afferent lymphatic pathways and blood vessels towards the T cell zones of secondary lymphoid organs, in which they directly interact with T cells [149]. The recognition of specific antigens presented by MHC molecules results in the activation of naïve T cells [157]. Further, differentiation of $CD8^+$ T cells is driven by costimulatory receptors like CD28 binding to ligands like CD80 or CD86, mainly expressed on professional APCs such as DCs [1]. A proper T cell activation requires both antigen contact and the costimulatory signal, which results in the induction of proliferation, cytokine production, and cell survival. Reencounter with their cognate antigen leads to a massive expansion and activation of their various effector functions. Additionally, inflammatory cytokines like IL-12 and Type I IFN (IFNα/β) can enhance clonal expansion and specifically contribute to the development of effector functions like cytolytic activity and IFNγ production [48–50]. Upon activation, T cells produce CD40 ligand, which in turn binds to CD40 on DCs and thereby can enhance activation via a positive feedback loop [128]. The third signal has a major impact on T cell polarization [102], whereas the absence of which can lead to insufficient

activation and thus tolerance and anergy of T cells [77]. In addition, TLR2 can provide costimulatory signals for T cell activation [46,184,261]. The establishment of an adequate immune response through antigen-dependent TCR-stimulation usually takes several days.

One of the earliest indications after T cell activation is the expression of cell surface glycoproteins like CD69, which can be found within a few hours after stimulation [224,257]. CD69 is known to form a complex with the sphingosine 1-phosphate receptor-1 (S1PR1), which is important for lymphocyte migration towards elevated S1P concentration [205]. The down-regulation can therefore prevent the egress of activated T cells from lymphoid tissues. After its initial activation resulting in cell proliferation and differentiation, the expression of CD69 is maintained for several days [262].

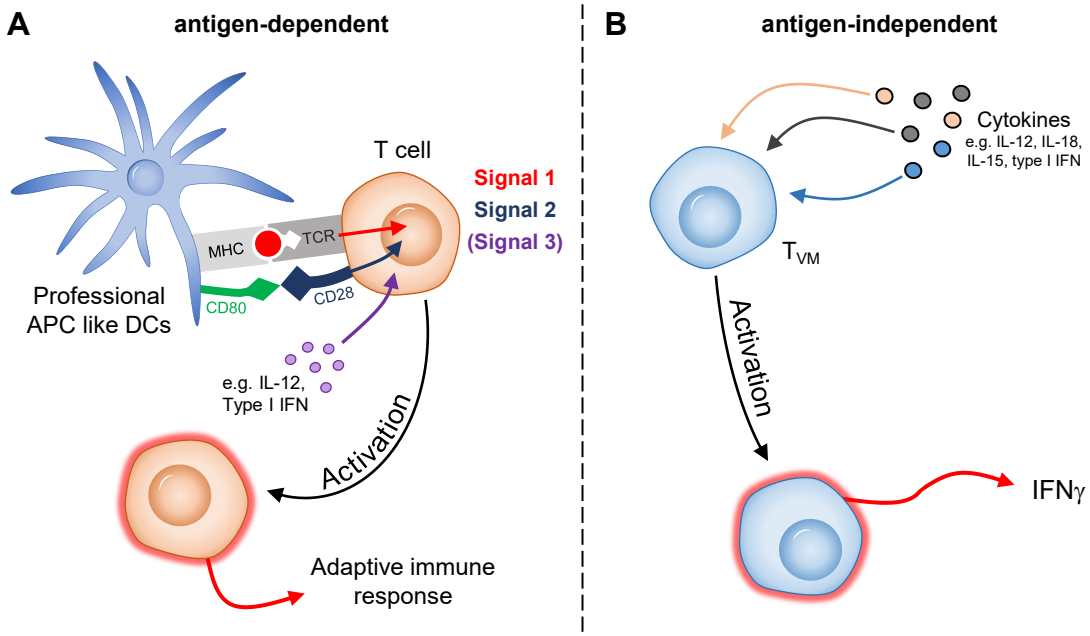

Figure 3 Comparison of antigen-dependent and antigen-independent T cell activation. Schematic representation of different T cell activation pathways. Adequate antigen-dependent activation requires three signals, namely antigen presentation via the MHC/TCR complex, costimulatory signals and specific cytokine stimulation (A). For antigen-independent "bystander" activation cytokines such as IL-12 and IL-18 are sufficient to induce a more rapid activation, for which specific virtual memory cells (T_{VM}) within the $CD8^+$ T cell subset are known (B).

A further T cell activation can solely be caused by innate cytokines (Figure 3B). This alternative activation mechanism, also called bystander activation, is much faster due to its independence from a cognate antigen and its presentation and can lead to an efficient

immune response within hours [78,116]. IL-12 and IL-18 but also IL-15, one of the most potent cytokine combinations, triggers a high production of IFNγ and up-regulation of CD69 in virus-specific $CD8^+$ effector and memory T cells [69]. Bystander activation has been shown in various studies, although the contribution in the immune response is diverse. Besides beneficial IFNγ production during *Listeria monocytogenes* infection [16,116], bystander activated T cells are associated with liver injury caused by IL-15-dependent innate-like cytolytic activity during acute hepatitis A [104].

In this context, a distinct $CD8^+$ T cell subtype that arises through homeostatic mechanisms was described in germ-free mice, which are particularly sensitive to bystander activation. These so-called virtual memory T cells (T_{VM}) are considered to take part in adaptive as well as innate immunity. Besides elevated proliferation compared to naïve T cells upon antigen encounter, rapid production of cytokines and even bystander killing via production of IFNγ or granzyme B upon stimulation with IL-12 and IL-18 was described [78,114,248]. These innate-like immune functions like IFNγ production upon cytokine stimulation were investigated in mouse models [78] and healthy humans [95]. T_{VM} are assumed to play a major role in patients with antiretroviral therapy against immunodeficiency virus (HIV) infection [100] or against infection with *Listeria monocytogenes* [114]. On the one hand, T_{VM} are described to constitutively express high levels of cytotoxic molecules like granzyme b, perforin and granulysin as well as secrete cytokines like IFNγ, IL-2 and TNFα or chemokines like C-C motif ligand (CCL)3, CCL4 and CCL5 in response to cytokine stimulation [100]. On the other hand, their TCR-induced IFNγ synthesis is very low even if infection with *Listeria monocytogenes* is efficiently controlled, which suggests a memory-like capacity to fight against specific pathogens [114].

1.3.2 T cells in the bone marrow

Maintenance of immunological memory is one of the key functions of adaptive immunity. Thereby, the immune memory is not gained by particularly long cellular lifespan but rather by frequent renewal of memory cells in the blood [82,129,151,236,247]. In this context, nonlymphoid and lymphoid tissues contain dividing memory cells, with the bone marrow as the preferred site of actively dividing memory $CD8^+$ T cells [14]. This was confirmed in

a recent study that investigated the frequent self-renewal and recirculation of memory cells between blood, lymph nodes and bone marrow [12].

In the early 2000s the bone marrow was identified to be a major reservoir of T_{CM} [144]. Under normal conditions, equal frequencies of $T_{E/EM}$, T_{CM} as well as naïve T cells can be found in all bones of which T_N represent the largest population [73]. The incidence of memory T cells was reported to be up to six times higher than in the spleen, which highlights the bone marrow in its role as memory T cell organ. The presence of IL-7 and IL-15, important for survival and long-term maintenance, is considered to favor the increased occurrence of memory T cells [14,83,203]. It is assumed that the bone marrow contains two niches for different groups of, on the one hand, proliferating and recirculating cells and, on the other hand, resting tissue-resident memory T cells [190]. The tissue-resident memory phenotype is characterized by the expression of CD69 instead of S1PR1 or CCR7 [130]. Human $CD69^+$ memory T cells reside in the bone marrow in a resting state regarding proliferation, transcription, and mobility [163,203]. However, local activation of these cells induces increased IFNγ production which results in stimulation of innate immunity and the recruitment of circulating $CD8^+$ T cells to the infectious site [5,194].

1.4 Sepsis

Sepsis is described in the third international consensus definition Sepsis-3 as a syndrome of physiologic, pathologic, and biochemical abnormalities caused by infection [208]. In order to fight against this infection, the host develops a dysregulated immune response, which in turn leads to life-threatening organ dysfunction. In a global study, sepsis was shown to comprise approximately 20 % of all annual deaths at 49 million cases and 11 million sepsis-related deaths in 2017 [191]. Thus, although increasingly reported, it is not only a major health problem in lower-middle-income countries. Only about 50 % of the patients recover, who initially survive sepsis. One third dies within the first year after sepsis, often due to direct sepsis-related complications in the first months [180,181]. But even in survivors, sepsis-related long-term consequences can be observed years afterward [94].

1.4.1 Diagnosis and disease progression

To determine the occurrence and severity of sepsis, the Sequential Organ Failure Assessment (SOFA) score is used. This score considers and evaluates six different organ systems, which are respiration, coagulation, liver, kidney as well as the cardiovascular and central nervous system with values from 0 (normal) to 4 (most abnormal) [233]. Depending on the severity of sepsis, it is divided into four different stages [23]. First, systemic inflammatory response syndrome (SIRS) describes the inflammatory process and, besides infection, can be caused by trauma, burns, or pancreatitis (Figure 4). For diagnosing SIRS, two or more clinical manifestations in terms of temperature, heart rate, respiratory rate, and white blood cell count must apply. In addition, if SIRS is caused by an infection, it is referred to as sepsis. Severe sepsis further triggers organ dysfunction, hypoperfusion abnormalities and hypotension. A special subtype of severe sepsis is septic shock, which is characterized by hypotension despite fluid resuscitation and is associated with a particularly increased mortality rate [232,245].

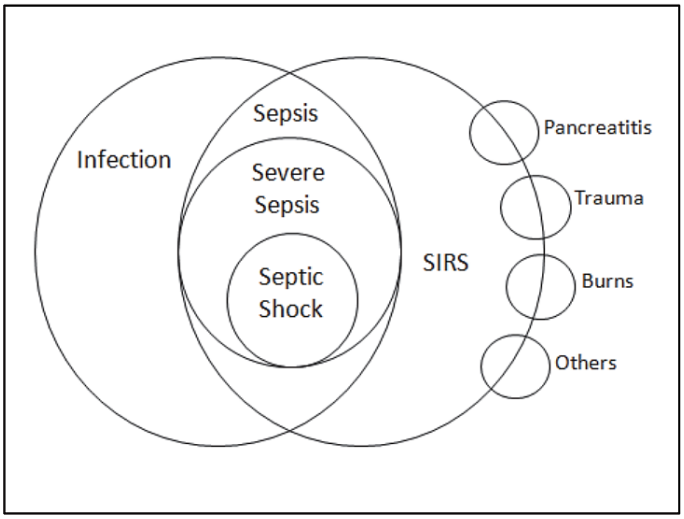

Figure 4 Relationship between infection, sepsis and the systemic inflammatory response syndrome (SIRS). While SIRS can also be caused by trauma, burns and other triggers, sepsis is only diagnosed with concomitant infection. Figure taken from [6]

In the early 1990s, sepsis was thought to consist only of increased production of pro-inflammatory cytokines. Through excessive release of pro-inflammatory mediators, this can lead to a so-called cytokine storm [188]. It soon became clear that increased

production of anti-inflammatory cytokines such as IL-10, IL-1 receptor antagonist (IL-1Ra), and transforming growth factor-β (TGFβ) occurs [63,136,137], which was believed to be a response to control systemic inflammation [155]. However, exacerbated production of these anti-inflammatory mediators and immunosuppressive effects of serum from septic patients was shown [136,182]. This sepsis-induced immunosuppression leads to an increased susceptibility to secondary infections, which was, for example, also described by the terms immunodepression [4] or immunoparalysis [235]. In 1997, the term compensatory anti-inflammatory response syndrome (CARS) was established [24]. It was formerly believed that CARS temporarily followed SIRS. However, it has since been shown that even if one of the syndromes might temporarily be predominant, these immune regulations are concomitant during sepsis [34,155]. The balance of these two syndromes is critically important, as the predominance of SIRS leads to septic shock, which potentially causes an early death of the patient, and increased CARS leads to immunosuppression, which can result in a late death even after the acute sepsis phase.

1.4.2 Pathogenesis

The initial phase of sepsis is mostly dominated by SIRS. Thereby, several mechanisms can lead to an exaggerated immune response that results in tissue and organ damage. Effector cells like macrophages and monocytes recognize the invading pathogens and secrete increased levels of pro-inflammatory cytokines like TNFα, IL-1β, IL-6, IL-12 or IL-18 [38,159]. This, in turn, results in an accumulation of other immune cells like neutrophils, T cells, B cells or platelets to the site of infection [22]. The immune cells are stimulated via TLR and NFkB signaling pathways to further secrete pro-inflammatory cytokines, chemokines and reactive oxygen species. These are, on the one hand, particularly important for killing pathogens, but, on the other hand, triggers tissue damage-induced vascular permeability and organ injury. Further, stimulation of CCR2 via its ligands CCL2 or CCL7 results in the infiltration of inflammatory monocytes [35]. Thereby, increased CCL2 levels have been associated with organ dysfunction and mortality in sepsis [25,26]. Other inflammatory mediators like complement factor C5a are able to control activity of innate immune cells during sepsis, for example, in causing hyperproduction of cytokines in macrophages and paralyzing neutrophils [186,243]. Further, it induces disseminated

intravascular coagulopathy (DIC) through activation of the coagulation system which results in the formation of blood clots [188]. Thereby, simultaneous inhibition of fibrinolysis, mainly caused by elevated levels of plasminogen activator inhibitor type-1 (PAI-1), leads to increasing disease complications and eventually death [18,259].

The secreted cytokines can have different roles during the immune response. For example, IL-6 activates B cells and T cells as well as the coagulation system [22,179,187]. However, it has anti-inflammatory effects by promoting production of IL-1Ra and IL-10 along with inhibiting the secretion of TNFα and IL-1β [195,212], which are able to induce vascular permeability and fever [32,53]. The initial SIRS is accompanied by CARS, in which increased production of anti-inflammatory cytokines such as IL-1, IL-4, IL-10 or TGFβ are thought to protect against an uncontrolled inflammatory reaction but eventually cause immunosuppression [24,235]. Sepsis-induced apoptosis is described for various cells of the innate and adaptive immune response. This includes a loss of $CD4^+$ T cells, B cells, and DCs in the spleen of septic patients [88,89]. Regulatory T cells and the Th2-polarizing myeloid-derived suppressor cells even increase in their proportion [52,231]. Pène et al. suggested the decrease of DCs to be regulated by TLR2 and TLR4 dependent signaling [172]. In addition, they showed in a more recent study TLR2ko mice to be less susceptible to secondary infections after sepsis [173]. In line with this, the TLR2 agonist P_3CSK_4 rather than TLR4 agonist LPS seemed to play a role during the development of DC dysfunction regarding impaired Th1-priming capacity [28]. This highlighted a specific role for TLR2 signaling on DC development resulting in a dysfunctional phenotype during sepsis.

Immunosuppression is characterized by dysfunctions of monocytes and macrophages [251], DCs [64,168,177] and lymphocytes [154]. This dysfunctional phenotype has been described in terms of DCs with increased IL-10 and decreased IL-12 production [64,177,246]. In the context of up-regulated anti-inflammatory mediators, IL-12 is of great relevance, which, besides DCs, is produced by monocytes and macrophages [157]. In contrast to IL-10, IL-12 stimulates T cells and NK cells to produce IFNγ and thereby induces a Th1-polarization. If this IFNγ production is missing, a higher susceptibility to bacteria is seen [90,241]. A balance between the pro-inflammatory and anti-inflammatory immune response is of great importance for the survival of sepsis

The murine cecal ligation and puncture (CLP) was developed to study these complex immune responses during sepsis and was initially established in rats [249]. The symptoms of sepsis can be well represented, for example, in the decrease of T lymphocytes in the thymus and a shift towards Th2-associated cytokine production [9,10]. The increased mortality of IFNγ-knockout (ko) mice highlights the loss of Th1-associated immune response as an important factor in sepsis-induced immunosuppression [139].
Previous studies demonstrated the CLP mouse model used in this group to induce immunosuppression indicated by diminished bacterial clearance after reinfection with *Pseudomonas aeruginosa* four days after sepsis [169]. In addition, DCs produced less IL-12 and instead secreted large amounts of IL-10 [64]. This was also observed in generated bone marrow-derived DCs (BMDCs), which leads to the assumption that this dysfunction is caused by an altered differentiation in the bone marrow. A short-term accumulation of activated pDCs 36 hours after sepsis was identified as an important mediator of this dysfunction, as depletion of pDCs induces a beneficial shift of the cytokine profile towards Th1 differentiation [210].

1.4.3 The relevance of cell metabolism

Sepsis-related organ damage has not only been associated with hyperinflammation but with energy deprivation [57]. Various mechanisms are available to the cells for energy production. During glycolysis, glucose is transported into the cell and processed in the cytosol to pyruvate, which is either further processed to lactate and produces NAD^+ for adenosine triphosphate (ATP) production or converted to acetyl coenzyme A (acetyl-CoA) in mitochondria, which drives the tricarboxylic acid (TCA) cycle [171]. This can support the electron transport chain and subsequently the oxidative phosphorylation (OXPHOS) in mitochondria through the production of NADH, which finally results in ATP production. The TCA cycle, in addition to acetyl-CoA, can be fueled by fatty acids or glutamine with citrate subsequently exported from mitochondria and stimulating acetyl-CoA production in the cytoplasm, which in turn is a substrate for fatty acid synthesis. This process is important in TLR-induced activation of DCs [61].
During sepsis, decreased OXPHOS initiates the energy production to shift to an anaerobic stage, in which a metabolic switch to glycolysis occurs that causes decreased generation

of ATP, similar to the Warburg effect in tumors [242]. The Warburg effect, also referred to as aerobic glycolysis, describes the behavior of tumor cells, which obtain their energy despite sufficient oxygen supply mainly by glycolysis with subsequent secretion of lactate. The metabolic shift from OXPHOS to glycolysis was observed during the acute septic phase in mice [39]. In the post-acute phase of sepsis, the glycolysis-dependence switches to fatty acid oxidation (FAO), which is regulated by sirtuins [124]. Decreased energy production may be observed in the heart, liver, lungs, kidneys, and brain of patients with septic shock and could be due to decreased OXPHOS. In addition, decreased peroxisomal proliferator-activated receptor y expression compromises FAO and glucose catabolism resulting in sepsis-induced organ failure [109,174]. Defects in both glycolysis and oxidative metabolism in sepsis patients were partially prevented by IFNγ therapy suggesting metabolic processes to be a good therapeutic target in sepsis [39].

1.5 Aims and scope of the work

Sepsis is a systemic infection that, in addition to the risk of dying from the acute hyperinflammatory reaction, increases the susceptibility to secondary infections. Previous studies have shown that this post-septic immunosuppression is caused by the dysfunctional phenotype of DCs maturing in the bone marrow, which is characterized by decreased IL-12 and increased IL-10 production [64,168]. Moreover, they are not able to initiate a sufficient adaptive immune response, but even inhibit IFNγ production in NK cells [168,169]. Further, activated pDCs accumulate in the bone marrow 36 hours after sepsis and play a detrimental role in generating dysfunctional DCs [210]. The sepsis-induced immunosuppressive effects of DCs regarding cytokine secretion and Th1-polarization and the accumulation of activated pDCs in the bone marrow was mimicked by application of the TLR2 stimulating reagent P_3CSK_4. In addition, it was prevented in TLR2ko mice, which indicates an important role of TLR2 signaling during the development of immunosuppression [28,178,211]. Preceding and accompanying the increase of pDCs, T cells accumulate in the bone marrow and show signs of increased activity [178,210].

The aim of this work was to analyze the accumulating T cells in the bone marrow in more detail with regard to their subpopulations and activation during sepsis. In addition, $CD8^+$ T cell functions that may be related to the development of immunosuppressive DCs in the bone marrow were investigated. To answer this question, the CLP model of post-septic immunosuppression was used, as in previous studies. Here, TLR2 was considered as a possible influencing signaling pathway, and in addition to wild-type mice, TLR2ko mice were used during the $CD8^+$ T cell characterization and functional studies.

2. Material and Methods

2.1 Material

2.1.1 Consumables

Consumables and equipment used for this work were ordered from Falcon BD (Heidelberg, DE), Becton, Dickinson and Company BD (Heidelberg, DE), STARLAB (Ahrensburg, DE), Greiner bio-one (Frickenhausen, DE), Eppendorf (Hamburg, DE), Sarstedt (Nümbrecht, DE), and Nunc (Wiesbaden, DE). Among other things, these included cell culture plates, pipettes and pipette tips, cannulae, single-use syringes, cell sieves and reaction as well as tubes for flow cytometry (Fluorescence-activated cell sorting (FACS) tube).

2.1.2 Instruments

All instruments and equipment used for this work are listed in Table 1.

Table 1 Instruments

Instruments	Model	Manufacturer
Anesthesia device	For small animals with isoflurane vaporizer	UNO, Netherlands
Blood analysis	Vet abc™ Spotchem II	Scil animal care, Viernheim, DE Arkray, Kyōto, Japan
Cell separation	autoMACS® pro	Miltenyi Biotec, Bergisch Gladbach, DE
Centrifuge	Varifuge 3.0RS, Hereaus Megafuge 40R Centrifuge 5417C IEC Micromax Fuge	Heraeus, Munich, DE Thermo Fisher Scientific, Dreieich, DE Eppendorf, Hamburg, DE Thermo Fisher Scientific, Dreieich, DE
Flow Cytometer	BD FACSCanto II TM CytoFLEX	BD Bioscience, San Jose, USA Beckman Coulter, Pasadena, USA
Heating devices	IL 11 Infrared lamp Heating and warming plate	Beurer, Ulm, DE Medax, Kiel, DE
Incubator	HerCell 150I CO_2 Incubator	Thermo Fisher Scientific, Dreieich, DE
Luminex	MAGPIX® System	Luminex Corporation, Austin, Texas, USA
Measuring devices	Scale Infrared Thermometer TM-65E	SCALTEC, Heiligenstadt, DE Medisana, Neuss, DE
Microscope	Axiovert 25, Axiostar plus	Carl Zeiss, Jena GmbH, DE

Instruments	Model	Manufacturer
Microplate reader	Labsystems Multiskan Ascent	Thermo Fisher Scientific, Dreieich, DE
Seahorse	Seahorse XFe24 Analyzer	Agilent Technologies, Santa Clara, USA
Spectrophotometer	Nanodrop 1000	Peqlab / VWR International, Darmstadt, DE
Mixing devices	Paramix II	JULABO GmbH, Seelbach, DE
	VF2	Janke&Kunkel IKA Labortechnik, DE
	MTS 4	Janke&Kunkel IKA Labortechnik, DE
	Test-Tube Rotator	Labinco, Breda, Netherlands
Water bath	TWB12	JULABO GmbH, Seelbach, DE
Workbench	antair BSK, antair HB	Bio-Flow Technik, Meckenheim, DE

2.1.3 Chemicals and stimuli

2.1.3.1 Chemicals

Unless otherwise stated, all chemicals used for this work were purchased from Sigma Aldrich (Taufkirchen, DE), Merck (Darmstadt, DE), Promega (Mannheim, DE) and Serva Elektrophoresis (Heidelberg, DE). The purity grade of the chemicals used was 'for analysis'. Ethanol used for disinfection was supplied by the pharmacy of the Essen University Hospital.

2.1.3.2 Reagents, cytokines and stimuli

Reagents, cytokines and stimuli used for isolation, cultivation and stimulation of cells or *in vivo* application are listed in Table 2.

Table 2 Reagents, cytokines, chemokines, stimuli and inhibitors

Reagents	Manufacturer
2-NBD glucose (2-NBDG)	Tocris Bioscience, Bristol, UK
Brefeldin A (GolgiPlug™)	BD Biosciences, Heidelberg, DE
Collagenase D	Roche Diagnostics GmbH, Penzberg, DE
GM-CSF mouse recombinant	PromoKine, PromoCell, Heidelberg, DE
recombinant mIL-2	R&D Systems, Wiesbaden, DE
recombinant mIL-12	R&D Systems, Wiesbaden, DE
recombinant hIL-15	PeproTech, Rocky Hill, USA
recombinant mIL-18	MBL CO., LTD., Naka-ku Nagoya, Japan
CpG-Oligonucleotide, ODN 1668	InvivoGen, San Diego, USA

Ionomycin calcium salt from *Streptomyces conglobatus*	Sigma-Aldrich, Taufkirchen, DE
LPS (E.coli 026:B6)	Sigma-Aldrich, Taufkirchen, DE
Pam_3CSK_4 (Pam_3CSK_4)	InvivoGen, San Diego, USA
Phorbol-12-myristat-13-acetat (PMA)	Sigma-Aldrich, Taufkirchen, DE
2-Deoxy-D-Glucose (2-DG)	Sigma-Aldrich, Taufkirchen, DE
Oligomycin	Calbiochem, Merck, Darmstadt, DE
6-Diazo-5-oxo-L-norleucine (DON)	Sigma-Aldrich, Taufkirchen, DE

2.1.4 Serum, Media, Buffers and Solutions

2.1.4.1 Serum

Fetal Calf Serum (FCS) was ordered from the company Biochrom (Berlin, DE). For inactivation of the complement components, FCS was heated for 30 minutes at 56°C in a water bath and stored in 50 ml aliquots at -20° C. Endotoxin levels were 1.00 EU mL-1.

2.1.4.2 Buffers and Solutions

If not mentioned separately, the chemicals of the companies specified in 2.1.3.1 were used for setting up buffers and solutions (see Table 3). Home-made deionized water, Phosphate-buffered Saline (PBS) or Aqua ad iniectabilia (Braun, Melsungen, DE) was used as a solvent. PBS used in cell culture and for *in vivo* application was obtained from Gibco/Invitrogen (Karlsruhe, DE) and had an endotoxin content of 1 EU mL^{-1}.

Table 3 Buffers and solutions

Name	Composition/Manufacturer
10x PBS	86,7 g/L NaCl 2,0 g/L KCl 2,0 g/L Na_2HPO_4 2,0 g/L KH_2PO_4 Ad aqua 1 L
autoMACS® Cleaning Solution	70 % v/v Ethanol
autoMACS® Pro Washing Solution	Miltenyi Biotec, Bergisch Gladbach, DE
autoMACS® Running Buffer	Miltenyi Biotec, Bergisch Gladbach, DE
Blocking buffer	1 % FCS in PBS / Reagent diluent Concentrate 2

Name	Composition/Manufacturer
Cellwash	BD Biosciences, Heidelberg, DE
Cytoperm/Cytofix	BD Biosciences, Heidelberg, DE
Dulbeccos phosphate buffered saline (Without $CaCl_2$ and $MgCl_2$)	Gibco/Invitrogen, Karlsruhe, DE
Ethylenediaminetetraacetic acid (EDTA)	250 mM stock solution
ELISA-Waschpuffer	0.05 % Tween 20 100 ml 10x PBS 900 ml Aqua dest.
Ethanol (100 % or 70 %)	Pharmacy of the Essen University Hospital, DE
Isoflurane	CP-pharma, Burgdorf, DE
Isotonic Sodium chloride solution (0.9 %)	Fresenius Kabi, DE / Berlin-Chemie, DE
Ketamine (10 %)	Medistar Arzneimittelvertrieb GmbH, Ascheberg, DE
PermWash	BD Biosciences, Heidelberg, DE
Reagent diluent Concentrate 2 (10x)	R&D Systems, Wiesbaden, DE
Red Blood Cell Lysing Buffer Hybri-Max™	Sigma-Aldrich, Taufkirchen, DE
Stop solution ELISA	27.15 ml H_2SO_4 (98 %) 472.85 ml H_2O
Temgesic® (Buprenorphine)	Indivior, Mannheim, DE
TMB Substrate Reagent Set	BD OptEIA™, BD Biosciences, Heidelberg, DE
Trypan Blue solution (0.4 %)	Sigma-Aldrich, Taufkirchen, DE
Tween 20 Molecular biology grade	AppliChem GmbH, Darmstadt, DE
Xylazine (20 mg/ml)	WDT, Garbsen, DE

2.1.4.3 Cell culture medium

The medium used for all experiments was *very low endotoxin medium*, VLE RPMI 1640 from Biochrom (Berlin, DE). Endotoxin-free additives were 10 mM HEPES (Biochrom, Berlin, DE), 0.06 mg mL^{-1} penicillin (Sigma-Aldrich, Taufkirchen, DE), 0.02 mg mL^{-1} gentamicin (Sigma-Aldrich, Taufkirchen, DE) and 0.05 mM of mercaptoethanol (Sigma-Aldrich, Taufkirchen, DE). L-glutamine was contained in the RPMI medium in stable form. Additionally, 10 % heat-inactivated FCS was added to the medium. The medium including these supplements mentioned above is from now on termed culture medium (CM). For cultivation of DCs, the CM additionally contained Granulocyte-macrophage colony-stimulating factor (GM-CSF). Each medium was stored at 4°C and was used for up to one month.

2.1.5 Antibodies

Flow cytometric characterization of cell surface molecules and intracellular cytokines or *in vivo* application was done with the following antibodies (Table 4).

Table 4 Antibodies

Antigen	Fluoro-chrome	Clonality	Manufacturer	Isotype control
B220	PE	RA3-6B2	BD Biosciences, Heidelberg, DE	Rat IgG 2a, κ
CD3	FITC	145-2C11	BD Biosciences, Heidelberg, DE	-
	APC	17A2	BD Biosciences, Heidelberg, DE	
	APC	145-2C11	Invitrogen, Darmstadt, DE	
	APC-Fire750	145-2C11	BioLegend, San Diego, USA	
CD4	PE	RM4-5	BD Biosciences, Heidelberg, DE	-
	Pacific Blue	RM4-5	BD Biosciences, Heidelberg, DE	
	BV510	RM4-5	BioLegend, San Diego, USA	
CD8	FITC	53-6.7	BD Biosciences, Heidelberg, DE	-
	PerCPCy5.5	53-6.7	BioLegend, San Diego, USA	
	BV510	53-6.7	BD Biosciences, Heidelberg, DE	
CD11b	PerCPCy5.5	M1/70	BD Biosciences, Heidelberg, DE	Rat IgG 2b, κ
	BV510	M1/70	BD Biosciences, Heidelberg, DE	Rat IgG 2b, κ
CD11c	APC	N418	Invitrogen, Darmstadt, DE	-
CD40	FITC	3/23	BD Biosciences, Heidelberg, DE	Rat IgG 2a, κ
CD44	AF488	IM7	BioLegend, San Diego, USA	-
CD45.1	APC	A20	BioLegend, San Diego, USA	-
CD62L	PE-Cy7	MEL-14	BioLegend, San Diego, USA	-
CD69	BV421	H1.2F3	BioLegend, San Diego, USA	Arm. Hamster IgG
CD86	PE	GL1	BD Biosciences, Heidelberg, DE	Rat IgG 2a, κ
CD115	APC-Cy7	AFS98	BioLegend, San Diego, USA	Rat IgG 2a, κ
CD122	PE	TM-β1	BioLegend, San Diego, USA	Rat IgG 2b, κ
CD135	BV421	A2F10	BioLegend, San Diego, USA	Rat IgG 2a, κ
TCR DO11.10	APC	KJ1-26	Invitrogen, Darmstadt, DE	-
F4/80	PE	BM8	eBioscience, Frankfurt, DE	-
Glut1	AF700	Polyclonal	Novus Biologicals, Colorado, USA	-
MHC II	PE-Cy7	M5/114.15.2	BD Biosciences, Heidelberg, DE	Rat IgG 2b, κ
IFNγ	PE	XMG.1.2	BD Biosciences, Heidelberg, DE	Rat IgG 1, κ
Ly6C	FITC	AL-21	BD Biosciences, Heidelberg, DE	Rat IgM, κ

Antigen	Fluoro-chrome	Clonality	Manufacturer	Isotype control
PD1	APC	29F.1A12	BioLegend, San Diego, USA	Rat IgG 2a, κ
Siglec-H	PerCPCy5.5	551	BioLegend, San Diego, USA	Rat IgG 1, κ
Fixable Viability Dye	eFluor™ 780	-	eBioscience, Frankfurt, DE	-
IgG from mouse serum (Block solution)			Sigma-Aldrich, Taufkirchen, DE	-
CD3, Purified		17A2	BD Biosciences, Heidelberg, DE	-
CD28, Functional Grade		37.51	Invitrogen, Darmstadt, DE	-
*InVivo*MAb CD8β		53-5.8	Bio X Cell, Lebanon, USA	HRPN

2.1.6 Commercial tests

The test kits given in Table 5 were used for quantification of cytokines and chemokines in cell culture and for cell purification using autoMACS®.

Table 5 Commercial tests

Name	Manufacturer
CD8a$^+$ T cell Isolation Kit, mouse	Miltenyi Biotec, Bergisch Gladbach, DE
CD11c MicroBeads UltraPure, mouse	Miltenyi Biotec, Bergisch Gladbach, DE
ELISA DuoSet Mouse GDF-15	R&D Systems, Wiesbaden, DE
ELISA DuoSet Mouse IL-6	R&D Systems, Wiesbaden, DE
ELISA DuoSet Mouse IL-10	R&D Systems, Wiesbaden, DE
ELISA DuoSet Mouse IL-12p70	R&D Systems, Wiesbaden, DE
ELISA DuoSet Mouse TNF- α	R&D Systems, Wiesbaden, DE

2.1.7 Animals

Female BALB/c mice obtained from Janvier (France) were used as experimental wild-type animals. Before starting the experiment, the animals had the opportunity to get used to the conditions in the central animal laboratory for at least one week. This was used to avoid any stress that may have arisen during transport. Other mouse strains used for this study were on BALB/c background and are summarized in Table 6 below. These animals were bred in the Central Animal Laboratory (ZTL) of the Essen University Hospital. At the start of the experiment, all animals had reached an age of 10-12 weeks (24 hours CLP or

transfer experiment) or 14-16 weeks (4 days CLP) and a weight of 19 to 24 g. The experimental animals were kept in accordance with the animal welfare regulations in the ZTL of the Essen University Hospital and had access to standard rodent food and water ad libitum.

Table 6 Mouse strains

Strain	Background	Breeder
BALB/c	BALB/c	Janvier Labs, France
TLR2ko	BALB/c	ZTL, Essen University Hospital, DE
IFNγko	BALB/c	ZTL, Essen University Hospital, DE / Dalton et al. [51]
DO11.10	BALB/c	ZTL, Essen University Hospital, DE / Jackson Laboratory, USA

2.2 Methods

2.2.1 Animal experiments

2.2.1.1 Induction of polymicrobial sepsis via cecal ligation and puncture

Sublethal polymicrobial sepsis was induced using the murine CLP model. This model was first established in rats [249] and was applied in a modified form during this work. After ligation and puncture of the cecum, bacteria are continuously released into the abdominal cavity and thereby trigger polymicrobial sepsis. The severity of sepsis can be modulated by varying the length of ligation, the size of needle used for puncture and the amount of initially released intestinal content. In the present work, animals were sacrificed after induction of sublethal sepsis at 12 hours, 24 hours (24 h CLP) or 4 days (4 d CLP) to analyze the influence of different sepsis durations on the immune system. For this purpose, female 10 to 16 week-old wild-type BALB/c, TLR2ko or VertX mice were used. After a short exposure of the mice to isoflurane, the anesthesia was carried out with an intramuscular (i. m.) injection into the foreleg of 115 mg kg^{-1} body weight ketamine and 13 mg kg^{-1} body weight xylazine.

Afterwards, the abdomen of the experimental animals was disinfected with Octenisept® (Schülke & Mayr GmbH, Norderstedt) and the fur in the lower abdominal area was cut to a length of approximately 1.5 cm. Subsequently, the abdominal cavity was opened along the linea alba (laparotomy) and the cecum was exposed by using blunt-nosed tweezers.

At least 50 % but a maximum of 1.5 cm length of the cecum was tied off using a loop of 5-0 non-absorbable surgical suture material (Prolene by Ethicon, Johnson & Johnson Medical GmbH, Norderstedt). During continuous pressure with the thumb and index finger, the ligated part was then punctured with a 27-gauge needle (BD Microlance™, BD Medical, Heidelberg) to release a small amount of the intestinal contents. Next, the cecum and intestinal content was placed back into the abdominal cavity. To resuscitate the experimental animals, 1 ml of a 0.9 % NaCl solution preheated to 37 °C body temperature was administered into the peritoneum. The incision was then closed with continuous sutures using 5-0 Prolene. For pain relief, 10 g per kg body weight of buprenorphine was injected subcutaneously.

As control treatment, mice underwent a sham operation in which no exposure or ligation and puncture of the cecum took place. Under the described operation conditions, the CLP animals developed symptoms of the disease, which were characterized by rough fur, limited motility and weight loss. Mortality within up to 24 hours of sepsis induction was 0 % and reaches 0-25 % after four days.

2.2.1.2 Adoptive cell transfer

To analyze the behavior of T cells and their influence on immune cell development during sepsis, $CD8^+$ T cell transfer experiments were performed, as depicted in Figure 5. $CD8^+$ T cells were isolated from BALB/c, TLR2ko or DO11.10 mice using a $CD8\alpha^+$ T cell Isolation Kit and the autoMACS® pro separator (See 2.2.3.2). Afterwards, the cells were transferred by intravenous (i.v. / See 2.2.5.1) injection of 100 µl cell suspension into the lateral tail vein of recipient mice. Subsequently, the mice were anesthetized and a CLP or sham operation was performed as described above. In case of a 24 h CLP, 10×10^6 $CD8^+$ T cells were transferred into BALB/c-CD45.1 mice aiming to characterize the phenotype of endogenous and transferred $CD8^+$ T cells. To analyze the influence of $CD8^+$ T cells on the development and functionality of DCs, 1×10^6 $CD8^+$ T cells were transferred into BALB/c mice, which were then subjected to a 4 d CLP.

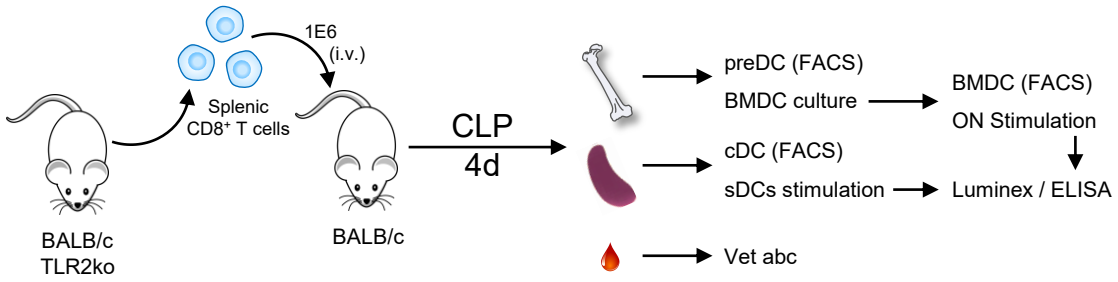

Figure 5 Experimental flow chart for CD8⁺ T cell transfer experiments. For transfer experiments, CD8⁺ T cells were isolated from BALB/c or TLR2ko mice and were injected intravenously (i.v.) into wild-type mice. After a CLP operation and additional four days, various parameters were examined in bone marrow, spleen, and blood.

2.2.1.3 CD8⁺ T cell Depletion

Anti-mouse CD8β antibody for *in vivo* applications was prepared sterile with the *InVivo*Pure pH 7.0 Dilution Buffer (Bio X Cell, Lebanon, USA) to a concentration of 1 µg/µl. Then, 100 µl depletion solution or the HRPN isotype control was intraperitoneally (i.p. / See 2.2.5.2) injected (Figure 6). After three days, CLP surgery was performed with a subsequent duration of four days. Various analyses were done, which are explained in more detail in the following method section.

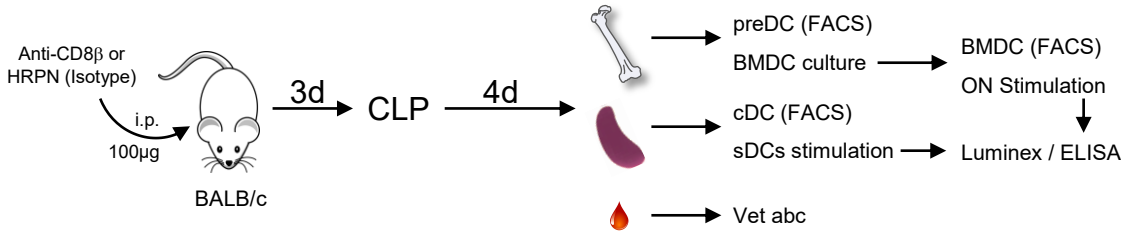

Figure 6 Experimental flow chart for CD8⁺ T cell depletion experiments. For depletion experiments, anti-CD8β or HRPN as isotype control was injected intraperitoneally (i.p.) into BALB/c mice. The mice underwent CLP surgery after three days. Various parameters were examined in bone marrow, spleen and blood four days later.

When cells from different animals were pooled in analyses, successful depletion was verified by FACS staining beforehand. Titration experiments demonstrated that depletion using this antibody was sufficient after three days and present for at least eight days in different organs (Figure 23A, Annex page 97).

2.2.2 Organ extraction

For the collection of bone marrow, spleen or peritoneal lavage, the test animals were killed by cervical dislocation after a short pre-anesthesia with isoflurane. Subsequently, all further steps for organ removal were performed under sterile conditions. In case of blood sampling, the animal was treated with ketamine and xylazine after pre-anesthesia (see 2.2.1.1) and the respective collection was performed under anesthesia.

2.2.2.1 Collection und preparation of whole blood and serum

Blood was collected either by cardiac puncture or by puncture of the ophthalmic vein. For both methods, the animals were anesthetized with ketamine and xylazine.

For cardiac puncture, the mouse was placed in the supine position and a 1 ml or 2 ml syringe with a 25-gauge needle was inserted centrally into the chest and laterally from the sternum until the heartbeat was noticed or the distance was sufficient. By slowly and continuously pulling out the plunger, blood was extracted from the heart.

For retrobulbar blood sampling, the mouse was placed in the prone position. A thin glass capillary was passed laterally past the eye in the direction of the opposite ear to the back wall of the orbit. Then, the retrobulbar venous plexus was punctured by a rapid twisting motion with the glass capillary, so that the blood was transferred into the desired tube. After both methods, the mouse was killed immediately by cervical dislocation.

The collected blood was transferred to a 1.3 ml K3E Membrane Micro tube (Sarstedt, Nümbrecht, DE), which include 1.6 mg EDTA/ml, and/or into a 1.2 ml S-Monovette for serum (Sarstedt, Nümbrecht, DE) including clot activator. The blood collected with EDTA was stored at room temperature for no longer than 1 hour while rotating slowly until further used to obtain a differential blood count using the Vet abc^{TM} animal blood counter. The determination of the leukocyte count, as well as its division into lymphocytes, monocytes and granulocytes, was used to assess the disease severity of the test animals.

For serum collection, blood was left to stand in the serum monovettes at room temperature for at least 30 min. The monovettes were centrifuged at 2000 g for 10 minutes and the serum, which is visible as a clear supernatant, was transferred to a fresh Eppendorf tube. After repeated centrifugation as an additional cleaning step, the sera were aliquoted and frozen at −80°C until further analyses (See 2.2.7.1).

2.2.2.2 Preparation of the bones

To remove the thigh (femur) and lower leg (tibia) bones, the test animals were placed in a supine position and the fur in the leg region was disinfected with 70 % ethanol. Using scissors, an incision was made along the hind legs of the mice and the fur was completely removed from the muscles. By carefully dislocating the hip joint and with a subsequent cut, the hind legs were separated from the hip joints. To remove the muscle tissue from the bones, the femur and tibia bones were separated from each other and from the foot bones through an incision with scissors. The bones thus separated were cleaned of muscle fibers and tendon tissue by careful rubbing with a rough paper tissue. Afterwards, they were disinfected with 70 % Ethanol and stored in PBS on ice until proceeding with the bone marrow cell isolation.

2.2.2.3 Preparation of the spleen

To remove the spleen, the test animals were placed on their right side and the peritoneum was disinfected with 70 % ethanol. Using scissors, a skin incision was made on the side of the animals in the area of the spleen. After the peritoneum was cut open, the spleen was carefully removed from the peritoneal cavity using blunt forceps, freed from the surrounding tissue and separated from the two blood vessels by an incision. The spleen was then processed depending on the desired cell isolation.

2.2.2.4 Isolation of bone marrow cells

After the bones were prepared and cleaned, they went through a disinfection cascade with two 70 % ethanol steps and then washed in PBS. Both ends of the tibia were cut with bone scissors and then rinsed with 5ml of cold CM using a syringe with a 27-gauge needle until all cells were flushed out of the bone. The same was done with the femur, which was only separated by a cut in the middle and both ends were carefully rinsed.

A 23-gauge needle was then placed on the syringe, the cells were resuspended twice and then transferred to a Falcon via a 30 µm filter. This was followed by lysis of the erythrocytes and then the cells were taken up in 2-5 ml of CM. Cell number determination using a Neubauer counting chamber was performed in 10 % trypan blue solution to

distinguish live from dead cells. If necessary, the cell suspension was adjusted to a desired concentration.

2.2.2.5 Isolation of spleen cells

After dissection, the spleen was placed in a small Petri dish and 1 ml of Collagenase D was injected into three different sites of the spleen using a syringe with a 27-gauge needle. Then the spleen was cut into three pieces, covered with about 2 ml of collagenase D and incubated for 12 minutes at 37°C and 5 % CO_2. The spleen pieces were then rubbed through a 70 qm filter into a petri dish containing 10 ml CM. After resuspension the cells were transferred through a 30µm filter into a falcon. This was followed by lysing the erythrocytes. Cells were resuspended in 5-10 ml CM, counted and stored on ice until further use. If only T cells were to be analyzed or purified in the experiment, the digestion step with collagenase D was skipped and the spleen was immediately cut and pressed through the 70 µm filter. If analysis or purification of DCs was intended, the procedure was performed as described above.

2.2.2.6 Red blood cell lysis

Red blood cell lysis was applied during the isolation of cells from bone marrow and spleen. For this purpose, after centrifugation and discarding the supernatant, the cells were gently resuspended in 1 ml of Red Blood Cell Lysing Buffer. Subsequently, another 1 ml lysis buffer was added up to a final volume of 2 ml and then incubated for approximately 30 seconds to one minute. The following addition of CM stopped the lysis and the cells were centrifuged again and then resuspended in CM at the desired concentration.

2.2.3 Cell purification using automated magnetic cell sorting (autoMACS®)

2.2.3.1 Principle

Magnetic cell separation can be used to separate individual cell populations in high purity from a cell mixture. For this purpose, the desired cells are coupled with superparamagnetic nano-sized beads (MACS® MicroBeads) indirectly via specific antibody binding. Then, the cell suspension is passed over a separation column filled with

steel beads and applied to a high magnetic field within the autoMACS® pro separator. The resulting high magnetic gradient retains the MicroBead-labeled cells in the column, while the negative fraction passes through and is collected. Subsequent elution of the column outside the magnetic field collects the positive fraction separately. Marking the desired cell population with the MACS® MicroBeads is called positive selection. In contrast, all unwanted cells can be marked with MACS® MicroBeads, which leads to a so-called depletion in which the desired cell population remains untouched.

2.2.3.2 Isolation of splenic $CD8^+$ T cells

The *$CD8a^+$ T cell Isolation Kit, mouse* from Miltenyi (Bergisch Gladbach, DE) was used to purify $CD8^+$ T cells from spleen. Isolation was performed using the *autoMACS® Pro Separator* according to the manufacturer's protocol. Since this is a Kit for depletion of unwanted cells, the isolated $CD8^+$ T cells were untouched. The purity of isolated $CD8^+$ T cells was more than 95 %. These cells were then used for *in vivo* transfer prior CLP operation.

2.2.3.3 Isolation of splenic DCs

The *CD11c MicroBeads UltraPure mouse* Kit from Miltenyi (Bergisch Gladbach, DE) was used to purify splenic DCs (sDCs). Isolation was performed using the *autoMACS® Pro Separator* according to the manufacturer's protocol. For the last step, cells were collected in CM additionally containing 0.3 ng/ml GM-CSF. The cells were stained for MHC II, F4/80, CD11b, CD11c and purity of isolated $CD11c^+$ cells was more than 95 %.

2.2.4 Cultivation and stimulation of murine cells

2.2.4.1 Cultivation and stimulation of bone marrow-derived dendritic cells

Generation of BMDCs was performed with CM containing 15 ng / ml recombinant murine GM-CSF. After isolation, 10 ml of BMC in a concentration of 2×10^5 /ml were incubated eight days at 37°C and 5 % CO_2. Cells were fed on day three by adding 10 ml of fresh medium and on day six by replacing 10 ml of consumed medium with fresh medium.

Non-adherent BMDCs were harvested and counted on day eight. A FACS staining was done to test composition and maturational level of the BMDCs using antibodies for MHC II, CD11c, CD11b, CD115, CD40, and CD86 including appropriate isotype controls.
For overnight stimulation, 5×10^5 cells were seeded in a 96 well f-bottom plate and rested for 1 hour. If indicated, BMDCs were incubated with the metabolic inhibitors 2-DG (0.25 to 2 mM), oligomycin (0.005 to 0.25 µM) or DON (1 to 50 µM) for 30 min. Afterwards, BMDCs were stimulated with 100 ng / ml LPS, 5 µg / ml CpG or 1 µg / ml CpG for 18-20 hours at 37°C and 5 % CO_2. Supernatants were stored at −20°C for further analyses.

2.2.4.2 Cultivation and stimulation of bone marrow cells

After isolation, 5×10^5 BMC were seeded in 96-well f-bottom plates and rested for 1 hour at 37°C and 5 % CO_2. Then, depending on the experimental setup, different stimulating reagents were added. The cells were stimulated with 10 ng / ml Phorbol 12-Myristate 13-Acetate (PMA), Ionomycin (1 µg / ml) or purified CD3 and CD28 (both 1.25 µg/ml) antibody with the addition of the protein transport inhibitor Brefeldin A for five hours. Cytokine stimulation was performed with 20 ng / ml recombinant mIL-12 and 20 ng / ml recombinant mIL-18 combined with 10 ng / ml hIL-15 or 10 ng / ml IL-2 for 18 hours and afterwards Brefeldin A was added for another four hours. If indicated, BMCs were prestimulated with 0.5 µg/ml,1 µg/ml or 2 µg/ml P_3CSK_4 and incubated for 18-20 hours prior PMA/Ionomycin stimulation as described above. Afterwards, cells were gently resuspended and analyzed with an intracellular staining for IFNγ production by T cells (See 2.2.6.3).

2.2.4.3 Cultivation and stimulation of splenic DCs

After purification (See 2.2.3.3), 1×10^5 sDCs were seeded in CM+0.3 ng/ml GM-CSF in a 96-well u-bottom plate and incubated at 37°C and 5 % CO_2. After one hour, the cells were stimulated with 5 µg/ml CpG and incubated overnight for 18-20 hours at 37°C and 5 % CO_2. The next day, supernatants were removed and frozen at –20°C until quantification analysis with the Luminex technology (See 2.2.7.2) was performed.

2.2.5 Applications

Substances were administered to the mice by different application routes. In addition to intramuscular (i.m.) and subcutaneous (s.c.) application for anesthetics and painkiller, intraperitoneal (i.p.) and intravenous (i.v.) injection were used for the initialization of $CD8^+$ T cell transfer and depletion experiments.

2.2.5.1 Intravenous

Mice were under a heat lamp for 15-20 seconds and then placed in a fixation chamber in which the tail remains accessible on the outside and was held in place. The tail was disinfected with 70 % Ethanol. The application solution was then injected in a volume of 100 µl into the lateral tail veins. For this purpose, a syringe with 30-gauge needle was placed very flat over the vein and then pushed slightly under the skin so that the liquid was injected into the vein without strong back pressure.

2.2.5.2 Intraperitoneal

The liquid to be injected was drawn up into a syringe with a 30-gauge needle. The mouse was then fixated with one hand and held slightly hanging down on the outstretched arm so that the organs in the abdominal cavity slid down. The needle was then inserted through the fur and peritoneum within the lower third of the body and on the right or left side of the linea alba. To exclude injury and injection into an internal organ, the syringe plunger was pulled up slightly and should form a vacuum. Subsequently, a volume of 100 µl was injected.

2.2.6 Flow cytometry

Measurement was done with a BD FACSCanto™ II or a CytoFLEX from Beckman Coulter.

2.2.6.1 Principle

Flow cytometry is a powerful and commonly used tool in immunology. Cells or beads passing in a stream are detected and counted by a laser beam [157]. A flow cytometer capable of separating different cell populations is called a fluorescence-activated cell

sorter (FACS). Forward scattering (FSC) and side scattering (SSC) are used to distinguish particles roughly based on their size (Forward) and cell granularity (Side). Cells are stained with fluorescent conjugated antibodies for further differentiation. Fluorogenic dyes used in this study were fluorescein isothyocyanate (FITC), Peridinin chlorophyll protein-Cyanine5.5 (PerCP-Cy5.5), phycoerythrin (PE), allophycocyanin (APC), the PE-Cy7 and APC-Cy7 tandem conjugate systems, APC/Fire™ 750, APC-eFluor™ 780, pacific blue (PB), Brilliant Violet™ 421 (BV421), Brilliant Violet™ 510 (BV510), and Alexa Fluor™ 700 (AF700).

2.2.6.2 Surface molecule staining

Desired cell suspension was transferred to a 96-well u-bottom plate. One million cells in a volume of 150-200 µl were used per staining. The plate was then centrifuged at 300 g and 4°C for 6 minutes, the supernatant discarded, and the cells incubated in 50 µl Mouse Immunoglobulin G (IgG) block buffer at 4°C for 6 minutes. Then 50 µl Cellwash® was incubated with desired antibodies for 12 minutes in refrigerator. This was followed by a wash step with Cellwash®. Finally, samples were resuspended in 150 µl Cellwash®, transferred to FACS tubes and stored in the dark and on ice until measured on the cytometer. If the cells were not freshly isolated but cultured, the block buffer step was skipped and 100 µl Cellwash® containing antibodies was added directly to the cells.

2.2.6.3 Intracellular staining (IFNγ)

At the beginning of intracellular staining, the surface molecules were stained as described above. However, instead of resuspending the cells in Cellwash® as the final step, 150 µl Cytofix/Cytoperm® was added here. Thereby, paraformaldehyde fixes the surface staining and saponin permeabilizes the cell membranes. After 20 minutes at room temperature in the dark, the permeabilization buffer Permwash®, which contains saponin, was added and the cells were centrifuged (300 g, 4°C). Afterwards, cells were incubated for 15 minutes at 4°C with antibodies for IFNγ or the appropriate isotype control in Permwash® buffer. After a last washing step, cells were resuspended in 100 µl Cellwash® and analyzed by flow cytometry.

2.2.6.4 Measurement of 2-NBDG uptake

$5*10^5$ BMDCs were transferred to a 96-well f-bottom cell culture plate and centrifuged at 300 g for 6 minutes. To wash out the CM, cells were then resuspended in 200 µl Cellwash® and centrifuged again. The cells were resuspended in 100 µl glucose-free medium (Gibco™, Thermo Fisher Scientific, Dreieich, DE) and were starved for 25 minutes at 37°C and 5 % CO_2. Then 200 µM 2-NBDG in glucose-free medium was added and incubated for another 20 minutes at 37°C and 5 % CO_2. This was followed by two washing steps with Cellwash® in a precooled centrifuge at 4°C. After the second washing step, cells were resuspended in 100 µl Cellwash® containing antibodies for MHC II, CD11c, CD11b, Glut1 as well as a fixable viability dye (FvD) and then incubated for 15 minutes at 4°C. After a last washing step, cells were then resuspended in Cellwash®, transferred to 5 ml FACS tubes and measured at the cytometer.

2.2.7 Quantification of (soluble) molecules or RNA expression

2.2.7.1 Enzyme-linked Immunosorbent Assay (ELISA)

So-called sandwich ELISAs were used to detect different mediators in cell culture supernatants and sera. First, the capture antibody was coated onto a 96-well microtiter plate. The sample was added and the desired protein bound to the antibody and remained immobilized on the plate. A detection antibody bound another epitope of the protein and was additionally coupled with a biotin. Streptavidin, which was coupled with a horseradish peroxidase, bound to the biotin in the next step. The horseradish peroxidase can oxidize tetramethylbenzidine (TMB) into a blue dye after the addition of H_2O_2. The reaction was stopped by the addition of 1 M H_2SO_4. This formed a stable yellow color complex that was quantified using a photometer. A standard series allowed the calculation of the respective antigen quantity via the OD values.

2.2.7.2 Luminex

The Luminex-technology was used for quantitative determination of a wide variety of molecules within cell culture supernatants of sDCs stimulated overnight with CpG (See 2.2.4.3). The principle of this measurement is based on the addition of beads, which can

be loaded with different detection reagents and individually identified by labeling with different fluorescent dyes in the Luminex. This allows the simultaneous detection of up to 100 different molecules within one sample.
The bead-based test using the MAGPIX® Luminex analysis system was performed by Mechthild Hemmler-Roloff who is part of the group headed by Prof. Dr. rer. nat. Astrid M. Westendorf (Infection Immunology, Essen University Hospital).

2.2.7.3 RNA analyses

The relative expression of messenger ribonucleic acid (mRNA) in cells can be determined by quantitative real-time polymerase chain reaction (PCR). The principle of this method is based on the amplification of nucleic acids within a specific frame limited by short single-stranded start molecules (primers). Real-time PCR additionally allows simultaneous quantification of the amplification via fluorescence measurement. Thereby, the expression of β-actin is used to normalize the levels.
RNA purification was performed using the RNeasy Mini Kit from Qiagen (Venlo, Netherlands) and according to the manufacturer's instructions. RNA was required for two different analyses during this study. If the cells had not previously been frozen in lysis buffer, this was added to the frozen cell pellet already in the –80° freezer. Sample by sample was brought directly to room temperature to prevent subsequent degradation of the samples. This was especially important for the RNA array (b).

a) Samples isolated from BMDC of 4 d CLPs were used to analyze metabolic expression patterns via real-time PCR. Therefore, concentration and purity of the RNA was measured with a Nanodrop 100 (Peqlab / VWR International, Darmstadt, DE). To perform the real-time PCR, the samples were sent to Thekla Kemper who is part of the group headed by Prof. Dr. rer. nat. Mengji Lu (Institute for Virology, Essen University Hospital).

b) Samples from BMC, which were isolated from a 24 h CLP transfer experiment, were used to analyze the influence of TLR2ko $CD8^+$ T cells on the RNA expression pattern in the bone marrow. For a comprehensive analysis by transcriptome

profiling, the *Clariom™ S Assay, mouse* (Thermo Fisher Scientific, Dreieich, DE) was performed in the BioChip Laboratory (Institute of Cell Biology, Essen University Hospital). In this case, the purity of the RNA samples was of particular importance, which was measured in the BioChip Laboratory before further processing.

2.2.7.4 Seahorse

Seahorse XF Analyzers were used to measure the oxygen consumption rate (OCR) and extracellular acidification rate (ECAR) of BMDCs from CLP operated animals. This allowed assessment of mitochondrial respiration (OCR) and glycolysis (ECAR) within living cells. In this work, the XF Cell Mito Stress Test was used. Therefore, cells were seeded on pretreated Seahorse Bioanalyzer XFe24 culture plates and were prepared for the assay. Within the assay, the basal rate of OCR and ECAR was measured first. Afterwards, metabolic pathway inhibitors were added to analyze specific metabolic capacities. First, Oligomycin was added, which inhibits the ATP Synthase (complex V), resulting in a reduction in mitochondrial respiration. Next, Carbonyl cyanide-4 (trifluoromethoxy) phenylhydrazone (FCCP) collapses the proton gradient and thereby disrupts the mitochondrial membrane potential. As a result, electron flow through the electron transport chain is uninhibited, and oxygen consumption by complex IV reached its maximum. Then a combination of Rotenone and Antimycin A was added, which inhibits complex I and III. This combination shuts down mitochondrial respiration. Any subsequent energy production occurs independently of mitochondrial respiration. The seahorse assay and analysis were performed by Dr. rer. nat. Andrea Engler from the Clinic for Anesthesiology and Intensive Care (Essen University Hospital).

2.2.8 Computational analysis and statistics

The *BD FACSDiva Software (BD Biosciences)* and *CytExpert software (Version 2.3.1.22 / Beckman Coulter)* were used to process samples at the respective flow cytometer. The received data was analyzed using *NovoExpress® (Version 1.2.4 /* ACEA Biosciences*)* from ACEA Biosciences. Organization of data was performed using *Microsoft® Excel® (Version 2008)*. Visualization and statistical analysis were performed with *GraphPad*

Prism (Version 5.0.1 and Version 8.0.1*).* The results are presented as median with interquartile range, individual values with median and interquartile range, or as mean with standard deviation, noted accordingly below the respective figure. Differences between groups of multiple experiments were examined using the unpaired and non-parametric *Mann-Whitney U*-test. A comparison of two groups from the same experiment with technical replicates was performed using an unpaired *t*-test. To examine correlations, the *Spearman rank correlation* test was performed. A p-value of ≤ 0.05 was considered statistically significant.

3. Results

All experiments were done using the CLP model known to mimic sepsis in mice. It was used in a mild form to study the causes and effects of post-septic immunosuppression.
As this model is very sensitive to various factors like the amount of released intestinal contents or the length of the ligated appendix, the course of disease was monitored using various sepsis-associated clinical parameters (Figure 7). Sepsis led to a significantly increased weight loss 24 hours after the operation and started to stagnate only late into the disease course (Figure 7A). Further, there was a change in the composition of white blood cells (WBC) four days after CLP (Figure 7B). While lymphocytes were drastically decreased to half, granulocytes doubled their cell number per µl blood. Monocytes also decreased after CLP, but due to their comparatively low cell count, their proportion within all WBC was always about 6 %. The sham animals had small changes in these parameters due to the performed laparotomy. In addition to the short weight loss after one and two days, this manifested in a slightly changed WBC composition compared to naïve animals four days after sepsis, which was significant for the increase in granulocyte number.

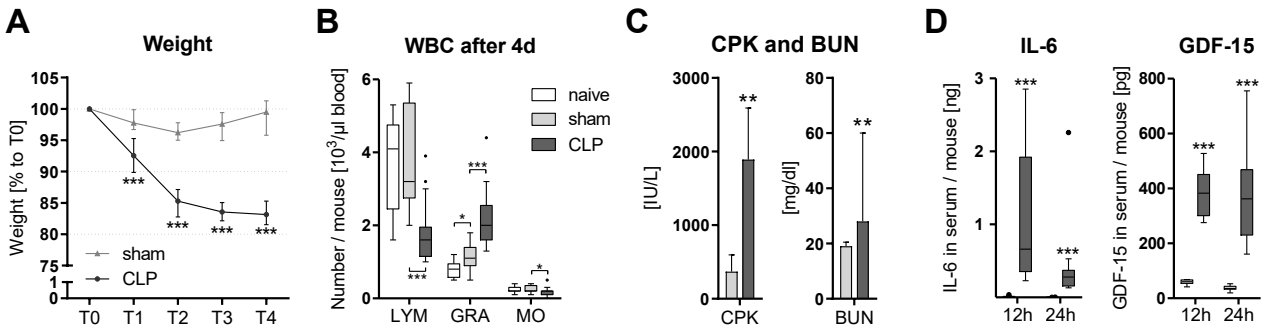

Figure 7 Evaluation of sepsis model based on various clinical parameters. Sepsis was induced in BALB/c wild-type mice. The mice were weighed daily and blood samples were taken after 12 h, 24 h, or 4 d CLP. The weight curve is shown as line chart of n = 12 mice per group (A). Further, the number of white blood cells (WBC) in whole blood samples four days after sepsis of n = 13-17 mice per group was calculated (B). These were separated into lymphocytes (LYM), granulocytes (GRA), and monocytes (MO). Serum was tested for creatine phosphokinase (CPK) and blood urea nitrogen (BUN) (C; n = 13-14 mice/group) as well as IL-6 (n = 10-15 mice/group) and GDF-15 (D; n = 7-14 mice/group) 12 or 24 hours after sepsis. A non-parametric *Mann-Whitney U*-test was performed for statistical analysis. Significant results are indicated as $p \leq 0.05$ (*), $p \leq 0.01$ (**) and $p \leq 0.001$ (***).

Serum samples were taken after 12 h and 24 h CLP. Hereby, creatine phosphokinase (CPK) and blood urea nitrogen (BUN) were up-regulated after CLP (Figure 7C). Among other things, these parameters indicate organ damage to kidney and muscle cells and are used to monitor the severity of various infectious diseases. In addition, an increased production of the pro-inflammatory mediators IL-6 and GDF-15 was measured (Figure 7D^{+}E). In the case of IL-6, a drop in production was detected after 24 hours, while GDF-15 was continuously increased up to 24 hours after sepsis.

3.1 Sepsis influences dendritic cell differentiation

It is known that sepsis causes an altered differentiation of DCs, which was described to play a major role in post-septic immunosuppression [64,168]. To examine this effect on DCs, the cDC population in the spleen (Figure 8) and the preDCs in the bone marrow (Figure 9) were examined over a period of up to four days after CLP.

3.1.1 Decreased numbers of cDC and the loss of CD4^{+} cDC after CLP

Generally, cDCs express MHC class II and high levels of CD11c (Figure 8A). Subdivision was done via gating for CD8, CD4 and CD11b. First, cDC1 (CD8^{+} CD11b^{-}) and cDC2 (CD8^{-} CD11b^{+}) were separated, whereas cDC1 equal CD8^{+} (CD4^{-}) cDCs. Second, cDC2 were further gated for CD4 expression distinguishing CD4^{+} cDCs and double negative (dN, CD4^{-} CD8^{-}) cDCs. The dot plots depict the decrease of the CD4^{+} cDC subtype of cDC2 from 85 % in sham to only 32 % in CLP.

Generally, the amount of cDC was continuously reducing during the measured period after sepsis (Figure 8A). A short-term increase in cDC number was observed in sham 24 hours after operation, but this dropped to about base level three days later. Thus, the normalization of the data to the sham median of the respective time point revealed a significant difference in cDC count between sham and CLP 24 hours after sepsis. This covered a reduction to initially 34 % and up to 22 % after 4 d CLP. Subdivision into CD4^{+}, CD8^{+}, and dN cDC revealed the specific loss of CD4^{+} cDCs and a significant decrease of CD8^{+} cDCs (Figure 8C). In sham operated mice, the initial rise in cDCs was about equal in all subpopulations. Thus, sepsis caused a dramatic loss of cDCs due to the loss of

CD4⁺ cDCs and reduction of CD8⁺ cDCs. The population of dN cDCs, however, remained almost unchanged.

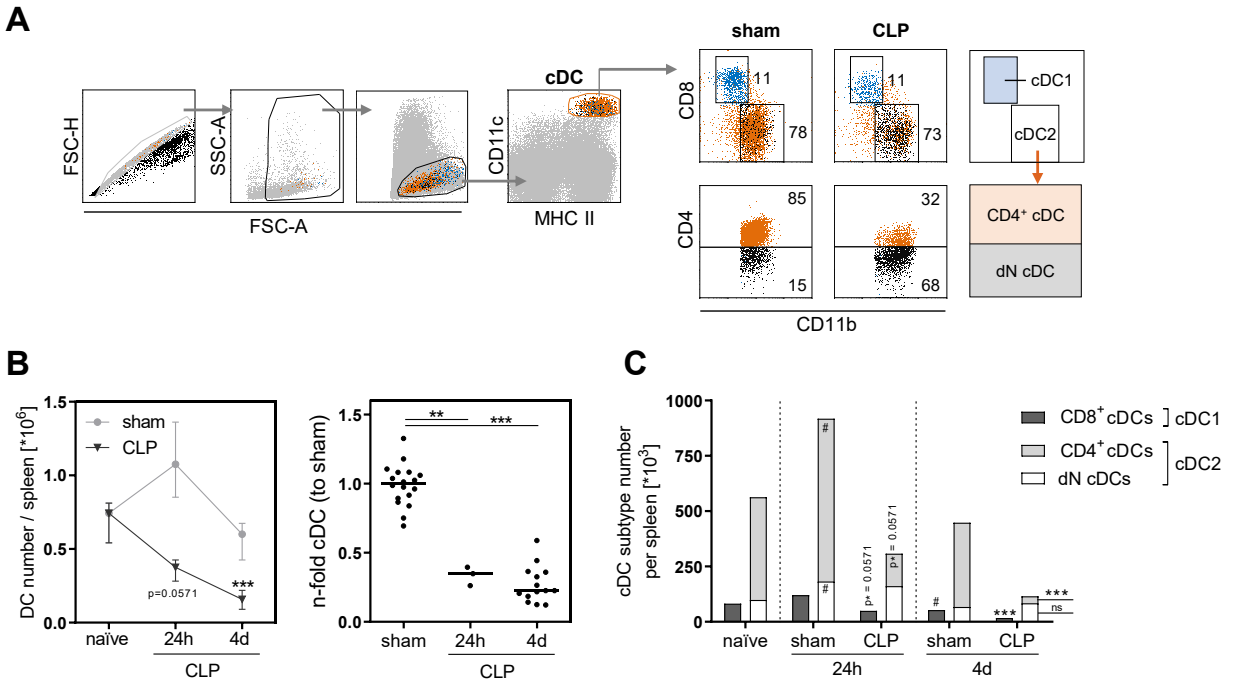

Figure 8 Numeric decrease of cDC and the loss of CD4⁺ cDCs after CLP over time. Sepsis was induced in wild-type mice and spleen cells were isolated at the indicated time points after CLP or sham surgery. The cDCs were analyzed by flow cytometry according to the given gating strategy (A). The identification of cDC was done via gating for CD11c^{hi} MHC II⁺ cells. The cDC subtypes are characterized as cDC1 / CD8⁺ cDC (CD8⁺ CD4⁻ CD11b⁻) and cDC2 separated into CD4⁺ cDC (CD4⁺ CD8⁻ CD11b⁺) and double negative cDC (dN cDC; CD8⁻ CD4⁻ CD11b⁺). Sham and CLP labeled dot plots shows exemplary data of 4 d CLPs, numbers indicate the percentage share. The progressive influence on the cDC population over time is shown as absolute numbers (B left) and normalized to the respective sham operation (B right). The distribution of cDC subtypes is visualized as a bar chart of CD8⁺ cDC and stacked CD4⁺ cDC and dN cDC for the indicated time points (C). The data is shown as the median, partly with interquartile range (B left), of n=3-4 (naïve, 24 h) or n=10-14 (4 d) mice per group. Non-parametric *Mann-Whitney U*-test was performed for statistical analysis. Significant results are indicated as p ≤ 0.05 (*, #), p ≤ 0.01 (**, # #) and p ≤ 0.001 (***, # # #). Unless stated otherwise, the asterisk (*) compares CLP with the corresponding time point of the sham operation and the number sign (#) compares the respective dataset with the naïve condition.

3.1.2 Numerical decrease and redistribution of preDC after CLP

The persistent alteration of cDC subset composition might be caused by changes in their production in the bone marrow. Thus, preDC were analyzed regarding their number and subset composition. The separation for preDCs in the bone marrow was done via the marker expression pattern of CD11c⁺ MHC II⁻ B220⁻ CD11b⁻ CD135⁺ (Figure 9A). It is known that preDCs are primed for distinct DC subsets which can be distinguished by surface marker expression of Siglec-H and Ly6c [196]. Ly6c⁻ Siglec-H⁺ preDCs still have

the potential to differentiate into pDCs (termed pDC-primed) while Ly6c$^+$ Siglec-H$^+$ preDCs (termed dP preDC) are found to mostly differentiate into cDCs. Siglec-H$^-$ preDCs are predominated to differentiate into cDC1 (Ly6c$^-$, termed preDC1) or cDC2 (Ly6c$^+$, termed preDC2).

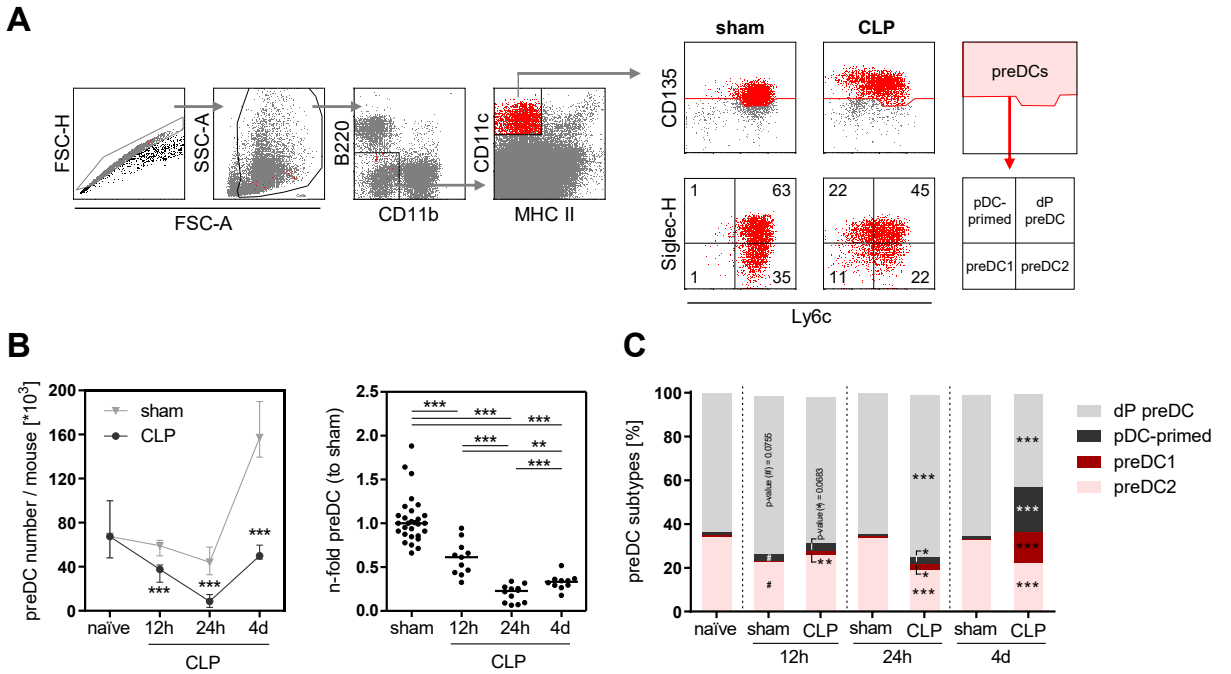

Figure 9 Numerical decrease and redistribution of preDC after CLP over time Sepsis was induced in wild-type mice and bone marrow cells were isolated at the indicated time points after CLP or sham surgery. PreDC were analyzed by flow cytometry according to the given gating strategy (A). PreDC are characterized as CD11c$^+$ CD135$^+$ B220$^-$ CD11b$^-$ MHCII$^-$ cells. The separation into subpopulations was done into double-positive preDC (dP preDC; Ly6c$^+$ Siglec-H$^+$), pDC-primed preDC (pDC-primed; Ly6c$^-$ Siglec-H$^+$), preDC1 (Ly6c$^-$ Siglec-H$^-$) and preDC2 (Ly6c$^+$ Siglec-H$^-$). Sham and CLP labeled dot plots shows exemplary data of 4 d CLPs, numbers in the quadrants indicate the percentage share. The progressive influence on the preDC population over time is shown as absolute numbers (B left) and normalized to the respective sham operation (B right). The distribution of preDC subtypes is visualized as a stacked bar chart for the indicated time points (C). The data is shown as the median, partly with interquartile range (B left), of n = 4 (naïve) or n = 7-14 mice per group. Non-parametric *Mann-Whitney U*-test was performed for statistical analysis. Significant results are indicated as $p \leq 0.05$ (*, #), $p \leq 0.01$ (**, # #) and $p \leq 0.001$ (***, # # #). Unless stated otherwise, the asterisk (*) compares CLP with the corresponding time point of the sham operation and the number sign (#) compares the respective dataset with the naïve condition.

The effect in the preDC population in the bone marrow was likely to be visible earlier than in the cDCs in the spleen. Thus, the analysis of the number and composition of preDCs was additionally performed 12 hours after sepsis. The number of preDC in the bone marrow significantly decreased from about 67 × 10^3 in naïve mice to a minimum of 8.7 × 10^3 cells 24 hours after CLP (Figure 9B). The population recovered in numbers but

was still significantly reduced to 37 % compared to the respective sham operated mice. The composition of preDC subsets in sham mice differed 12 hours after operation as there was an increased proportion of dP preDCs and a significant shift to more pDC-primed and less preDC2 (Figure 9C). However, this stabilized 24 hours after operation and remained unchanged up to four days later. The situation was different for CLP operated animals. First, a similar loss of preDC2 and increase of dP preDC was observed 12 hours after CLP. However, pDC-primed and preDC1 significantly increased in CLP compared to sham. In the further progression, the amount of preDC2 significantly reduced 24 hours after CLP. This shifted the proportional distribution further towards the differentially unpredicted dP preDCs. Another three days later, the dP preDCs were 0.42-fold reduced which contrasted with a significant increase of the preDC1 and pDC-primed population. The amount of preDC2 was still reduced compared to sham.

In general, the sepsis-induced loss of preDCs might be initially caused by the increased loss of preDC2, whereas the slow numerical regeneration of preDCs resulted in increased generation of Ly6c$^-$ preDCs, namely pDC-primed and preDC1.

3.2 Accumulation of T cells in the bone marrow after sepsis

The preDC data suggested an early sepsis-induced effect on the progenitor cells in the bone marrow. Therefore, the bone marrow was analyzed for other cell populations that might influence the progenitor cells directly or via modulating the environment in the bone marrow. For this purpose, T cells were characterized using flow cytometry according to the given gating strategies (Figure 10). First, T cells were separated for CD4$^+$ and CD8$^+$ T cells and their respective activation was analyzed by gating for CD69$^+$ expression (Figure 10A). Results regarding this analysis can be found in the next section. Further, T cells were subdivided via CD44, CD62L and CD122 expression (Figure 10B). This allowed the separation into T_N (CD44$^-$ CD62L$^+$), $T_{E/EM}$ (CD44$^+$ CD62L$^-$), T_{CM} (CD44$^+$ CD62L$^+$ CD122$^-$), and T_{VM} (CD44$^+$ CD62L$^+$ CD122$^+$). Results regarding CD8$^+$ T cell composition and their specific activation can be found in section 3.2.2 on page 46.

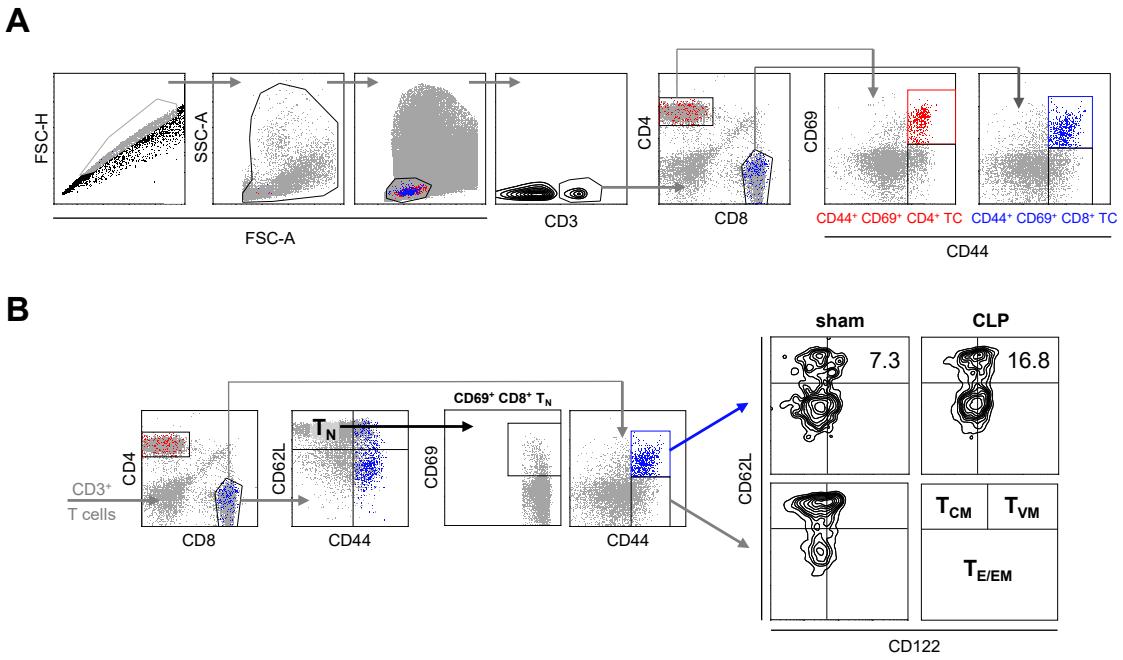

Figure 10 Gating strategy for T cells, CD8⁺ T cell subset composition and their activation. T cells were analyzed by flow cytometry according to the given gating strategies. T cells were separated for CD4⁺ T cells and CD8⁺ T cells (A). Their activation was investigated via CD69 expression on total T cell level as well as each individual T cell subset. The separation of T cell subtypes was done for the CD8⁺ T cell compartment (B). The study distinguishes between naïve (T_N ; CD62L⁺ CD44⁻), effector/effector memory ($T_{E/EM}$; CD62L⁻ CD44⁺), central memory (T_{CM} ; CD62L⁺ CD44⁺ CD122⁻) and virtual memory (T_{VM} ; CD62L⁺ CD44⁺ CD122⁺) CD8⁺ T cells. The upper gating strategy is used for the data described in Figure 11 and the lower one for the data described in Figure 12.

3.2.1 T cell number and activation in spleen and bone marrow over time

The number and activation of T cells was analyzed after CLP compared to sham surgery over a time course of four days. In this regard, bone marrow and spleen cells decreased over time (Figure 11A) – from an initial average of about 100 × 10^6 (spleen) or 60 × 10^6 (bone marrow) cells to a minimum of 86 × 10^6 and 30 × 10^6 cells respectively. While the number continuously decreased in the spleen, the minimum of bone marrow cells was reached as early as 24 hours after sepsis and started to increase three days later.

After sham operation, CD4⁺ T cells were almost unchanged and CD8⁺ T cells just slightly increased at early time points in the spleen (Figure 11B). In contrast, sepsis induced a continuous loss of especially CD4⁺ but also CD8⁺ T cells. A different picture was visible in the bone marrow, which was similar between CD4⁺ and CD8⁺ T cells. The sham operation led to an increase in T cells in the beginning but returned to lower levels over time. This was not observed after CLP, instead, the cell number continuously increased to a T cell

maximum after 24 hours. With the last measurement on day four, the T cell number reached a low point below base level.

Because of the effect on T cell number in the early time points after sham operation, the cell numbers were normalized to the sham level of the respective experiments (Figure 11C). This nicely showed the quite similar increase of $CD4^+$ as well as $CD8^+$ T cells spiking at 24 hours after sepsis. Looking on the respective numbers of activated effector and memory T cells, meaning the $CD69^+$ expression on $CD44^+$ T cells, first differences were spotted between $CD4^+$ and $CD8^+$ T cells (Figure 11D). While there was only a slight 1.2-fold increase of activated $CD4^+$ $CD44^+$ T cells 24 hours after sepsis, $CD8^+$ $CD44^+$ T cells had a fast increase of about 2.1-fold as early as 12 hours and still visible 24 hours after CLP.

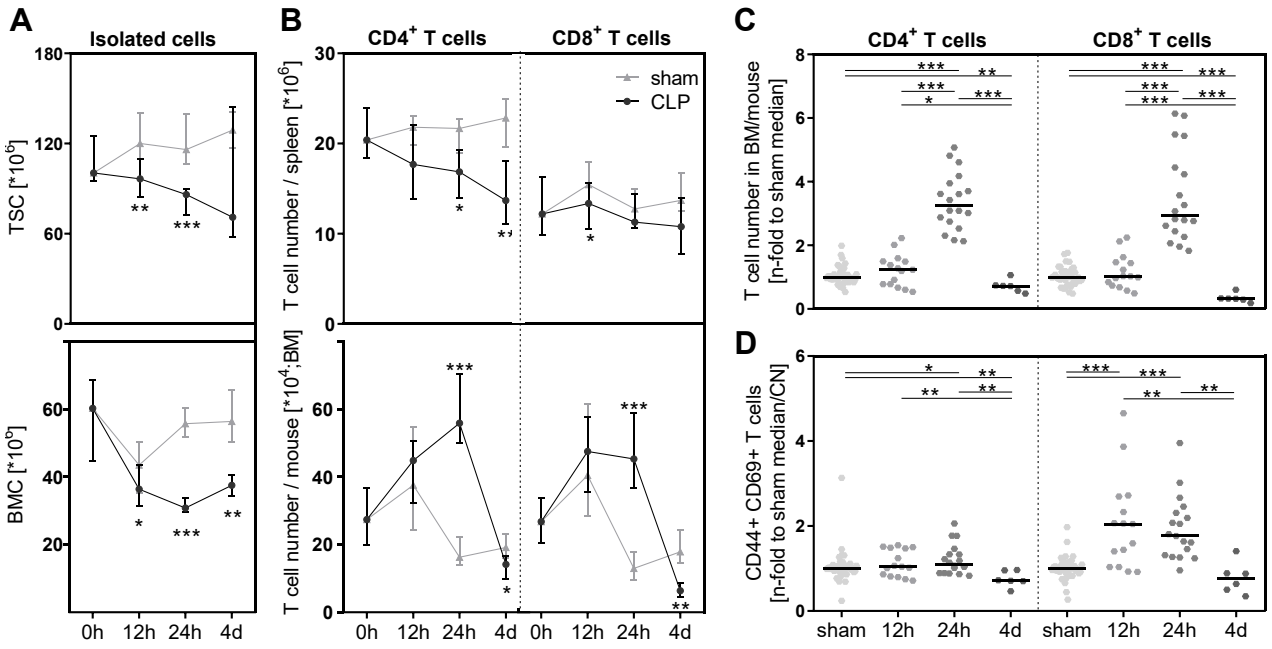

Figure 11 T cell number and their activation over time in spleen and bone marrow after CLP. Sepsis was induced in wild-type mice and bone marrow cells (BMC) as well as total spleen cells (TSC) were isolated at the indicated time points after CLP or sham surgery. The influence of sham or CLP operation on isolated BMC or TSC (A) and the number of $CD4^+$ and $CD8^+$ T cells (B) is shown as line charts with interquartile range of n = 7-15 (TSC) or n = 10-16 (BMC) mice per group. To consider the influence of the sham operation, especially at early time points, the number of $CD4^+$ and $CD8^+$ T cells (C) and the activation level of $CD44^+$ effector and memory T cells by CD69 expression (D) in the bone marrow (BM) was normalized to the respective sham operation. Non-parametric *Mann-Whitney U*-test was performed for statistical analysis. Significant results are indicated as $p \leq 0.05$ (*), $p \leq 0.01$ (**) and $p \leq 0.001$ (***).

In summary, a decrease of cell number was observed in both organs, while there was an accumulation of activated T cells in the bone marrow with a peak 24 hours after CLP in contrast to sepsis-induced continuous T cell loss in the spleen. Further, $CD8^+$ T cells were more prominently activated than $CD4^+$ T cells starting as early as 12 hours after sepsis induction. Thus, the following T cell analysis focused on $CD8^+$ T cells.

3.2.2 $CD8^+$ T cell subset composition and their activation

As described above, the comparatively high increase in T cell number with a still high activation level was present 24 hours after CLP. Therefore, $CD8^+$ T cells were examined in more detail regarding their subpopulations and activity after a 24 h CLP.

The number of T_N increased by a multiple after CLP in wild-type mice (Figure 12A). In addition, T_{CM} nearly tripled while T_{VM} had an about 4-fold increase. The number of $T_{E/EM}$ did not change. Looking on the activation of the T cell subsets (Figure 12B), again, no difference was found for $T_{E/EM}$. However, their general activation level was highest between all T cell subsets. In relation to this, the increase in activated naïve cells, even if significant, was negligible. Besides the increasing tendency of activated T_{CM}, particularly outstanding was the sepsis-induced 1.3-fold higher activation of T_{VM}.

The investigated time point after sepsis was relatively short for antigen-dependent T cell activation. However, the selectively activated T_{VM} are known to have the ability to get activated very quickly by innate cytokines. This process is termed bystander activation. To investigate the possibility of bystander activation, $CD8^+$ T cells isolated from DO11.10 mice were intravenously transferred into BALB/c-CD45.1 mice prior operation. Afterwards, the activation of T_{VM} was measured (Figure 12D). DO11.10 mice have an altered T cell receptor, so they require ovalbumin (ova)-peptide for successful antigen-dependent T cell activation. In this experiment no ova-peptide was provided as well as this requirement is only true for $CD4^+$ but not $CD8^+$ T cells. Despite the lack of ova as the cognate antigen of DO11.10 for antigen-dependent activation, the $CD8^+$ T_{VM} had sepsis-induced increased activation from 4 % to 17 %, which indicated antigen-independent bystander activation of these cells.

Following this, the question arose as to the mechanism by which T cell activation might occur. One possible signaling pathway is TLR2, as besides other cytokines and

molecules, a lot of TLR2 ligands are known to circulate after sepsis. This pathway is additionally interesting, since a reduced susceptibility to secondary infections after sepsis in TLR2ko mice is known. For this purpose, TLR2ko mice were subjected to the same operation and $CD8^+$ T cells were subsequently characterized. The number of T_N, T_{CM} and T_{VM} but not $T_{E/EM}$ increased in a comparable manner to the wild-type (D). Further, increased T cell activation was visible in the same subsets, even significant for T_{CM}. Summarizing, a specific accumulation of T_N, T_{CM} and T_{VM} in the bone marrow after sepsis was found. T_{VM} were specifically activated, which was identified as bystander activation of these cells. In addition, $CD8^+$ T cells from wild-type and TLR2ko animals behaved in the same way regarding their accumulation and activation.

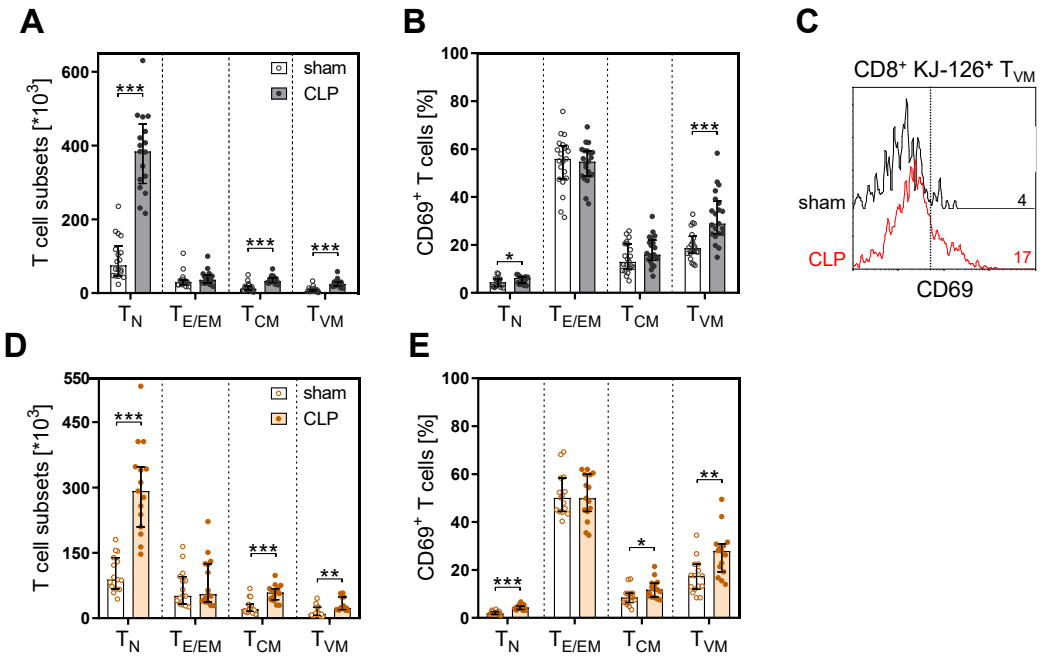

Figure 12 Composition and activation of $CD8^+$ T cells in wild-type and TLR2ko mice 24 hours after CLP. Sepsis was induced in wild-type or TLR2ko mice and BMC were isolated 24 hours later. Number (A) and activation (B) of wild-type as well as number (D) and activation (E) of TLR2ko $CD8^+$ T cell subsets are shown as median with interquartile range and individual values of n = 15-18 mice per group. T cells were separated into naïve (T_N), effector/effector memory ($T_{E/EM}$), central memory (T_{CM}) and virtual memory (T_{VM}) $CD8^+$ T cells. Significant results are indicated as $p \leq 0.05$ (*), $p \leq 0.01$ (**) and $p \leq 0.001$ (***). Further, $CD8^+$ T cells from DO11.10 mice were adoptively transferred in wild-type mice prior CLP operation to investigate their antigen-independent bystander activation. The result is shown with an exemplary histogram (C).

3.3 Altered cytokine secretion pattern of CD8⁺ T cells after sepsis

After a striking accumulation and activation of CD8⁺ T cells in the wild-type as well as TLR2ko mice was observed, the T cell functionality was subsequently addressed. For this purpose, the IFNγ production of CD8⁺ T cells was determined according to the given gating strategy (Figure 13A). Here, the comparison between wild-type sham and CLP revealed a loss of IFNγ production after sepsis. Measurement of the PD1 expression on CD8⁺ T cells excluded an effect induced by T cell exhaustion, because no increase but rather no changes or a decrease in expression after sepsis was visible. Therefore, the effect of decreased IFNγ production in the wild-type was further investigated after treatment with different stimulation reagents and compared with the functionality of TLR2ko CD8⁺ T cells (Figure 13B). In this regard, stimulation was performed either with PMA and Ionomycin for 5 hours, with CD3 and CD28 or with different mixed cytokine setups aiming to mimic bystander activation.

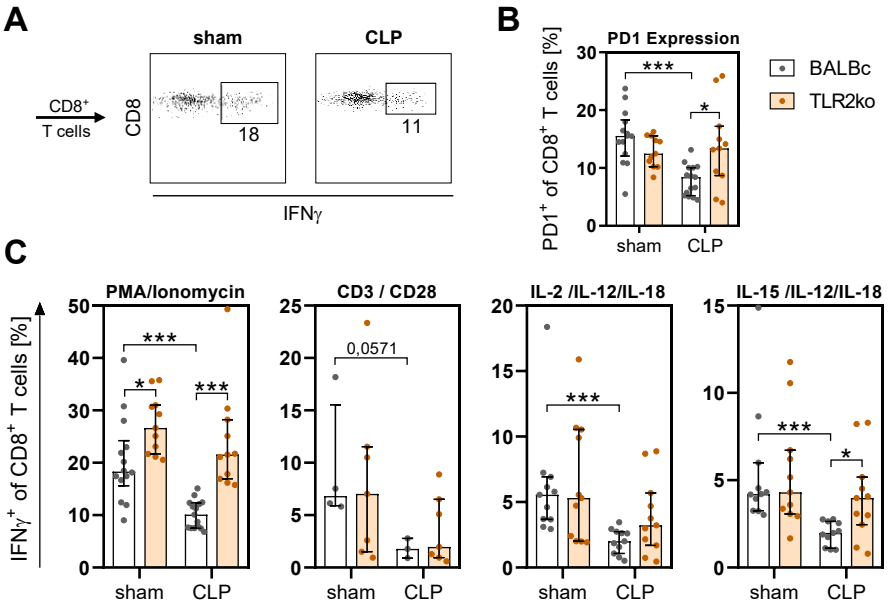

Figure 13 IFNγ production by CD8⁺ T cells in wild-type and TLR2ko mice 24 hours after CLP. Sepsis was induced in wild-type (WT; white) or TLR2ko (orange) mice and BMC were isolated 24 hours later. IFNγ production was measured by flow cytometry according to the given gating strategy (A). Sham and CLP labeled dot plots shows exemplary data after PMA/Ionomycin stimulation, numbers indicate the percentage share. PD1 expression of CD8⁺ T cells was used to monitor T cell exhaustion (B). IFNγ production of CD8⁺ T cells is shown as median with interquartile range and individual values of n = 11-15 mice per group (C). Stimulation was done with PMA and Ionomycin, CD3 and CD28 as well as with cytokines. Non-parametric *Mann-Whitney U*-test was performed for statistical analysis. Significant results are indicated as $p \leq 0.05$ (*), $p \leq 0.01$ (**) and $p \leq 0.001$ (***).

Indeed, the loss of IFNγ producing $CD8^+$ T cells in the wild-type was independent of the particular type of stimulation. However, the percentage loss was greater after stimulation with cytokines. While PMA/Ionomycin-induced IFNγ production dropped to 55 %, a significant decrease to 47 % ($IL\text{-}15^+$) and 36 % ($IL\text{-}2^+$) was observed after cytokine stimulation. Further, CD3/CD28-induced IFNγ production was 0.26-fold but only almost significantly reduced, which was probably due to the limited data available. This sepsis-induced decrease was not visible in TLR2ko $CD8^+$ T cells. Instead, the IFNγ production significantly increased compared to wild-type after stimulation with PMA and Ionomycin or the cytokine mix of IL-12, IL-18, and IL-15. Thus, the inhibition of IFNγ production in $CD8^+$ T cells after sepsis have to be TLR2-dependent.

To check whether this effect was caused by T cell independent effects in the TLR2ko animals or whether it was a T cell intrinsic effect, TLR2ko or wild-type $CD8^+$ T cells were transferred into a CD45.1-BALB/c wild-type animal prior CLP operation (Figure 14A). The loss of IFNγ producing $CD8^+$ T cells was visible in wild-type independent of their origin (endogenous or transferred T cells). In contrast, transferred TLR2ko $CD8^+$ T cells slightly increased in their IFNγ production. RNA from BMCs isolated after this transfer experiment was then subjected to an RNA array. Thereby, sepsis-induced IFNγ signaling increased bone marrow-wide after transfer of TLR2ko $CD8^+$ T cells compared to down-regulation after wild-type $CD8^+$ T cell transfer (Figure 14B). Thus, transfer of TLR2ko $CD8^+$ T cells resulted in increased IFNγ signaling in CLP animals which contrasted with the loss that occurred in wild-type. To investigate a general effect of regulation via TLR2, naïve $CD8^+$ T cells were stimulated with the TLR2 ligand P_3CSK_4 overnight followed by restimulation with PMA and ionomycin. Again, there was a moderate decrease of IFNγ producing $CD8^+$ T cells, which further decreased with higher concentration of P_3CSK_4.

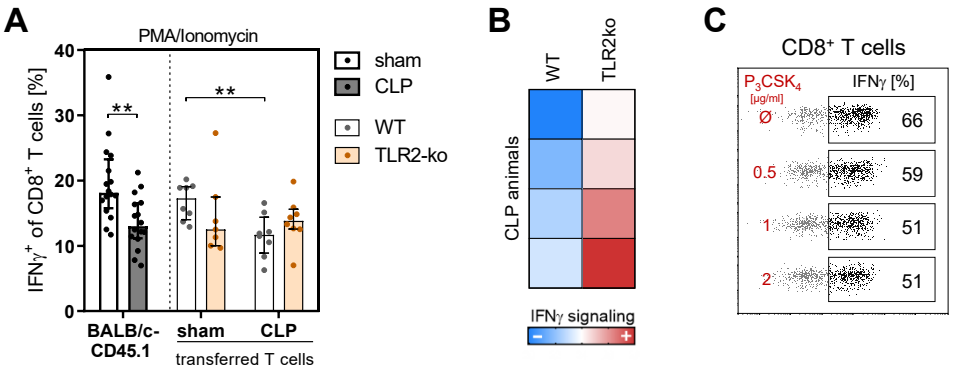

Figure 14 IFNγ is decreased in a TLR2-dependent T cell intrinsic manner after sepsis. IFNγ production after an adoptive transfer of TLR2ko (orange) or wild-type (WT; white) $CD8^+$ T cells into BALBc-CD45.1 wild-type mice was investigated to examine T cell extrinsic or intrinsic effects of TLR2 (A). The data of this experiment is shown as median with interquartile range and individual values of n = 16 (BALBc-CD45.1) or n = 7-8 (transferred T cells) mice per group. RNA isolated from BMC after wild-type or TLR2ko transfer was submitted to an RNA array (B). The results regarding the IFNγ signaling pathway analysis are summarized in a heatmap, whereas each square corresponds to an individual mouse with comparable low (blue) or high (red) IFNγ signaling values. Last, PMA/Ionomycin-induced IFNγ production of naïve BMCs was measured in response to overnight prestimulation with the TLR2 ligand P_3CSK_4 (C). This data is shown of one representative experiment, whereas red numbers indicate the amount of P_3CSK_4 in µg/ml and black numbers indicate the percentage share of $IFN\gamma^+$ $CD8^+$ T cells. Non-parametric *Mann-Whitney U*-test was performed for statistical analysis. Significant results are indicated as $p \leq 0.01$ (**) and $p \leq 0.001$ (***).

In summary, $CD8^+$ T cells from wild-type but not from TLR2ko mice had an impaired ability to produce IFNγ. This was also evident after transfer of $CD8^+$ T cells, which suggests a T cell intrinsic effect of TLR2 on IFNγ production after sepsis. This was generally confirmed for BMCs by mRNA pathway analysis. Prestimulation with P_3CSK_4 revealed a general effect of TLR2 on the regulation of IFNγ production by $CD8^+$ T cells. As the cytokine environment plays a crucial role in myeloid cell development, $CD8^+$ T cells might be a possible candidate to modulate the cytokine microenvironment in the bone marrow.

3.4 Impact of $CD8^+$ T cells on DC differentiation and functionality

Whether the different cytokine secretion pattern of $CD8^+$ T cells has an influence on DC differentiation were examined in the following experiments. Therefore, $CD8^+$ T cell depletion as well as transfer of $CD8^+$ T cells from TLR2ko mice was done. Subsequently, preDC and cDC as well as BMDCs generated in GM-CSF culture were analyzed four days after sepsis induction. According to the previous results, the increased production of IFNγ in TLR2ko $CD8^+$ T cells might counteract the loss of IFNγ predominant in wild-type. Application of the antibody induced a clear depletion of $CD8^+$ T cells in the spleen and

bone marrow compared to the isotype (Figure 23B, Annex page 97). Furthermore, results regarding clinical parameters did not notably differ between the depletion or transfer experiments and compared to normal CLP (data not shown).

3.4.1 Phenotype and function of DCs after CD8⁺ T cell transfer or depletion

The influence of CD8⁺ T cells on the parameters with respect to the cDC and preDC subsets[4] was analyzed. Thereby, the depletion of CD8⁺ T cells led to a decreasing trend in cDC cell count to about 85 % after CLP. However, there was no significant influence on cDC subset composition (Figure 15A⁺B). In contrast to the cDC, the preDC significantly decreased in their number from about 66 × 10^3 to 46 × 10^3 after CD8⁺ T cell depletion. The distribution among the different preDC subsets remained unaffected (Figure 15C⁺D). Transfer of CD8⁺ T cells from TLR2ko mice did not affect the cDC and preDC neither in their number nor in their composition (Figure 15 E-H). A general positive correlation of preDC cell number and DC number was found to be highly significant (Figure 15I).

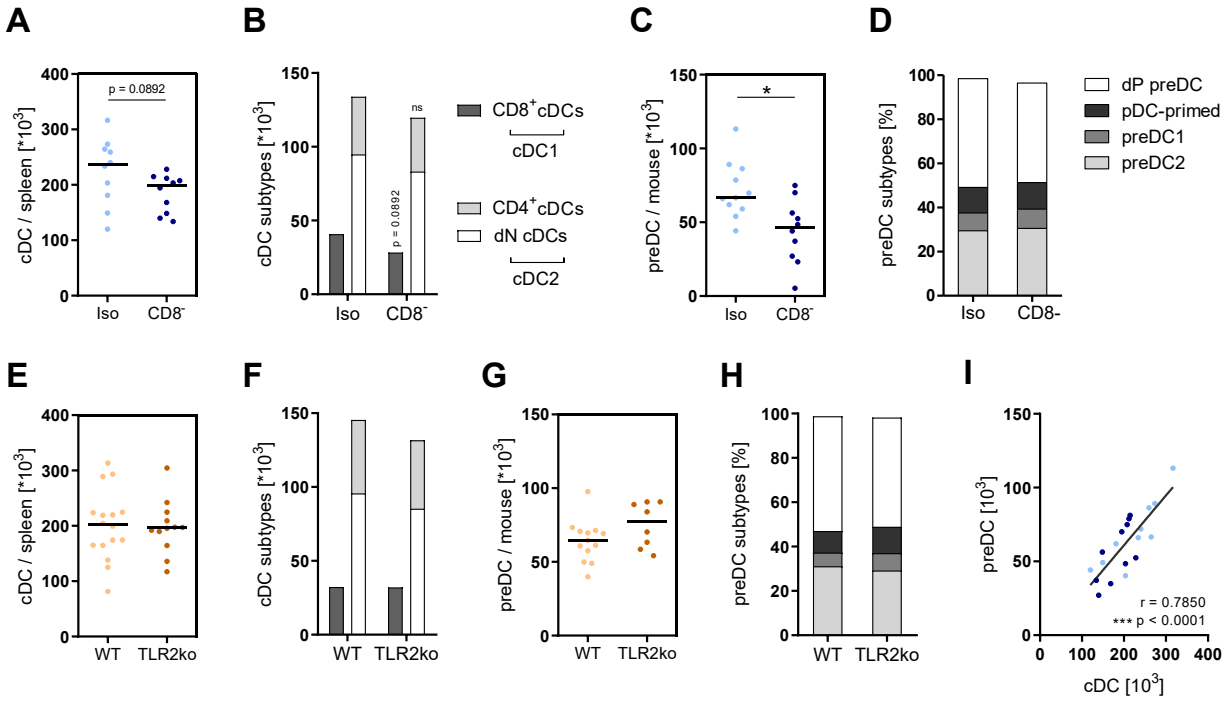

Figure 15 Influence of CD8⁺ T cell depletion or transfer on cDC and preDC after CLP. Sepsis was induced in wild-type mice after CD8⁺ T cell depletion or transfer. Total spleen cells or bone marrow cells were isolated after 4 d CLP or

[4] Described above in section 3.1.1 (p. 40) and 3.1.2 (p. 41)

sham surgery and cDC or preDC were analyzed by flow cytometry. Number (A, E) and composition (B, F) of cDC as well as number (C, G) and composition (D, H) of preDC is shown. In this regard, the upper part compares $CD8^+$ T cell depletion (blue) while the lower part compares $CD8^+$ T cell transfer from TLR2ko mice (orange) with the respective control CLPs. The data is shown as the median of n = 10-14 mice per group. In addition, the number of cDCs was plotted against the respective preDC number per mouse to detect a possible correlation of these values. For statistical analysis, the *Spearman rank correlation* test was performed. The resulting correlation coefficient r and p-value are noted on the diagram. Non-parametric *Mann-Whitney U*-test was performed for statistical analysis. Significant results are indicated as $p \leq 0.05$ (*).

In addition to the investigation of phenotypic influences, functional studies were performed. Therefore, sDCs were purified and stimulated overnight with CpG. Subsequently, the supernatant was analyzed for the production of various cytokines and chemokines using a Luminex assay. Thereby, CCL2 production was measured to be increased after transfer of TLR2ko $CD8^+$ T cells but significantly decreased after $CD8^+$ T cell depletion (Figure 16A). A similar regulation was observed for CCL22 (Figure 16B) and PAI-1 (Figure 16C), both even with a significant increase after the transfer of TLR2ko $CD8^+$ T cells.

In summary, the presence of T cells in the bone marrow influenced the number of preDCs. Further, the number of preDCs in the bone marrow was positively correlated with the number of DCs in the spleen. In addition, $CD8^+$ T cells had an influence on the function like cytokine and chemokine secretion of sDCs. Although the transfer of TLR2ko $CD8^+$ T cells had no influence on the number and composition of DCs, a functional influence was described.

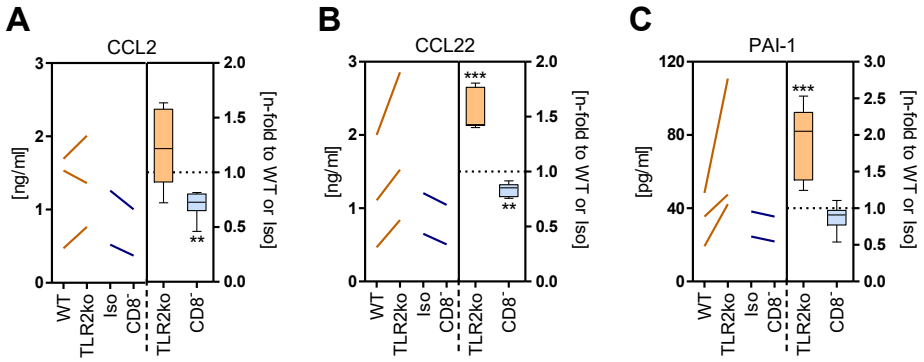

Figure 16 Influence of $CD8^+$ T cell depletion or transfer on functionality of sDCs after CLP. Sepsis was induced in wild-type mice after $CD8^+$ T cell depletion or transfer. Splenic DCs were isolated after a 4 d CLP and stimulated over night with CpG. Supernatants were then analyzed regarding different Cytokine and chemokine concentrations via Luminex. The influence of $CD8^+$ T cell transfer or depletion on the production of CCL2 (A), CCL22 (B), and PAI-1 (C) after sepsis was compared. The data is shown in absolute amounts and normalized to the respective control operation with tukey box plots of two to three experiments each. Non-parametric *Mann-Whitney U*-test was performed for statistical analysis. Significant results are indicated as $p \leq 0.05$ (*), $p \leq 0.01$ (**) and $p \leq 0.001$ (***).

3.4.2 The BMDC phenotype is not influenced by $CD8^+$ T cells

The generation and analysis of BMDCs was proven to be a good model to study immunosuppressive effects by DCs after sepsis [168]. Therefore, further investigations were performed with BMDC cultures. In the presence of GM-CSF hematopoietic precursor differentiate into a heterogeneous $CD11c^+$ MHC II^+ population, which can be separated into monocyte-derived macrophages and CDP-derived DCs [81]. In this study, the BMDCs were separated into these monocyte-derived BMDCs (mdDCs) with the expression pattern of MHC II^{int} $CD11c^+$ $CD11b^{hi}$ $CD115^+$ and cDC like BMDCs (termed cDC-like) with MHC II^{hi} $CD11c^+$ $CD11b^{int}$ $CD115^-$.

Although BMDC cultures were not further separated into their subpopulations for functional studies, a distinction was made between these subpopulations as described above for the assessment of the culture components using the given gating strategy (Figure 17A). Additionally, the state of maturation was analyzed by CD40 and CD86 expression on the BMDCs in general. In order to investigate any influence of $CD8^+$ T cell depletion or transfer on BMDC differentiation, the composition and maturation state of the cultures were compared after treatment. The remarkable sepsis-induced shift towards more mdDCs (about 80 %) compared to sham was largely unaffected by $CD8^+$ T cell depletion or transfer (Figure 17B). Further, the maturational state of BMDCs did not have a clear trend or were rather unaffected (Figure 17C^+D).

All in all, sepsis led to an increased proportion of mdDCs and less cDC-like BMDCs, which was not dependent on the availability of $CD8^+$ T cells or their suggested IFNγ production after transfer of TLR2ko $CD8^+$ T cells. Further, the maturational state of these cells was rather independent or unchanged by the experimental setups.

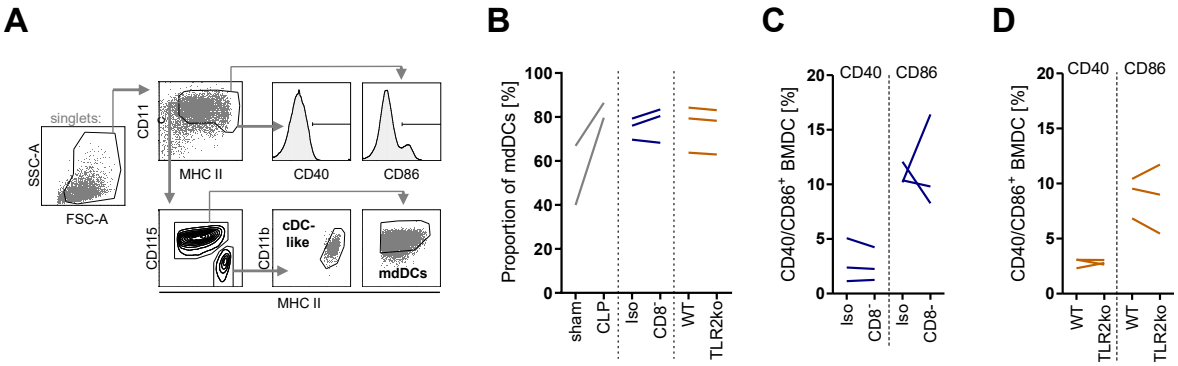

Figure 17 Composition and maturation of BMDC after CLP is independent of CD8⁺ T cells. Sepsis was induced in wild-type mice and BMC were isolated after a 4 d CLP or sham surgery. For $CD8^+$ T cell depletion or transfer group, anti-CD8β antibody ($CD8^-$) or HRPN as isotype control (Iso) was injected three days before operation or $CD8^+$ T cells from wild-type or TLR2ko mice were transferred intravenously directly prior CLP operation. Bone marrow-derived DCs (BMDCs) were generated in cell culture media including GM-CSF and analyzed via flow cytometry according to the given gating strategy (A). BMDCs were separated into MHC II^{int} $CD11c^+$ $CD11b^{hi}$ $CD115^+$ monocyte-derived DCs (mdDCs) and MHC II^{hi} $CD11c^+$ $CD11b^{int}$ $CD115^-$ CDP-derived DCs (cDC-like). The proportion of mdDCs (B) and the general maturation state of BMDCs examined by CD40 and CD86 expression after $CD8^+$ T cell depletion (C) or transfer (D) is shown as line charts whereas each line compares the groups of individual experiment.

3.4.3 Cytokine production of BMDC can be influenced by CD8⁺ T cells

Although $CD8^+$ T cells did not affect the general phenotype of BMDCs, an influence on the functionality was not unlikely. Thus, the cytokine production of BMDCs, which is a particularly important regulatory property of DCs, was investigated after $CD8^+$ T cell depletion or transfer. Besides the pro-inflammatory cytokines TNFα and the active heterodimer IL-12p70, the anti-inflammatory IL-10 was measured.

The CpG-induced production of the pro-inflammatory cytokines TNFα (Figure 18A) and IL-12p70 (Figure 18B) significantly decreased after sepsis, whereas the production of IL-10 significantly increased (Figure 18C). This therefore led to a decreased IL-12p70 / IL-10 ratio (Figure 18D). The calculation of the IL-12p70 / IL-10 ratio allows the examination of a potential shift towards more pro- or anti-inflammatory cytokine production. In this regard, an increased ratio corresponds to a more pro-inflammatory secretion pattern. Vice versa, a decreased ratio corresponds to a more anti-inflammatory cytokine production. Thus, BMDCs had a sepsis-induced shift towards a more anti-inflammatory phenotype. In contrast, LPS-induced TNFα production was unchanged while IL-12p70 increased and IL-10 slightly decreased. Accordingly, this led to an increased ratio, which indicated a more pro-inflammatory phenotype.

Further, the influence of $CD8^+$ T cell depletion on BMDC functionality was analyzed. Although not significant, BMDCs tended to produce less TNFα (Figure 18E). Similarly, a significant loss in IL-12p70 was observed (Figure 18F), both independent of the stimulation. In contrast, the production of IL-10 significantly increased (Figure 18G). As a consequence, the IL-12p70 / IL-10 ratio decreased after LPS stimulation which corresponded to a more anti-inflammatory phenotype (Figure 18H). This revealed the ability of $CD8^+$ T cells to affect the functionality of BMDCs, which was, however, independent of the particular stimulation pathway of BMDCs.

In the following, the influence of TLR2ko $CD8^+$ T cell transfer on BMDC functionality was investigated. In contrast to $CD8^+$ T cell depletion, there was no decrease in TNFα production after LPS stimulation, but a significant increase after CpG stimulation (Figure 18K). Similar to depletion, T cell transfer led to significantly lower IL-12p70 production after LPS (Figure 18L) and an overall increased IL-10 production (Figure 18M). In contrast, IL-12p70 production significantly increased in the case of CpG stimulation as it was the case for TNFα. Consequently, the LPS-induced IL12p70 / IL-10 ratio decreased indicating a more anti-inflammatory phenotype of the BMDCs while it was rather unchanged after CpG stimulation (Figure 18N).

All in all, $CD8^+$ T cells had the ability to influence the functionality of BMDCs. Here, a general shift towards a more anti-inflammatory cytokine production after LPS stimulation was particularly outstanding and contrasted the general regulation after CLP. However, the IL-12p70 production was influenced differently after TLR2ko $CD8^+$ T cell transfer depending on the respective stimulation pathway. Based on the previous results, an influence of the altered IFNγ production by the transfer was assumed.

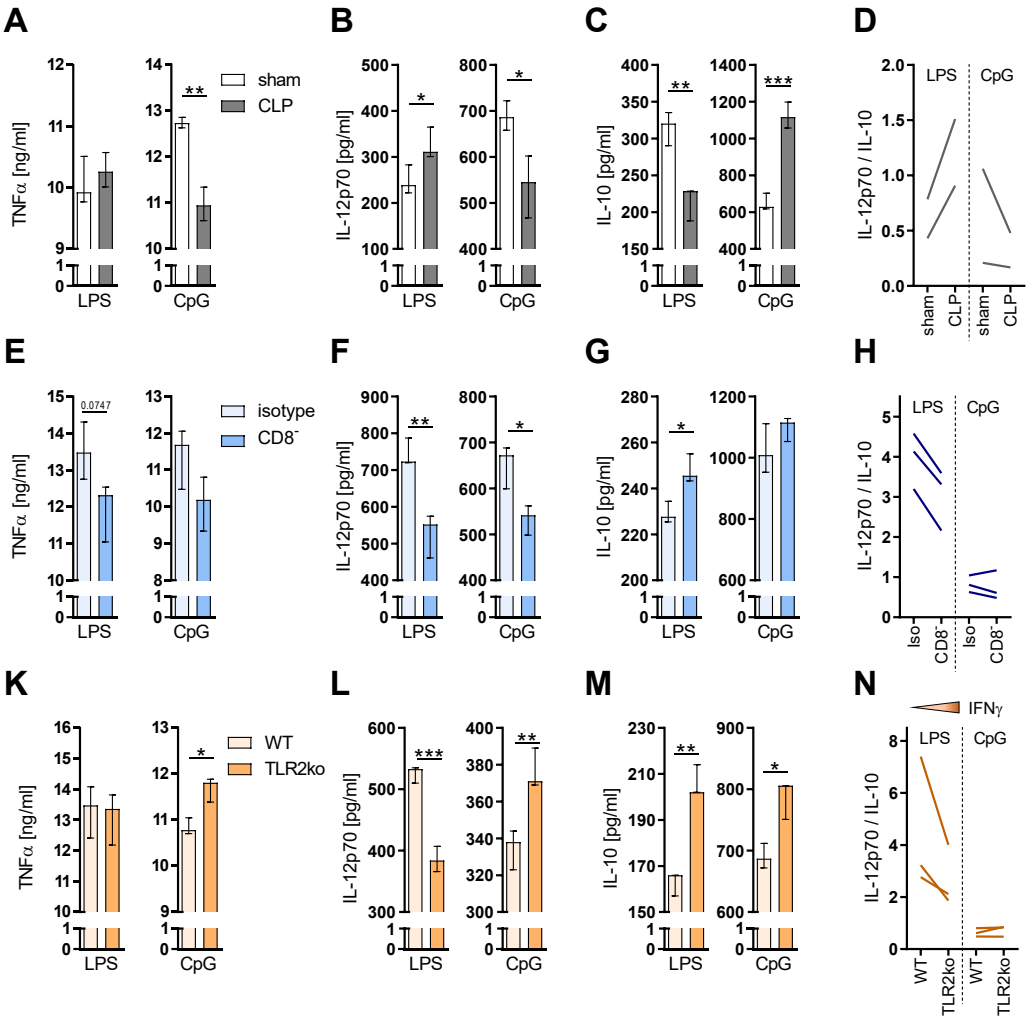

Figure 18 Cytokine production of BMDC after CLP and CD8⁺ T cell depletion or transfer. Sepsis and CD8⁺ T cell depletion or transfer was induced as described in Figure 17. Cytokine production by BMDCs of TNFα (A/E/K), IL12p70 (B/F/L), and IL-10 (C/G/M) after CpG or LPS stimulation is shown with representative data of one out of two to three experiments. The first row shows data from sham and CLP experiments (grey), while the second one shows depletion (blue) and the third one shows transfer (orange) data. An unpaired *t*-test was performed for statistical analysis. Significant results are indicated as $p \leq 0.05$ (*), $p \leq 0.01$ (**) and $p \leq 0.001$ (***). Further, the shift between anti- and pro-inflammatory cytokine production represented by the IL12p70 / IL-10 ratio is analyzed for all experimental setups (D/H/N).

3.4.4 Functionality of BMDCs can be influenced by IFNγ availability

To investigate this assumption, naïve BMDC were generated from wild-type or IFNγko mice aiming to analyze the ability of IFNγ availability to influence BMDC differentiation. The distribution among the different subtypes and the maturation level of BMDCs were not majorly changed by the absence of IFNγ in the cultures (Figure 19A+B). However, the cytokine production was regulated differently in BMDCs from IFNγko mice (Figure 19C).

This was dependent on the respective TLR ligand. Stimulation with LPS via TLR4 resulted in increased production of IL-12p70 while lower levels of TNFα and IL-10 were detected. This led to an increased anti-inflammatory cytokine response of IFNγko BMDCs (Figure 19D). In contrast, CpG stimulation via TLR9 revealed an opposite effect on IL-12p70 and IL-10 production while TNFα was still reduced. This led to an increased pro-inflammatory cytokine pattern in IFNγko BMDCs compared to the wild-type.

According to these results, a strong influence of IFNγ on the functionality of BMDCs in terms of cytokine production was suggested. A similar regulation after the transfer of $CD8^+$ T cells from TLR2ko mice in view of the assumed IFNγ production strengthened the hypothesis of a dependence on IFNγ.

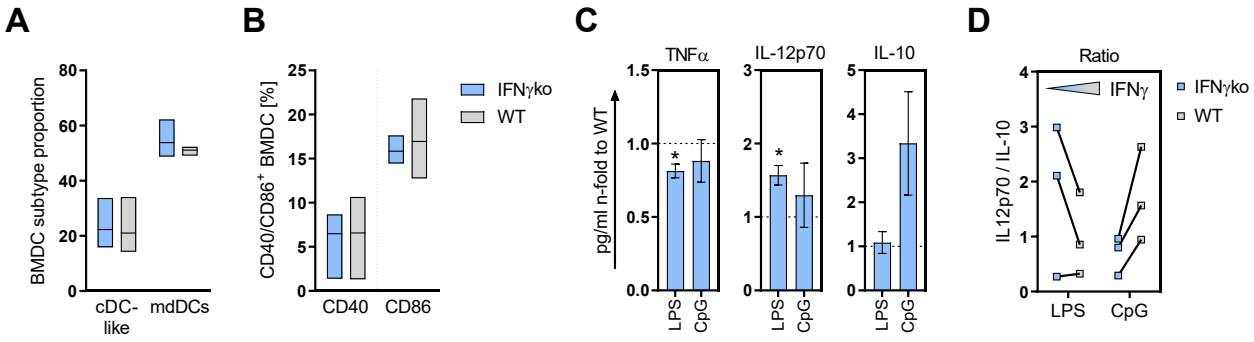

Figure 19 Altered differentiation of BMDC regarding cytokine production in IFNγko mice. BMDCs were generated from wild-type or IFNγko mice and analyzed regarding their subdivision into cDC-like and mdDCs (A). The maturational state of BMDC was measured by their expression of costimulatory molecules like CD40 and CD86 (B). The cytokine production of TNFα, IL12p70, and IL-10 after LPS or CpG stimulation was quantified and normalized for IFNγko to the respective wild-type BMDCs. (C). Further, the shift between anti- and pro-inflammatory cytokine production represented by the IL12p70 / IL-10 ratio is analyzed for both mouse strains (D). The data is depicted as bar charts or floating bars (min to max) with indicated mean of two individual experiments.

3.5 Sepsis-induced shift to a more glycolytic phenotype of BMDC

The question arose in which way cytokines like IFNγ can alter the functionality of newly differentiated DCs. One possible option is the regulation of cell metabolism, which is known to fundamentally affect the functionality of cells.

First, a general analysis of the metabolic profile of BMDCs after sepsis was done. A possible influence on mitochondrial respiration or glycolysis of DCs was analyzed using a Seahorse assay. A schematic overview (Figure 20A) serves to better interpret the

following energy profile of BMDC from sham or CLP mice (Figure 20B). The displayed baseline values describe the energy state of the cells after CpG stimulation. BMDCs after sepsis clearly shifted towards a less metabolically active phenotype. Subsequently, oligomycin, an ATPase synthase inhibitor, was added to the cells to inhibit mitochondrial respiration. This initiated the stress-typical up-regulation of glycolysis, which was evident in BMDC after sham and CLP operation. The resulting gap is the metabolic potential of the cells. In this regard, BMDCs had a reduced metabolic potential after sepsis. By calculating the OCR/ECAR ratio, a general shift towards mitochondrial respiration or glycolytic metabolism can be analyzed (Figure 20C). The significant reduced ratio after sepsis indicated a shift to a more glycolytic metabolism of these cells. Glycolysis thus had been confirmed as an important metabolism in stressed BMDCs. In addition, sepsis led to a reduced metabolic potential of these cells.

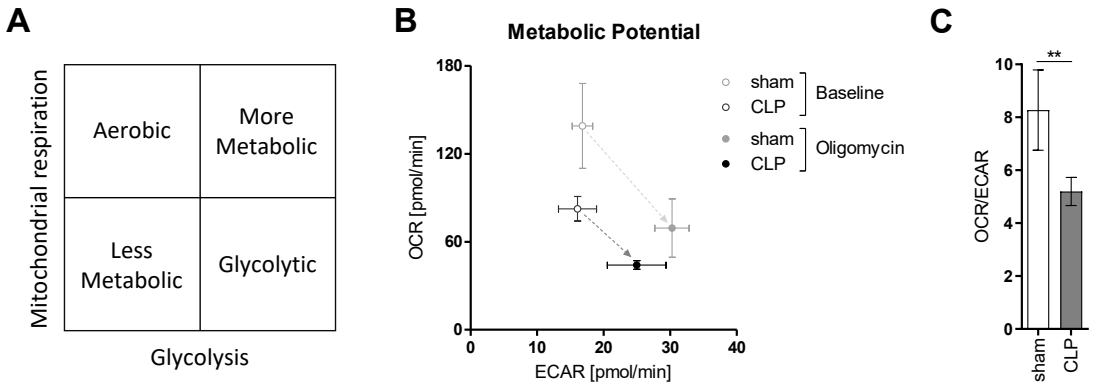

Figure 20 Metabolic potential of BMDCs after Sepsis. BMDCs processed in a metabolic assay using a Seahorse XF Analyzer. A schematic diagram is shown for better interpretation of the metabolic energy profile (A). The measured oxygen consumption rate (OCR) corresponds to cell metabolism via mitochondrial respiration and the extracellular acidification rate (ECAR) to cell metabolism via glycolysis. The corresponding profile compares sham and CLP Baseline values and after addition of oligomycin (B). The dotted arrows indicate the metabolic potential of these cells. Calculating a ratio of OCR/ECAR allows the identification of a shift from mitochondrial respiration to a more glycolytic metabolism (C). All data shows one representative experiment out of two with four technical replicates. A parametric *t*-test was performed for statistical analysis. Significant results are indicated as $p \leq 0.01$ (**).

Thus, glycolytic parameters of BMDCs were analyzed in more detail. Therefore, the glucose analogue 2-NBDG was used to quantify the glucose uptake of BMDCs in a specific time frame (Figure 21A). Thereby, the BMDC subtypes were differently regulated as there was slightly decreased uptake for mdDCs but increased uptake for cDC-like BMDCs visible. Further, the expression of the insulin-independent glucose transporter

Glut1 decreased in mdDCs but was differently regulated in cDC-like BMDCs (Figure 21B). In addition, the dot plots for 2-NBDG as well as Glut1 expression revealed a general increased glycolytic activity in mdDCs compared to cDC-like BMDCs. Looking onto the RNA expression of all BMDCs, Glut1 had no clear trend (Figure 21C). However, the hexokinase 2 (HK2), important for the phosphorylation of glucose to glucose-6-phosphate during the glycolysis, was increasingly expressed after CLP. Furthermore, despite the measured parameters regarding glycolysis, the glutamine metabolism was analyzed during the RNA quantification (Figure 21D). Thereby, the expression of the glutaminase GLS2 increased, which, in addition to enhanced glycolysis, revealed increased activity of the glutamine metabolism after sepsis.

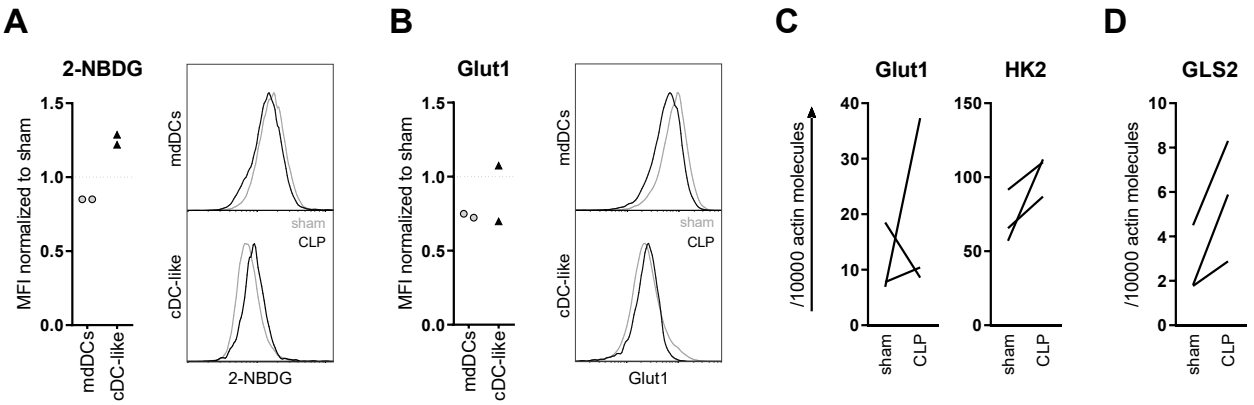

Figure 21 Glucose consumption and metabolic RNA expression in BMDCs after sepsis. BMDCs after a 4 d CLP were subjected to an assay to quantify 2-NBDG via FACS analysis (A) including a staining for the glucose transporter protein Glut1 (B). The data was collected in two individual experiments and is depicted as the median fluorescence intensity (MFI) normalized to the respective sham expression and exemplary dot plots each. Further, RNA isolated out of three individual experiments was analyzed for its expression of Glut1, the hexokinase 2 (HK2) (C), and the glutaminase GLS2 (D).

3.6 The glutamine metabolism selectively inhibits IL-10 production

The following experiments now determined the possibility of an influence of metabolism on cytokine production by BMDCs. Therefore, cytokine production was quantified after inhibition of different metabolic pathways. In addition to the ATP synthase inhibitor oligomycin, the glucose analogue 2-DG was used, which competitively inhibits glycolysis at its second step. Furthermore, the glutamine antagonist DON was chosen. The BMDCs were stimulated overnight in the presence of increasing inhibitor concentrations.

Representative data after LPS stimulation comparing sham and CLP is depicted in Figure 22. All measured cytokines decreased evenly after addition of 2-DG in a dose-dependent manner (Figure 22A). The addition of oligomycin caused an initial slight inhibition of TNFα, IL-10 and IL-12p70, which then remained almost unchanged or was rather random even with highly increasing inhibitor quantity (Figure 22B). The glutamine antagonist DON on the other hand led to a specific inhibition. While TNFα and IL-12p70 were mainly unaffected or might be slightly increased with higher inhibitor concentrations, IL-10 production was selectively down-regulated (Figure 22C).

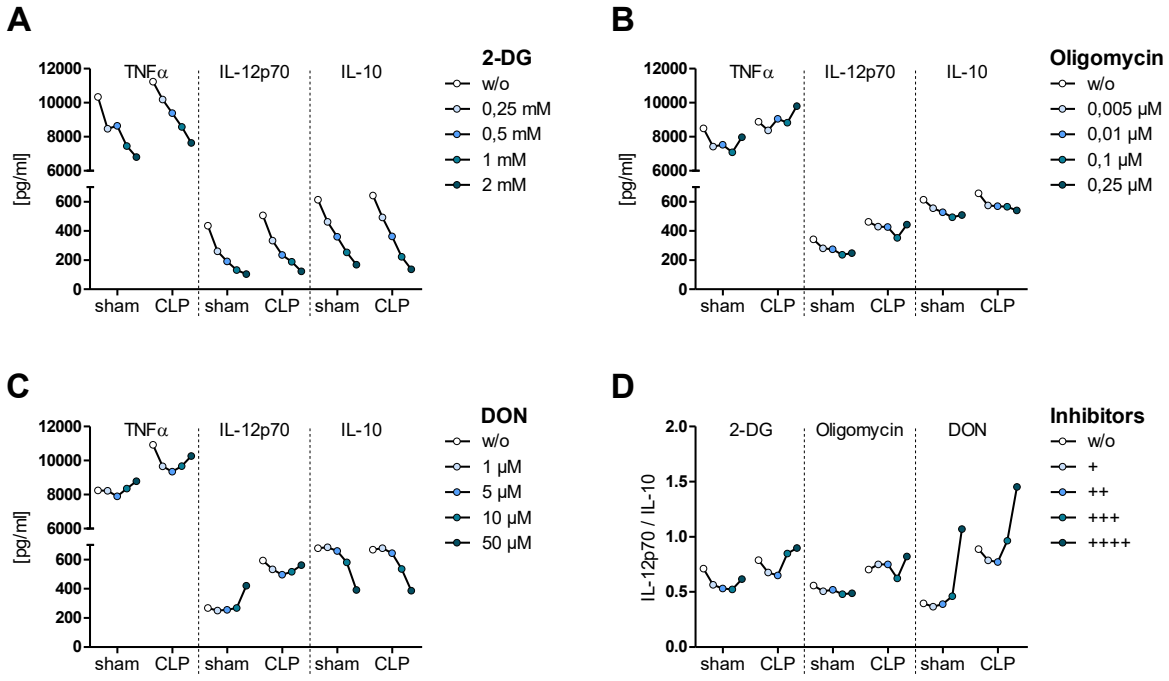

Figure 22 Impact on BMDC cytokine production by various metabolic pathways. Sepsis was induced in wild-type mice and BMC were isolated after a 4 d CLP or sham surgery. BMDCs were stimulated with LPS in the presence of increasing amounts of inhibitors for various metabolic pathways. These were 2-Deoxy-D-glucose (2-DG), a competitive inhibitor of glycolysis, the ATPase synthase inhibitor Oligomycin (mitochondrial respiration) and 6-Diazo-5-oxo-L-norleucine (DON), which is a glutamine antagonist. The cytokine production of TNFα, IL12p70 and IL-10 after LPS stimulation was measured. These were treated with different inhibitor amounts of 2-DG (A), Oligomycin (B) or DON (C) and are depicted in a line chart with one exemplary experiment. Further, the shift between anti- and pro-inflammatory cytokine production represented by the IL12p70 / IL-10 ratio after inhibitor treatment was analyzed (D).

Looking at the IL-12p70/IL-10 ratio under these different inhibitory conditions, 2-DG and oligomycin did not have a clear influence, as the ratio was initially decreasing and subsequently increased with higher inhibitor amounts (Figure 22D). This indicated that

BMDCs tended to have a more anti-inflammatory immune response at first and a more pro-inflammatory immune response with stronger inhibition. In addition, the influence of oligomycin was opposite between sham and CLP, which might be caused by a glycolysis-preferred metabolism of the cells after sepsis. The strongest changes were caused after the addition of DON, where an increased pro-inflammatory immune response occurred with increasing inhibitor concentration due to the selective up- and down-regulation of the measured cytokines. This specific regulatory effect of DON was confirmed in further experiments in the bachelor thesis of Nadine Gausmann [72]. In addition, she provided evidence for a TLR independence as she measured the same IL-10 specific regulation after stimulation of TLR2, TLR4, and TLR9.

In summary, the cytokine production of BMDCs was tightly regulated by its metabolic pathways. Glycolysis was important for the various cytokines investigated here in a rather nonspecific but dose-dependent manner while oligomycin just seemed to have minor effects. The glutamine metabolism, however, had a selective importance for IL-10 production in BMDCs. This offers the possibility of targeted treatment against immunosuppressive effects regarding cytokine balance during sepsis by considering the glutamine metabolism.

4. Discussion

Sepsis is a systemic infection in which hyperproduction of pro-inflammatory mediators can lead to organ failure. Thereby, formation of anti-inflammatory mediators accompanying and following this anti-inflammatory phase can induce a suppression of the immune system causing a late death of the patient. The development of this immunosuppression has been attributed to dysfunctional DCs, which could similarly be induced by stimulation with a TLR2 ligand. Since DCs originate in the bone marrow, preDCs should be investigated in the bone marrow. The observed parallel accumulation and activation of T cells in the bone marrow, led to the aim of this work to examine the distribution, activity, and function of these cells. Furthermore, it should be analyzed to what extent these cells have an influence on the altered development of DCs and whether TLR2 signaling plays a role.

4.1 Evaluation of the murine sepsis model

The first goal was to validate the used sepsis model and to exclude experiments with a too severe sepsis course, as this could lead to essentially altered immune reactions. Since this study was intended to investigate the causes and effects of post-septic immunosuppression, a mild form of sepsis was used.

Different clinical parameters were measured to determine the disease severity. Thereby, the frequency of WBCs shifted from fewer lymphocytes to increasing numbers of granulocytes after CLP. This is in line with the fact that the percentage of granulocytes is significantly higher and lymphocytes significantly decreased in septic patients [140]. However, even if increasing, most of the granulocytes are immature [11]. This immaturity can be assumed for the granulocytes in the present sepsis model and, in addition, decreasing lymphocyte counts are a sign of ongoing immunosuppression.

The levels of early inflammation parameters like CPK, BUN, IL-6 and GDF-15 were measured in the serum 24 hours after sepsis. Elevated CPK levels can be released after muscle damage and are used as a marker for acute myocardial infarction [193,234]. The condition of rapid breakdown of skeletal muscle, called rhabdomyolysis, is associated with sepsis [17,111]. It can be caused by invasion of pathogens directly into the muscles,

generation of toxins, cytokine-mediated muscle cell toxicity as well as muscle ischemia due to shock [111]. Although septic shock can be excluded in this model, the rising CPK level clearly shows known sepsis complications. Further, the body weight of septic mice significantly declined over the first two days, which can be mostly attributed to muscle damage.

Since BUN is a parameter that indicates acute kidney injury, its increase is particularly important to better mimic human sepsis [55]. Based on the increased levels in this sepsis model, it can be assumed that such a course is present in the early stage of the disease. Li et al. investigated a variety of clinical sepsis-associated biomarkers in the CLP model with C57Bl/6 mice [118]. They found BUN to peak at 16 hours after sepsis induction and being below the normal level two days later. Besides, IL-6 has a high peak as early as eight hours after sepsis rapidly decreasing from 16 to 48 hours. This is consistent with the results obtained in this study, as IL-6 was highly increased 12 hours after sepsis and, even if still up-regulated compared to sham, decreasing over time.

GDF-15 has been linked to poor survival in sepsis and is proposed as a possible predictive marker for mortality in septic patients. Serum levels correlate positively with disease severity [29] and are enhanced in critically ill patients with systemic inflammation that later on acquired septic complications [105]. Recently, production of GDF-15 was demonstrated in a CLP mouse model, mediated by TLR2-Myd88 signaling [192]. Thus, the fact that elevated GDF-15 was measured in this sepsis model not only confirms septic symptoms but may allow further research on the correlation of GDF-15 and sepsis disease progression in the mouse model.

In this study, these parameters were used for severity control and to exclude an influence of different treatments on the general sepsis course. The applied sepsis model shows known clinical parameters of sepsis-induced immunosuppression and was suitable for further investigations.

4.2 DCs diminish in spleen and bone marrow after sepsis

Loss of different immune cell populations is a striking feature of sepsis-induced immunosuppression. The systemic loss of DCs has been shown in multiple studies not only in the spleen but also in lymph nodes, whereas occurrence could be narrowed down

to later than 15 hours after sepsis [59,64,89,168,226]. This is in line with the observed loss of cDCs in this study.

It was noticeable that the number of dN cDCs was almost unchanged, whereas $CD4^+$ and $CD8^+$ cDCs significantly reduced after sepsis. This corresponds to previous studies, in which $CD4^+$ and $CD8^+$ cDCs in the spleen are significantly reduced compared to sham as early as 24 hours after CLP [64,168,172,210]. This is suggested to be caused by newly generated DC from septic mice predominantly to differentiate towards dN instead of $CD4^+$ DCs. Thus, the sepsis-induced DC number and composition described in this study corresponds to the current state of knowledge and resembles clear signs of immunosuppression.

To further investigate the impact of polymicrobial sepsis on the differentiation of DCs, preDCs in the bone marrow were analyzed in the present study. Significant reduction of the preDC cell count visible as early as 12 hours after CLP was evident. A decrease in DC progenitors has been described after systemic infection with various Gram-negative and Gram-positive bacteria [167]. Impaired proliferation, apoptosis, or mobilization into the periphery as a cause for this reduction was mainly excluded. In turn, Pasquevich et al. provided evidence that the decreased DC differentiation is at the expense of a shift towards monocytic innate immune response after systemic bacterial infection [167]. Further, they proposed DC depletion in mouse models after bacterial infection to be explained by this shift towards emergency myelopoiesis and the increased apoptosis as well as turnover of DCs (e.g. [8,172,217,227]). Data obtained in this study can support this theory, especially since the preDCs decreased in the bone marrow before cDC loss in the spleen was visible. Thus, the trigger must act on the preDC development in the bone marrow approximately 12 hours or earlier after sepsis.

PreDCs in the bone marrow can be divided into different subtypes, which are predetermined to develop into different DC populations. In this study, the model from Schlitzer et al. was used to interpret the data [196]. During preDC stage 1, termed pDC-primed preDCs in this study, the progenitor cells can still differentiate into pDCs. This DC subtype is mostly known for its ability to produce IFNα upon viral infection [36]. Further preDCs during stage 2, termed dP preDCs, only differentiate into cDCs. They can develop into the committed $Ly6c^-$ $Siglec\text{-}H^-$ preDC1 and $Ly6c^+$ $Siglec\text{-}H^+$ preDC2, respectively.

Thereby, preDC1 differentiate into cDC1 corresponding to the $CD8^+$ cDC and preDC2 differentiate into cDC2 corresponding to the dN and $CD4^+$ cDC subsets.

In this study, a clear shift towards more $Ly6c^-$ preDCs became apparent. Thereby, the dP preDCs increased on the first day but ultimately seemed to differentiate further into preDC1 instead of preDC2. An impairment in the developmental step from pDC-primed preDCs (stage 1) to dP preDCs (stage 2) might explain the shift to $Ly6c^-$ cells [196]. Thus, although formation of the $Ly6c^-$ Siglec-H^+ pDC-primed preDCs would occur, the number of dP preDCs would decrease. The dP preDCs would then increasingly differentiate into preDC1 for reasons unknown so far. Alternatively, at this stage of differentiation towards preDC2, there might be a developmental separation in their cDC-commitment between dP cDCs and $CD4^+$ cDCs. Thus, the shift from preDC2 to preDC1 would not necessarily be a favoring of the preDC1 population but could be due to the absence of the preDC2 type, which would develop into $CD4^+$ cDCs. However, a possible mechanism or commitment causing preferential development of dN cDCs rather than $CD4^+$ cDCs remains unknown and has to be analyzed in future studies.

The simultaneous measurement of cDC and preDC allows the analysis of a possible correlation in number and composition. Besides the loss in absolute DC count described in this and other studies, a strong decrease in *de novo* differentiated $CD4^+$ DCs via BrdU application was shown by Pastille et al. [168], which is reflected in the loss of preDC2 in this study. In addition, the absolute number of cDC1/$CD8^+$ DCs dropped but was not affected in *de novo* differentiated DCs. This is in line with the shift towards preDC1 possibly able to replenish the decreased cDC1 numbers after a general loss of preDC investigated in this study.

In the following, the question arose which changes in the bone marrow were responsible for this restructuring in the preDC compartment. Developmental processes in the bone marrow are tightly controlled by the cytokine milieu, which in turn depends on bone marrow cell composition and activity. In a previous study, a short-term increase in activated $CD4^+$ pDCs was found in the bone marrow [210]. While the increase of pDCs is not visible before 24 hours after sepsis [178,210,211], the results of this study indicate that an impact on preDC populations must have occurred around 12 hours earlier. An event preceding the rising of pDCs is the enrichment of T cells in the bone marrow

[178,210]. Consequently, as an objective of this study, T cells were characterized in more detail and evaluated for their ability to affect DC development in the bone marrow.

4.3 Characterization of T cells in the bone marrow after sepsis

4.3.1 Accumulation and specific activation in the CD8$^+$ T cell compartment

The cytokine milieu can have a strong influence on the development of DCs in the bone marrow [200,238]. Since T cells have the regulatory capabilities and are prominent cytokine producers, they can directly or indirectly intervene in the differentiation processes in the bone marrow and thus mediate the altered DC functionality.

It has been shown by numerous studies that T cells undergo sepsis-induced apoptosis in the spleen, other lymphoid organs, and the blood as early as within 24 hours to two days after sepsis induction [10,37,58,88]. This is in line with the CD4$^+$ T cell loss visible in the spleen during this study. In addition, the visible decrease of bone marrow cells after CLP might be largely characterized by decreased numbers of granulocytes, B cells and monocytes [178]. The increasing absolute cell number of T cells, however, stands in very clear contrast to this. This confirms results from previous studies, in which especially CD4$^+$ T cells are increased in the bone marrow 24 and 36 hours after sepsis induction [178,210]. The normalized values revealed that this temporary increase was proportionally comparable between CD4$^+$ and CD8$^+$ T cells. However, CD8$^+$ T cells showed increased signs of activity. This was present as early as 12 hours after sepsis induction, which is in parallel to the occurring loss of preDC. Thus, the appearance of activated T cells might be associated with the loss and/or restructuring of preDCs.

4.3.2 Antigen-independent activation of virtual memory T cells

How does increased and rapid activation appear in CD8$^+$ T cells, while this is not visible in CD4$^+$ T cells? There are several ways in which a T cell can be activated. Besides stimulation of the TCR, which requires antigen presentation by APCs like DCs, T cells can get bystander activated via innate cytokines. In addition, the TLR2 receptor, which is expressed on activated CD4$^+$ and CD8$^+$ memory T cells, is able to function as a

costimulatory molecule and therefore plays a role in T cell activation, function, and survival [46,184,261].

A large proportion of the incoming T cells consisted of T_N, but they did not show any relevant signs of CD69 expression. In contrast, T_{CM} and T_{VM} appeared in the bone marrow, where T_{VM} particularly displayed increased CLP-induced activation in both wild-type and TLR2ko mice. Naturally occurring memory $CD8^+$ T cells, characterized by $CD44^{hi}$ $CD122^{hi}$ $Ly6C^{hi}$ expression, are significantly lower in proportion and number in TLR2ko than in wild-type mice [47]. This was explained by the costimulatory effect of TLR2, which was reflected in the increased formation of memory T cells in the presence of IL-7. However, this was not the case in this study, as the memory $CD8^+$ T cells count was not lower in TLR2ko mice compared to the wild-type. Since sham operation has an impact on the immune system, this might explain the altered composition of T cells not only in the CLP but also in the control group. However, Cottalorda et al. used the C57BL/6 background while this study used BALB/c mice, which could be a reason for a cell composition possibly altered right from the start.

Since there are no differences in T cell activation between the mouse strains, a costimulatory role of TLR2 during sepsis can be excluded. Furthermore, the early onset of activity argues against stimulation of the TCR, which usually takes days rather than hours to establish an appropriate antigen-dependent T cell response [157]. As described, an alternative is the possibility of activation via cytokines, the so-called bystander activation. The T_{VM} are a T cell type that is particularly known for this activation.

The significantly increased activity observed exclusively in T_{VM} strongly suggests bystander activation of these cells. Further, the clear increase in activated T_{VM} of DO10.11 mice in the absence of OVA-peptide as the cognate antigen confirmed antigen-independent activation of T_{VM} under the influences of sepsis. It has been shown in the last years that T_{VM} play a role in various infections [114,119,189]. Thereby, the ability to perform NK cell-like cytotoxic functions like killing of target cells might play a role during sepsis. This mechanism has been analyzed in mouse models and humans [95,248]. The relevance of T_{VM} in different infections as well as the possibilities to intervene rapidly in the immune response, placed T_{VM} in a particular focus during this study.

All in all, TLR2-independent accumulation and activation of $CD8^+$ T cells was observed. The specific appearance of activated T_{VM} particularly early after sepsis and without providing a cognate antigen indicates sepsis-induced bystander activation of these cells.

4.3.3 TLR2 signaling impairs the IFNγ production of $CD8^+$ T cells after sepsis

The production of various effector molecules is an important feature of $CD8^+$ T cells to fulfill and shape immune responses [157]. $CD8^+$ memory T cells are especially described for their ability to rapidly produce IFNγ after stimulation of the TCR or with cytokines like IL-12 or IL-18 [116,176]. Recently, Taylor et al. provided evidence that IFNγ was produced by mostly memory than naïve $CD4^+$ and $CD8^+$ T cells in spleen and liver after CLP [223]. Different stimulating reagents were used in this study, including cytokine mixes with IL-12, IL-18 and IL-15 or IL-2 to induce TCR-independent bystander stimulation. Interestingly, despite the described increase in $CD8^+$ T cells and especially activated T_{VM}, we observed a highly significant and mostly decreasing production of IFNγ by wild-type $CD8^+$ T cells. Reduced IFNγ production during bacterial infections is associated with an increased bacterial load as a consequence of insufficient bacterial clearance [156]. Since previous studies attributed the decreased IFNγ production to the functions of dysfunctional DCs, the question arose as to what led to the decreased production by $CD8^+$ T cells in the bone marrow.

Thereby, TLR2 signaling came into consideration because no loss of IFN production was detected in TLR2ko $CD8^+$ T cells in this study. Significantly higher levels of IFNγ producing cells were maintained compared to the wild-type after stimulation with PMA and Ionomycin or IL-12, IL-18, and IL-15. In this context, a similar effect by CLP in decreasing the IFNγ production of pre-existing LCMV-specific memory $CD8^+$ T cells has been described after rechallenge with *Listeria monocytogenes* [58]. This was caused by severe impairment of antigen-dependent but also antigen-independent functions of the remaining memory cells. This reduced sensitivity to bystander activation was caused by T cell extrinsic effects during sepsis, which was enhancing the susceptibility to secondary infections.

Following this, the question arose whether this dependence on TLR2 signaling was also an environmental or rather a T cell-intrinsic effect. Here, transfer of TLR2ko $CD8^+$ T cells

demonstrated that, contrary to the findings of Duong et al. [58], a TLR2-dependent and T cell-intrinsic effect led to the reduction of IFNγ in wild-type. The transfer of TLR2ko T cells positively affected the RNA expression of the IFNγ signaling pathway among all bone marrow cells. Thus, $CD8^+$ T cells can have a strong influence on the cytokine environment in the bone marrow during sepsis.

A general mechanism of TLR2 signaling was identified by prestimulation with the TLR2 ligand P_3CSK_4, as PMA stimulation on the next day resulted in lower IFNγ production by $CD8^+$ T cells. Stimulation of $CD8^+$ T cells with P_3CSK_4 induce a reduced requirement of costimulatory signals provided by APCs for them to develop into functional memory cells [150], which is consistent with TLR2 being able to function as a costimulatory molecule in T cells. To my knowledge, no literature exists in which a comparable P_3CSK_4 prestimulation was done as mostly a simultaneous incubation of P_3CSK_4 and other stimulating reagents was applied. For example, simultaneous stimulation with IL-2 and P_3CSK_4 induces a strong increase in IFNγ production by memory phenotype $CD8^+$ T cells in the absence of specific antigens [47]. Cottalorda et al. therefore proposed a new TLR2-dependent mechanism which seemed to be involved in the Ag-independent control of memory $CD8^+$ T cell homeostasis and function. In this study, however, the stimulation via TLR2 appeared to inhibit IFNγ production in $CD8^+$ T cells. A TLR2-dependent down-regulation of IFN expression had been described after rhinovirus infection [256]. Xander et al. demonstrated the underlying mechanisms to be via induction of TLR2-dependent SIRT-1 expression, which in turn reduced IFN production by inhibiting the JAK-STAT signaling pathway. Furthermore, TLR2 signaling depletes interleukin receptor associated kinase −1 (IRAK-1), which thereby inhibits the expression of IFN after stimulation with single strand (ss) RNA signaling through MyD88-dependent TLR7/TLR9 [126]. The activation of TLR2 suppresses IFN responses to virus infection [70,229]. It is possible that TLR2-activation during sepsis triggers similar processes that subsequently led to the decreased IFNγ production.

In summary, a TLR2-dependent and T cell intrinsic regulation reduced the IFNγ production of bone marrow $CD8^+$ T cells after sepsis. Thereby, transfer of TLR2ko $CD8^+$ T cells was able to alter the whole IFNγ signaling RNA expression in the bone marrow. The sepsis-induced loss of IFNγ production may play a role during the altered differentiation

processes after sepsis. However, the exact mechanisms involved in this down-regulation during sepsis remain unclear. For further investigation, possible factors like increased SIRT-1 expression, inhibited JAK/STAT signaling, or depletion of IRAK-1 could be analyzed using the *in vitro* P_3CSK_4 prestimulation assay and subsequently be addressed in the sepsis model.

4.4 What is the impact of $CD8^+$ T cells on altered DCs after sepsis?

4.4.1 Numerical reduction of preDCs correlating cDC numbers

The impact of IFNγ on cell development in the bone marrow has been shown in various scenarios. Besides controlling the odontoblastic differentiation [260], IFNγ plays a role during lymphopoiesis and the development of the myeloid lineage [183]. Thus, the reduced IFNγ production in the bone marrow might interfere with developmental processes during sepsis.

The numerical loss of preDC in the bone marrow and DCs in the periphery after sepsis might be caused by the shift towards emergency myelopoiesis. In this study, the depletion of $CD8^+$ T cells in CLP mice did influence a further decreasing tendency of cDCs as well as significantly reduced preDC numbers in the bone marrow. This indeed was a general influence on the DC development as there was no influence on specific subtypes. Thus, $CD8^+$ T cell depletion seem to worsen the sepsis-induced preDC loss. DCs are significantly decreased in mature B and T cell-deficient SCID or RAG2ko mice and can be proportionally restored by T cell reconstitution [206]. This reveals the dependency of DC development on T cells, which was by part evident in this study if only $CD8^+$ T cell depletion was applied. In this context, the expression of FL on T cells might play a role [145]. In this regard, cytokines such as IL-2, IL-4, IL-7 and IL-15 enhance the expression of membrane bound and soluble FL on T cells [42]. It is known that FL is involved early in hematopoiesis and especially in the formation of functional cells of mature DCs [216].

Furthermore, T cells are able to influence the differentiation of DCs via the interaction of CD40 and CD40 ligand [65]. Fas-induced apoptosis is disrupted through CD40 ligation [19], which enables T cells to specifically regulate DC composition and number. Also, naïve T cells are able to condition DCs upon microbial challenge via B7-H1 [220]. In this

study, $CD8^+$ T cells were sufficient to induce preDC development, which may be in addition to cytokine milieu control regulated by direct cell-cell contact. To investigate the latter, the localization of T cells and preDCs in the bone marrow during sepsis must be investigated. Here, *Clec9a*$^{+/cre}$*Rosa*$^{+/EYFP}$ mice generated by Schraml et al. [198] could be used, which have been tested with CLP in preliminary experiments and a well-detectable fluorescence was found in cDCs.

After TLR2ko $CD8^+$ T cell transfer a slightly increasing tendency of preDC number was seen. It is possible that an effect might have been enhanced by the transfer of more cells. An experiment directly comparing the groups of CLP animals with and without transfer of increasing numbers of wild-type or TLR2ko $CD8^+$ T cells might provide more insight into an improving effect of increasing numbers of $CD8^+$ T cells and a potential TLR2 dependence. One could now speculate that, although if low IFNγ production compared to sham, the depletion of $CD8^+$ T cells led to decreased preDC number due to complete loss, while the increased IFNγ production after TLR2ko $CD8^+$ T cell transfer changed this to a slightly increasing trend.

For example, Pasquevich et al. reported that TLR4ko, TLR2ko and double ko mice are not reduced in their preDCs after *Yersenia enterocolitica* infection [167]. IFNγ is suggested to act directly on progenitor cells [131] and is required for infection-induced changes of bone marrow hematopoiesis in malaria by indirectly acting on the chemokine receptor CCR2 [15]. Thus, it is possible that the decreased preDC count might be attributed to decreased IFNγ production in the bone marrow acting on preDC development. However, this theory is contradicted by the fact that IFNγ is essential for functional myelopoiesis upon infection [15,27,131] which is thereby competing with DC development. Blocking of IFNγ prior infection with *Yersinia enterocolitica* restores the impaired DC development, which suggested infection induced monopoiesis and impaired DC development to be dependent on IFNγ signaling [167]. However, this process could be indirectly mediated via the regulatory capabilities of IFNγ on other cytokines [260]. To test a possible correlation between the decreased preDC number and the availability of IFNγ, a CLP could be combined with the application of IFNγ with subsequent examination of the preDCs.

In summary, $CD8^+$ T cells support the formation of preDCs. Here, the expression of FL might play a role. However, the underlying mechanisms remain unclear and a direct or indirect influence of IFNγ production needs to be investigated in future studies. Other possibilities such as signaling via CCR2 could be considered.

4.4.2 $CD8^+$ T cells alter the production of sepsis-related proteins by sDCs

Regulation of cell development via cytokines is not only able to control the quantity but also the quality of immune cells. Therefore, the question arose whether $CD8^+$ T cells, especially in view of their altered IFNγ production, may have an impact on the function of sDCs.

Increased CCL2 is correlated with organ dysfunction and mortality in sepsis patients [25,26] and is a negative prognostic factor in septic dogs and CLP mice [74,228]. However, neutralization of CCL2 increased the sepsis-induced lethality due to inhibiting the beneficial effects like the recruitment and activation of macrophages and neutrophils in mice [141]. Thereby, CCL2 influences the systemic cytokine balance in positively regulating the IL-10 production [75,142]. Similar beneficial effects like accumulation and activation of macrophages during CLP are known for CCL22 [143]. Thus, the roles of CCL2 and CCL22 are very much dependent on the current course of the disease – increased inflammation during SIRS or the anti-inflammatory effects of CARS. According to the results of this study, transfer of TLR2ko $CD8^+$ T cells induced even more elevated production of the chemokines CCL2 and CCL22 in sDCs, whereas depletion of $CD8^+$ T cells decreased them. $CD8^+$ T cells thereby had an impact on DC functionality which might be negatively regulated by TLR2. This influence would be quite helpful for the initial hyperinflammatory phase but might subsequently support the DC-dependent immunosuppressive effects and thus be counterproductive for the further course of the disease.

In many cases, sepsis is associated with altered coagulation factors, which can range from a weak activation of coagulation noticeable by a subtle decrease in platelet count to a severe hemostatic activation, for example, in the form of microvascular thrombosis [117]. Among numerous other processes, strong inhibition of fibrin degradation plays a

role in this sepsis complications, which is mainly caused by up-regulation of PAI-1 [18]. For example, PAI-1 serum levels are increased in patients with burn sepsis [41].
As with the production of the chemokines CCL2 and CCL22, PAI-1 was up-regulated by $CD8^+$ T cell transfer and down-regulated by its depletion. Thus, $CD8^+$ T cells might be involved in a regulation that leads to an increased production of PAI-1 by sDCs. Such regulation could in turn play a role in the maintenance of fibrin degradation.
All in all, $CD8^+$ T cells influence the functionality of newly differentiated DCs, which might be negatively regulated by TLR2 signaling. Further experiments would be necessary to investigate an exact influence of $CD8^+$ T cells as well as underlying mechanisms regarding the different molecules.

4.4.3 TLR2-dependent alteration of BMDC function by $CD8^+$ T cells

The cell number of sDCs after sepsis is severely limited by DC loss to make extensive functional studies. Thus, more functional analyses were performed in a cell culture model using BMDCs generated from septic mice with or without $CD8^+$ T cell treatment. Altered differentiation of DCs results in increased IL-10 production contributing to the development of immunosuppression and can be resembled by BMDC cultured *in vitro* with GM-CSF [168,210]. BMDC cultures are a heterogeneous composition of various DC subtypes with distinct functions [81]. Examination of the BMDC cultures with or without T cell depletion or transfer revealed that BMDCs were not altered in their maturation or subset composition.
The measured cytokine production of the BMDCs after sham and CLP operation served, on the one hand, as evaluation of the BMDC cultures compared with those from previous studies and, on the other hand, as a comparative value for the different $CD8^+$ T cell treatments. The shift towards increased IL-10 instead of IL-12p70 production is a key feature of post-septic BMDCs after restimulation with CpG [28,168,210]. The same was true for the BMDC culture in this study, in which the IL-12p70/IL-10 ratio decreased towards a more anti-inflammatory BMDC phenotype. It is striking that this is regulated differently depending on the TLR ligand, since after LPS stimulation there was an increased IL-12p70 but decreased IL-10 production. In this regard, it is important to note that IL-12p70 production increases with progressively delayed LPS stimulation, while IL-

10 levels are lower [102]. This was attributed to the different maturation of BMDCs. Thus, the day of harvesting the cells during this study might have an influence on the subsequent LPS-induced cytokine secretion and thereby might support this regulation different to stimulation with CpG.

The investigation of LPS-induced cytokine production after T cell depletion revealed a regulation by $CD8^+$ T cells into a more pro-inflammatory cytokine secretion pattern. $CD8^+$ T cells might mediate the cytokine milieu which then directly affects the progenitor cells. Mediators like IFNγ, IFNα or IL-10 are known to mediate DC differentiation resulting in altered function and phenotype [33,238,255].

Following this, the data of the transfer experiment were of particular interest, since TLR2ko $CD8^+$ T cells had an increased IFNγ production after CLP. Indeed, transfer resulted in an altered cytokine secretion pattern of BMDCs, leading to a striking regulation towards an increased anti-inflammatory immune response after LPS stimulation. Thus, TLR2 signaling on T cells might have a direct influence on this regulation. Interestingly, the regulation of IL-12p70 production depended on the stimulation pathway, differently regulated after TLR4- or TLR9-signaling and in total contrast to the regulation after CLP. Again, this could be influenced by the aforementioned timing dependence of stimulation with LPS.

Wu et al. showed *in vitro* generated DCs after LPS stimulation from IFNγko mice to be unaffected in their maturation but producing increased IL-12 [255]. The same was observed in BMDC culture of IFNγko mice compared with wild-type animals in this study. In contrast, generation of BMDCs in the presence of IFNγ enhances their IL-10 and slightly reduces their IL-12 production [98]. In this study, this regulation was observed in LPS-stimulated BMDCs after transfer of TLR2ko $CD8^+$ T cells. As these cells maintained the IFNγ production after sepsis, the altered DC phenotype after CLP might be associated with the TLR2-dependent loss of IFNγ production by $CD8^+$ T cells in the bone marrow. This regulatory impact may explain why IFNγ treatment during sepsis yields controversial results. For example, positive effects on monocyte functions have been observed in septic patients after IFNγ application [54,170]. However, the amount of data is rather limited to make a reliable statement of improvement in terms of infection and mortality after sepsis. In contrast, mortality was even increased after IFNγ treatment in the CLP model [152]. A

cause might be the potential regulation by IFNγ on the cytokine production of the DCs and the resulting shift of the IL-12p70/IL-10 ratio. This could have a negative impact depending on the predominant syndrome.

4.5 Metabolic changes as a possible factor of altered DC function

The question arose in which way the T cells might interfere with the functionality of the DCs, characterized by their altered cytokine production. Here, cell metabolism came into focus since energy supply is important during immune responses and can influence cell functions. Also, sepsis-induced organ damage has been associated with energy deprivation [57].

The investigation of this study revealed an increasing glycolytic metabolism of BMDCs after sepsis, which, moreover, reduced the metabolic potential of the cells important for resilience during stress. The switch of activated DCs to glycolysis has been investigated in multiple studies upon stimulation with various molecules like CpG [61,110], P_3CSK_4 [61], LPS [60,61,97,110,138,175], and many more, concisely reviewed by Wculek et al. [244]. This increased glycolysis occurs within minutes after TLR stimulation in BMDCs and various cDC populations [61]. The enhanced glycolysis is triggered due to OXPHOS down-regulated by NO and is assumed to be a survival response to maintain ATP levels [60]. Several studies are providing evidence that enhanced glycolysis occurs in immunogenic or pro-inflammatory DCs [60,61,110], whereas increased OXPHOS and FAO can be observed in tolerogenic DCs [61,132].

In this context, it is not surprising that the use of the glucose antagonist 2-DG led to a comprehensive and dose-dependent reduction of the measured cytokines IL-10, IL-12p70 and TNFα. A corresponding regulation was shown by other researchers in the form of reduced IL-6, IL-12p70 and TNFα after addition of 2-DG [61] or similar effects due to glucose limitations eventually causing the death of DCs [110]. However, 2-DG not only inhibits glycolysis, but also activates the endoplasmic reticulum stress response [138] and impairs OXPHOS or JAK-STAT6 signaling by reducing ATP levels [239]. For example, 2-DG reduced glycolysis starting at amounts as low as 0.156 mM in bone marrow-derived macrophages (BMDMs), whereas OXPHOS decreased at 10 mM but increased at amounts below 1.25 mM. ATP production was not affected in doses under 0.3 mM. This

vividly demonstrates how the additional effects of 2-DG are particularly dose dependent. However, since the lowest dose of 0.25 mM applied in this study induced a general reduction in cytokine production, an influence of, for example, reduced ATP production can be considered unlikely. Moreover, the consistent reduction in cytokine production underlines the relevance of glycolysis for the activation and functionality of DCs. For further experiments, the effects of 2-DG must be taken with caution and investigation of glycolysis should rather be performed using glucose limitation to exclude any influence on other systems.

Glut1 transcript and protein is increased after various TLR stimulations of DCs indicating increased glucose uptake after activation [110]. However, FACS analysis and RNA quantification in this study did not show a clear correlation between the glycolytic shift and the expression of the glucose transporter Glut1 or more enhanced glucose uptake measured via 2-NBDG after CLP. Thus, the sepsis-induced up-regulation of glycolysis did not seem to be caused by higher availability of intracellular glucose. However, the increased transcription of HK2 indicated an elevated glycolytic activity. This is in line with significantly increased HK2 expression relevant during general LPS-induced monocyte-derived DC activation in human while intracellular glucose levels measured via 2-NBDG did not change [175]. However, this was already visible in BMDCs from septic mice before re-stimulation. Thus, this study further demonstrated that sepsis-induced altered differentiation of DCs was, besides changes in their cytokine production and T cell priming, characterized by differences in their metabolism.

The use of oligomycin had very little effect on the activation of BMDCs and their production of IL-6, IL-12 and TNFα after LPS stimulation [61]. These results were confirmed and extended by the almost unchanged IL-10 production. Due to the increased glycolysis as a consequence of inhibited OXPHOS and down-regulated FAO [60,110], mitochondrial respiration can be assumed to be of minor relevance for BMDC activation and resulting functions during sepsis.

The continuous sepsis-induced up-regulation of the glutaminase GLS2 was quite striking, which suggests an increased glutamine metabolism after CLP. Thus, since the milieu during the generation of BMDCs is identical between sham and CLP, the reprogramming of metabolism must already be present in the progenitor cells. To further investigate the

influence of glutamine metabolism on BMDC functionality, the glutamine antagonist DON was added during DC stimulation. This revealed a specific inhibition of IL-10 production, whereas the immunogenic mediators IL-12p70 and TNFα were unchanged or, in case of IL-12p70, slightly enhanced in sham animals. This specific regulation was recently observed in naïve BMDM, in which addition of DON results in increased TNFα but decreased IL-10 secretion [162]. The development of a more pro-inflammatory macrophage phenotype was attributed to enhanced NF-κB and decreased STAT3 signaling. This was confirmed in another study after glutamine deprivation indicated by increased expression of M1 macrophage marker genes including *Tnf*, *Il6* and *Il12* [123]. Further, *Il10* mRNA is reduced in DCs after L-glutamine starvation [138]. These studies show that glutamine metabolism has a distinct effect on the development of macrophages and DCs. This was confirmed for BMDCs in this study. However, the underlying mechanisms would need to be investigated in future experiments.

Moreover, glutamine treatment has been analyzed in the context of experimental sepsis in various studies. Application prior or immediately after operation results in histologically evaluated improvements and reduces sepsis symptoms 24 hours to two days after CLP [62,164,215,240]. Thereby, glutamine suppressed the pro-inflammatory response indicated by low levels of IL-6 or TNFα but enhanced levels of anti-inflammatory IL-10. Thus, administration of glutamine led to a significant improvement in the initial sepsis phase dominated by SIRS. On the contrary, the results of this work in terms of increased IL-12 and decreased IL-10 production after glutamine inhibition indicate that the influence of glutamine metabolism on DC functionality might worsen the course of sepsis during CARS. Thus, for a successful regulation of the glutamine metabolism, reliable factors would have to be analyzed to determine the current stage of disease in the sepsis patient. Especially, since significant beneficial effects of glutamine treatment of, for example, critically ill patients are still under debate [21,222]. Nevertheless, this provides therapeutic possibilities to reduce the susceptibility to secondary infections after sepsis.

Furthermore, this is providing evidence that a specific functional change in DCs can be induced by altering metabolic processes. Thus, it is possible that $CD8^+$ T cells in the bone marrow can cause a functional change of the DCs as early as in the preDC stage by, for example, inducing metabolic alteration.

5. References

1. Acuto O, Michel F (2003). CD28-mediated co-stimulation: a quantitative support for TCR signalling. *Nature Reviews Immunology*, 3(12):939–951.
2. Akashi K et al. (2000). A clonogenic common myeloid progenitor that gives rise to all myeloid lineages. *Nature*, 404(6774):193–197.
3. Akira S, Uematsu S, Takeuchi O (2006). Pathogen Recognition and Innate Immunity. *Cell*, 124(4):783–801.
4. Angele MK, Faist E (2002). Clinical review: immunodepression in the surgical patient and increased susceptibility to infection. *Critical care (London, England)*, 6(4):298–305.
5. Ariotti S et al. (2014). Skin-resident memory $CD8^+$ T cells trigger a state of tissue-wide pathogen alert. *Science*, 346(6205):101–105.
6. Artero A, Zaragoza R, Miguel J (2012). Epidemiology of Severe Sepsis and Septic Shock. In: *Severe Sepsis and Septic Shock - Understanding a Serious Killer*. InTech,2012:3–25.
7. Ausubel FM (2005). Are innate immune signaling pathways in plants and animals conserved? *Nature Immunology*, 6(10):973–979.
8. Autenrieth SE et al. (2010). Immune Evasion by *Yersinia enterocolitica*: Differential Targeting of Dendritic Cell Subpopulations *In Vivo*. Cookson BT, ed. *PLoS Pathogens*, 6(11):e1001212.
9. Ayala A et al. (1994). Polymicrobial Sepsis but Not Low-Dose Endotoxin Infusion Causes Decreased Splenocyte IL-2/IFN-γ Release While Increasing IL-4/IL-10 Production. *Journal of Surgical Research*, 56(6):579–585.
10. Ayala A et al. (1996). Differential induction of apoptosis in lymphoid tissues during sepsis: variation in onset, frequency, and the nature of the mediators. *Blood*, 87(10):4261–4275.
11. Ayres LS, Sgnaolin V, Munhoz TP (2019). Immature granulocytes index as early marker of sepsis. *International Journal of Laboratory Hematology*, 41(3):392–396.
12. Baliu-Piqué M et al. (2018). Short Lifespans of Memory T-cells in Bone Marrow, Blood, and Lymph Nodes Suggest That T-cell Memory Is Maintained by Continuous Self-Renewal of Recirculating Cells. *Frontiers in Immunology*, 9(SEP):2054.
13. Banchereau J, Steinman RM (1998). Dendritic cells and the control of immunity. *Nature*, 392(6673):245–252.
14. Becker TC et al. (2005). Bone Marrow Is a Preferred Site for Homeostatic Proliferation of Memory CD8 T Cells. *The Journal of Immunology*, 174(3):1269–1273.
15. Belyaev NN et al. (2013). Extramedullary Myelopoiesis in Malaria Depends on Mobilization of Myeloid-Restricted Progenitors by IFN-γ Induced Chemokines. Stevenson MM, ed. *PLoS*

Pathogens, 9(6):e1003406.

16. Berg RE et al. (2003). Memory $CD8^+$ T cells provide innate immune protection against *Listeria monocytogenes* in the absence of cognate antigen. *The Journal of experimental medicine*, 198(10):1583–93.
17. Betrosian A et al. (1999). Bacterial sepsis-induced rhabdomyolysis. *Intensive Care Medicine*, 25(5):469–474.
18. Biemond BJ et al. (1995). Plasminogen Activator and Plasminogen Activator Inhibitor I Release during Experimental Endotoxaemia in Chimpanzees: Effect of Interventions in the Cytokine and Coagulation Cascades. *Clinical Science*, 88(5):587–594.
19. Björck P, Banchereau J, Flores-Romo L (1997). CD40 ligation counteracts Fas-induced apoptosis of human dendritic cells. *International Immunology*, 9(3):365–372.
20. Boehm T, Iwanami N, Hess I (2012). Evolution of the Immune System in the Lower Vertebrates. *Annual Review of Genomics and Human Genetics*, 13(1):127–149.
21. Bollhalder L et al. (2013). A systematic literature review and meta-analysis of randomized clinical trials of parenteral glutamine supplementation. *Clinical Nutrition*, 32(2):213–223.
22. Bone RC (1991). The Pathogenesis of Sepsis. *Annals of Internal Medicine*, 115(6):457.
23. Bone RC et al. (1992). Definitions for Sepsis and Organ Failure and Guidelines for the Use of Innovative Therapies in Sepsis. *Chest*, 101(6):1644–1655.
24. Bone RC, Grodzin CJ, Balk RA (1997). Sepsis: A New Hypothesis for Pathogenesis of the Disease Process. *Chest*, 112(1):235–243.
25. Bossink A et al. (1995). Plasma levels of the chemokines monocyte chemotactic proteins-1 and -2 are elevated in human sepsis. *Blood*, 86(10):3841–3847.
26. Bozza FA et al. (2007). Cytokine profiles as markers of disease severity in sepsis: a multiplex analysis. *Critical Care*, 11(2):R49.
27. de Bruin AM et al. (2012). IFNγ induces monopoiesis and inhibits neutrophil development during inflammation. *Blood*, 119(6):1543–1554.
28. Bruns S et al. (2013). Lipopeptides rather than lipopolysaccharide favor the development of dendritic cell dysfunction similar to polymicrobial sepsis in mice. *Inflammation Research*, 62(6):627–636.
29. Buendgens L et al. (2017). Growth Differentiation Factor-15 Is a Predictor of Mortality in Critically Ill Patients with Sepsis. *Disease Markers*, 2017.
30. Call ME et al. (2002). The Organizing Principle in the Formation of the T Cell Receptor-CD3 Complex. *Cell*, 111(7):967–979.
31. Campbell JJ et al. (2001). CCR7 Expression and Memory T Cell Diversity in Humans. *The*

Journal of Immunology, 166(2):877–884.

32. Cannon JG et al. (1990). Circulating Interleukin-1 and Tumor Necrosis Factor in Septic Shock and Experimental Endotoxin Fever. *Journal of Infectious Diseases*, 161(1):79–84.
33. Carbonneil C (2004). Dendritic cells generated in the presence of interferon-a stimulate allogeneic $CD4^+$ T-cell proliferation: modulation by autocrine IL-10, enhanced T-cell apoptosis and T regulatory type 1 cells. *International Immunology*, 16(7):1037–1052.
34. Cavaillon J-M et al. (2001). Review: Immunodepression in sepsis and SIRS assessed by ex vivo cytokine production is not a generalized phenomenon: a review. *Journal of Endotoxin Research*, 7(2):85–93.
35. Cebinelli GCM et al. (2020). CCR2-deficient mice are protected to sepsis by the disruption of the inflammatory monocytes emigration from the bone marrow. *Journal of Leukocyte Biology*, (September):JLB.4MR0820-049RR.
36. Cella M et al. (1999). Plasmacytoid monocytes migrate to inflamed lymph nodes and produce large amounts of type I interferon. *Nature Medicine*, 5(8):919–923.
37. Chang KC et al. (2007). Multiple triggers of cell death in sepsis: death receptor and mitochondrial-mediated apoptosis. *FASEB journal : official publication of the Federation of American Societies for Experimental Biology*, 21(3):708–19.
38. Chaudhry H et al. (2013). Role of cytokines as a double-edged sword in sepsis. *In vivo (Athens, Greece)*, 27(6):669–684.
39. Cheng S-C et al. (2016). Broad defects in the energy metabolism of leukocytes underlie immunoparalysis in sepsis. *Nature Immunology*, 17(4):406–413.
40. Cheong C et al. (2010). Microbial Stimulation Fully Differentiates Monocytes to DC-SIGN/$CD209^+$ Dendritic Cells for Immune T Cell Areas. *Cell*, 143(3):416–429.
41. Chi YF et al. (2015). Association between PAI-1 polymorphisms and plasma PAI-1 level with sepsis in severely burned patients. *Genetics and Molecular Research*, 14(3):10081–10086.
42. Chklovskaia E et al. (2001). Cell-surface trafficking and release of flt3 ligand from T lymphocytes is induced by common cytokine receptor γ-chain signaling and inhibited by cyclosporin A. *Blood*, 97(4):1027–1034.
43. Chow DA (2005). Natural Immune Activation: Stimulators/Receptors. In: *NeuroImmune Biology*.Vol5. Elsevier Masson SAS,2005:123–150.
44. Clemens MJ, Elia A (1997). The Double-Stranded RNA-Dependent Protein Kinase PKR: Structure and Function. *Journal of Interferon & Cytokine Research*, 17(9):503–524.
45. Cooper MD, Alder MN (2006). The Evolution of Adaptive Immune Systems. *Cell*, 124(4):815–822.

46. Cottalorda A et al. (2006). TLR2 engagement on $CD8^+$ T cells lowers the thresholdfor optimal antigen-induced T cell activation. *European Journal of Immunology*, 36(7):1684–1693.
47. Cottalorda A et al. (2009). TLR2 engagement on memory $CD8^+$ T cells improves their cytokine-mediated proliferation and IFN-γ secretion in the absence of Ag. *European Journal of Immunology*, 39(10):2673–2681.
48. Curtsinger JM et al. (1999). Inflammatory cytokines provide a third signal for activation of naïve $CD4^+$ and $CD8^+$ T cells. *Journal of immunology*, 162(6):3256–3262.
49. Curtsinger JM et al. (2005). Cutting Edge: Type I IFNs Provide a Third Signal to $CD8^+$ T Cells to Stimulate Clonal Expansion and Differentiation. *The Journal of Immunology*, 174(8):4465–4469.
50. Curtsinger JM, Mescher MF (2010). Inflammatory cytokines as a third signal for T cell activation. *Current Opinion in Immunology*, 22(3):333–340.
51. Dalton D et al. (1993). Multiple defects of immune cell function in mice with disrupted interferon-gamma genes. *Science*, 259(5102):1739–1742.
52. Delano MJ et al. (2007). MyD88-dependent expansion of an immature $GR\text{-}1^+CD11b^+$ population induces T cell suppression and Th2 polarization in sepsis. *Journal of Experimental Medicine*, 204(6):1463–1474.
53. Dinarello CA (2004). Infection, fever, and exogenous and endogenous pyrogens: some concepts have changed. *Journal of Endotoxin Research*, 10(4):201–222.
54. Döcke W-D et al. (1997). Monocyte deactivation in septic patients: Restoration by IFN-γ treatment. *Nature Medicine*, 3(6):678–681.
55. Doi K et al. (2009). Animal models of sepsis and sepsis-induced kidney injury. *Journal of Clinical Investigation*, 119(10):2868–2878.
56. Dranoff G (2004). Cytokines in cancer pathogenesis and cancer therapy. *Nature Reviews Cancer*, 4(1):11–22.
57. Drosatos K et al. (2013). Peroxisome Proliferator–Activated Receptor-γ Activation Prevents Sepsis-Related Cardiac Dysfunction and Mortality In Mice. *Circulation: Heart Failure*, 6(3):550–562.
58. Duong S et al. (2014). Polymicrobial Sepsis Alters Antigen-Dependent and -Independent Memory $CD8^+$ T Cell Functions. *The Journal of Immunology*, 192(8):3618–3625.
59. Efron PA et al. (2004). Characterization of the Systemic Loss of Dendritic Cells in Murine Lymph Nodes During Polymicrobial Sepsis. *The Journal of Immunology*, 173(5):3035–3043.
60. Everts B et al. (2012). Commitment to glycolysis sustains survival of NO-producing inflammatory dendritic cells. *Blood*, 120(7):1422–1431.

61. Everts B et al. (2014). TLR-driven early glycolytic reprogramming via the kinases TBK1-IKKε supports the anabolic demands of dendritic cell activation. *Nature Immunology*, 15(4):323–332.
62. Fabiani IM, Rocha SL (2017). Evaluation of sepsis treatment with enteral glutamine in rats. *Revista do Colégio Brasileiro de Cirurgiões*, 44(3):231–237.
63. Fischer E et al. (1992). Interleukin-1 receptor antagonist circulates in experimental inflammation and in human disease. *Blood*, 79(9):2196–2200.
64. Flohé SB et al. (2006). Dendritic cells during polymicrobial sepsis rapidly mature but fail to initiate a protective Th1-type immune response. *Journal of Leukocyte Biology*, 79(3):473–481.
65. Flores-Romo L et al. (1997). CD40 Ligation on Human Cord Blood CD34+Hematopoietic Progenitors Induces Their Proliferation and Differentiation into Functional Dendritic Cells. *Journal of Experimental Medicine*, 185(2):341–350.
66. Fogg DK et al. (2006). A Clonogenic Bone Marrow Progenitor Specific for Macrophages and Dendritic Cells. *Science*, 311(5757):83–87.
67. Förster R et al. (1999). CCR7 coordinates the primary immune response by establishing functional microenvironments in secondary lymphoid organs. *Cell*, 99(1):23–33.
68. Fraser IP, Koziel H, Ezekowitz RAB (1998). The serum mannose-binding protein and the macrophage mannose receptor are pattern recognition molecules that link innate and adaptive immunity. *Seminars in Immunology*, 10(5):363–372.
69. Freeman BE et al. (2012). Regulation of innate $CD8^+$ T-cell activation mediated by cytokines. *Proceedings of the National Academy of Sciences of the United States of America*, 109(25):9971–6.
70. Ganesan S et al. (2016). TLR2 Activation Limits Rhinovirus-Stimulated CXCL-10 by Attenuating IRAK-1–Dependent IL-33 Receptor Signaling in Human Bronchial Epithelial Cells. *The Journal of Immunology*, 197(6):2409–2420.
71. García-González P et al. (2016). Tolerogenic dendritic cells for reprogramming of lymphocyte responses in autoimmune diseases. *Autoimmunity Reviews*, 15(11):1071–1080.
72. Gausmann N (2020). Einfluss verschiedener Stoffwechselwege auf die Zytokinproduktion und T-Zell Aktivierung durch dendritische Zellen im Zusammenhang mit bakterieller Infektion. [Impact of different metabolic pathways on cytokine production and T-cell activation by dendritic cells in the context of bacterial infection.] *Unpublished bachelor thesis, University of Duisburg-Essen*:1–80.
73. Geerman S et al. (2016). Quantitative and Qualitative Analysis of Bone Marrow $CD8^+$ T Cells

from Different Bones Uncovers a Major Contribution of the Bone Marrow in the Vertebrae. *Frontiers in Immunology*, 6(JAN):1–11.

74. Goggs R, Letendre J (2019). Evaluation of the host cytokine response in dogs with sepsis and noninfectious systemic inflammatory response syndrome. *Journal of Veterinary Emergency and Critical Care*, 29(6):593–603.
75. Gomes RN et al. (2006). Increased susceptibility to septic and endotoxic shock in monocyte chemoattractant protein 1/CC chemokine ligand 2-deficient mice correlates with reduced interleukin 10 and enhanced macrophage migration inhibitory factor production. *Shock*, 26(5):457–463.
76. Grajales-Reyes GE et al. (2015). Batf3 maintains autoactivation of Irf8 for commitment of a CD8α$^+$ conventional DC clonogenic progenitor. *Nature Immunology*, 16(7):708–717.
77. Gutcher I, Becher B (2007). APC-derived cytokines and T cell polarization in autoimmune inflammation. *Journal of Clinical Investigation*, 117(5):1119–1127.
78. Haluszczak C et al. (2009). The antigen-specific CD8$^+$ T cell repertoire in unimmunized mice includes memory phenotype cells bearing markers of homeostatic expansion. *Journal of Experimental Medicine*, 206(2):435–448.
79. Harty JT, Tvinnereim AR, White DW (2000). CD8$^+$ T Cell Effector Mechanisms in Resistance to Infection. *Annual Review of Immunology*, 18(1):275–308.
80. Hassin D et al. (2011). Cytotoxic T lymphocyte perforin and Fas ligand working in concert even when Fas ligand lytic action is still not detectable. *Immunology*, 133(2):190–6.
81. Helft J et al. (2015). GM-CSF Mouse Bone Marrow Cultures Comprise a Heterogeneous Population of CD11c$^+$MHCII$^+$ Macrophages and Dendritic Cells. *Immunity*, 42(6):1197–1211.
82. Hellerstein MK et al. (2003). Subpopulations of long-lived and short-lived T cells in advanced HIV-1 infection. *Journal of Clinical Investigation*, 112(6):956–966.
83. Herndler-Brandstetter D et al. (2011). Human Bone Marrow Hosts Polyfunctional Memory CD4$^+$ and CD8$^+$ T Cells with Close Contact to IL-15–Producing Cells. *The Journal of Immunology*, 186(12):6965–6971.
84. Hilkens CMU et al. (1997). Human Dendritic Cells Require Exogenous Interleukin-12–Inducing Factors to Direct the Development of Naive T-Helper Cells Toward the Th1 Phenotype. *Blood*, 90(5):1920–1926.
85. Hoffmann JA et al. (1999). Phylogenetic perspectives in innate immunity. *Science (New York, N.Y.)*, 284(5418):1313–8.
86. Hooper L V, Midtvedt T, Gordon JI (2002). How host-microbial interactions shape the nutrient environment of the mammalian intestine. *Annual review of nutrition*, 22:283–307.

87. Hoshino K et al. (1999). Cutting edge: Toll-like receptor 4 (TLR4)-deficient mice are hyporesponsive to lipopolysaccharide: evidence for TLR4 as the Lps gene product. *Journal of immunology*, 162(7):3749–52.
88. Hotchkiss RS et al. (2001). Sepsis-Induced Apoptosis Causes Progressive Profound Depletion of B and $CD4^+$ T Lymphocytes in Humans. *The Journal of Immunology*, 166(11):6952–6963.
89. Hotchkiss RS et al. (2002). Depletion of Dendritic Cells, But Not Macrophages, in Patients with Sepsis. *The Journal of Immunology*, 168(5):2493–2500.
90. Huang S et al. (1993). Immune response in mice that lack the interferon-gamma receptor. *Science*, 259(5102):1742–1745.
91. Huber M et al. (2013). IL-17A secretion by $CD8^+$ T cells supports Th17-mediated autoimmune encephalomyelitis. *Journal of Clinical Investigation*, 123(1):247–260.
92. Inohara N et al. (2001). Human Nod1 Confers Responsiveness to Bacterial Lipopolysaccharides. *Journal of Biological Chemistry*, 276(4):2551–2554.
93. Iwasaki A, Medzhitov R (2010). Regulation of Adaptive Immunity by the Innate Immune System. *Science (New York, N.Y.)*, 327(5963):291–295.
94. Iwashyna TJ et al. (2010). Long-term Cognitive Impairment and Functional Disability Among Survivors of Severe Sepsis. *JAMA*, 304(16):1787.
95. Jacomet F et al. (2015). Evidence for eomesodermin-expressing innate-like $CD8^+$ KIR/$NKG2A^+$ T cells in human adults and cord blood samples. *European Journal of Immunology*, 45(7):1926–1933.
96. Janeway CA, Medzhitov R (2002). Innate Immune Recognition. *Annual Review of Immunology*, 20(1):197–216.
97. Jantsch J et al. (2008). Hypoxia and Hypoxia-Inducible Factor-1α Modulate Lipopolysaccharide-Induced Dendritic Cell Activation and Function. *The Journal of Immunology*, 180(7):4697–4705.
98. Jiang H-R et al. (2002). Secretion of interleukin-10 or interleukin-12 by LPS-activated dendritic cells is critically dependent on time of stimulus relative to initiation of purified DC culture. *Journal of leukocyte biology*, 72(5):978–85.
99. Jiang W et al. (1995). The receptor DEC-205 expressed by dendritic cells and thymic epithelial cells is involved in antigen processing. *Nature*, 375(6527):151–155.
100. Jin J-H et al. (2020). Virtual memory $CD8^+$ T cells restrain the viral reservoir in HIV-1-infected patients with antiretroviral therapy through derepressing KIR-mediated inhibition. *Cellular & Molecular Immunology*, (March):1–9.
101. Kaech SM, Cui W (2012). Transcriptional control of effector and memory $CD8^+$ T cell

differentiation. *Nature Reviews Immunology*, 12(11):749–761.

102. Kaliński P et al. (1999). T-cell priming by type-1and type-2 polarized dendritic cells: the concept of a third signal. *Immunology Today*, 20(12):561–567.
103. Kim H-J, Cantor H (2011). Regulation of self-tolerance by Qa-1-restricted $CD8^+$ regulatory T cells. *Seminars in Immunology*, 23(6):446–452.
104. Kim J et al. (2018). Innate-like Cytotoxic Function of Bystander-Activated $CD8^+$ T Cells Is Associated with Liver Injury in Acute Hepatitis A. *Immunity*, 48(1):161-173.e5.
105. Kleinertz H et al. (2019). Circulating growth/differentiation factor 15 is associated with human CD56bright natural killer cell dysfunction and nosocomial infection in severe systemic inflammation. *EBioMedicine*, 43:380–391.
106. Klenerman P, Hill A (2005). T cells and viral persistence: lessons from diverse infections. *Nature immunology*, 6(9):873–9.
107. Komai-Koma M et al. (2004). TLR2 is expressed on activated T cells as a costimulatory receptor. *Proceedings of the National Academy of Sciences*, 101(9):3029–3034.
108. Kondo M, Weissman IL, Akashi K (1997). Identification of Clonogenic Common Lymphoid Progenitors in Mouse Bone Marrow. *Cell*, 91(5):661–672.
109. Koutroulis I et al. (2019). Sepsis Immunometabolism. *Critical Care Explorations*, 1(11):e0061.
110. Krawczyk CM et al. (2010). Toll-like receptor–induced changes in glycolytic metabolism regulate dendritic cell activation. *Blood*, 115(23):4742–4749.
111. Kumar AA et al. (2009). Rhabdomyolysis in Community Acquired Bacterial Sepsis – A Retrospective Cohort StudyBozza PT, ed. *PLoS ONE*, 4(9):e7182.
112. Langerhans P (1868). Über die Nerven der menschlichen Haut. [About the nerves of the human skin] *Archiv für Pathologische Anatomie und Physiologie und für Klinische Medicin*, 44(2–3):325–337.
113. Lanzavecchia A, Sallusto F (2004). Lead and follow: the dance of the dendritic cell and T cell. *Nature Immunology*, 5(12):1201–1202.
114. Lee J-Y et al. (2013). Virtual memory $CD8^+$ T cells display unique functional properties. *Proceedings of the National Academy of Sciences*, 110(33):13498–13503.
115. León B, López-Bravo M, Ardavín C (2007). Monocyte-Derived Dendritic Cells Formed at the Infection Site Control the Induction of Protective T Helper 1 Responses against *Leishmania*. *Immunity*, 26(4):519–531.
116. Lertmemongkolchai G et al. (2001). Bystander activation of $CD8^+$ T cells contributes to the rapid production of IFN-gamma in response to bacterial pathogens. *Journal of immunology*, 166(2):1097–105.

117. Levi M, van der Poll T (2017). Coagulation and sepsis. *Thrombosis Research*, 149:38–44.
118. Li J-L et al. (2018). Assessment of clinical sepsis-associated biomarkers in a septic mouse model. *Journal of International Medical Research*, 46(6):2410–2422.
119. Lin JS et al. (2019). Virtual memory $CD8^+$ T cells expanded by helminth infection confer broad protection against bacterial infection. *Mucosal Immunology*, 12(1):258–264.
120. Liu K et al. (2007). Origin of dendritic cells in peripheral lymphoid organs of mice. *Nature Immunology*, 8(6):578–583.
121. Liu K et al. (2009). *In Vivo* Analysis of Dendritic Cell Development and Homeostasis. *Science*, 324(5925):392–397.
122. Liu L et al. (1998). Induction of Th2 cell differentiation in the primary immune response: dendritic cells isolated from adherent cell culture treated with IL-10 prime naïve $CD4^+$ T cells to secrete IL-4. *International Immunology*, 10(8):1017–1026.
123. Liu P-S et al. (2017). α-ketoglutarate orchestrates macrophage activation through metabolic and epigenetic reprogramming. *Nature Immunology*, 18(9):985–994.
124. Liu TF et al. (2015). Sequential Actions of SIRT1-RELB-SIRT3 Coordinate Nuclear-Mitochondrial Communication during Immunometabolic Adaptation to Acute Inflammation and Sepsis. *Journal of Biological Chemistry*, 290(1):396–408.
125. Liu Y-J (2005). IPC: Professional Type 1 Interferon-Producing Cells and Plasmacytoid Dendritic Cell Precursors. *Annual Review of Immunology*, 23(1):275–306.
126. Liu YC et al. (2012). TLR2 Signaling Depletes IRAK1 and Inhibits Induction of Type I IFN by TLR7/9. *The Journal of Immunology*, 188(3):1019–1026.
127. Lu Y et al. (2014). Tumor-specific IL-9-producing $CD8^+$ Tc9 cells are superior effector than type-I cytotoxic Tc1 cells for adoptive immunotherapy of cancers. *Proceedings of the National Academy of Sciences of the United States of America*, 111(6):2265–70.
128. Ma DY, Clark EA (2009). The role of CD40 and CD154/CD40L in dendritic cells. *Seminars in Immunology*, 21(5):265–272.
129. Macallan DC et al. (2004). Rapid Turnover of Effector–Memory $CD4^+$ T Cells in Healthy Humans. *Journal of Experimental Medicine*, 200(2):255–260.
130. Mackay LK et al. (2015). Cutting Edge: CD69 Interference with Sphingosine-1-Phosphate Receptor Function Regulates Peripheral T Cell Retention. *The Journal of Immunology*, 194(5):2059–2063.
131. MacNamara KC et al. (2011). Infection-Induced Myelopoiesis during Intracellular Bacterial Infection Is Critically Dependent upon IFN-γ Signaling. *The Journal of Immunology*, 186(2):1032–1043.

132. Malinarich F et al. (2015). High Mitochondrial Respiration and Glycolytic Capacity Represent a Metabolic Phenotype of Human Tolerogenic Dendritic Cells. *The Journal of Immunology*, 194(11):5174–5186.
133. Manetti R et al. (1993). Natural killer cell stimulatory factor (interleukin 12 [IL-12]) induces T helper type 1 (Th1)-specific immune responses and inhibits the development of IL-4-producing Th cells. *Journal of Experimental Medicine*, 177(4):1199–1204.
134. Manz MG et al. (2006). Dendritic Cell Development from Common Myeloid Progenitors. *Annals of the New York Academy of Sciences*, 938(1):167–174.
135. Maraskovsky E et al. (1997). Dramatic Numerical Increase of Functionally Mature Dendritic Cells in FLT3 Ligand-Treated Mice. In: *Advances in Experimental Medicine and Biology*.Vol417.,1997:33–40.
136. Marchant A et al. (1994). Interleukin-10 production during septicaemia. *The Lancet*, 343(8899):707–708.
137. Marie C, Cavaillon J-M, Losser M-R (1996). Elevated Levels of Circulating Transforming Growth Factor-β1 in Patients with the Sepsis Syndrome. *Annals of Internal Medicine*, 125(6):520.
138. Márquez S et al. (2017). Endoplasmic Reticulum Stress Sensor IRE1α Enhances IL-23 Expression by Human Dendritic Cells. *Frontiers in Immunology*, 8(JUN):1–19.
139. Martignoni A et al. (2008). CD4-expressing cells are early mediators of the innate immune system during sepsis. *Shock (Augusta, Ga.)*, 29(5):591–7.
140. Martins EC et al. (2019). Neutrophil-lymphocyte ratio in the early diagnosis of sepsis in an intensive care unit: a case-control study. *Revista Brasileira de Terapia Intensiva*, 31(1):63–70.
141. Matsukawa A et al. (1999). Endogenous monocyte chemoattractant protein-1 (MCP-1) protects mice in a model of acute septic peritonitis: cross-talk between MCP-1 and leukotriene B4. *Journal of immunology*, 163(11):6148–54.
142. Matsukawa A et al. (2000). Endogenous MCP-1 Influences Systemic Cytokine Balance in a Murine Model of Acute Septic Peritonitis. *Experimental and Molecular Pathology*, 68(2):77–84.
143. Matsukawa A et al. (2000). Pivotal Role of the CC Chemokine, Macrophage-Derived Chemokine, in the Innate Immune Response. *The Journal of Immunology*, 164(10):5362–5368.
144. Mazo IB et al. (2005). Bone Marrow Is a Major Reservoir and Site of Recruitment for Central Memory $CD8^+$ T Cells. *Immunity*, 22(2):259–270.

145. McClanahan T et al. (1996). Biochemical and genetic characterization of multiple splice variants of the Flt3 ligand. *Blood*, 88(9):3371–3382.
146. McKenna HJ et al. (2000). Mice lacking flt3 ligand have deficient hematopoiesis affecting hematopoietic progenitor cells, dendritic cells, and natural killer cells. *Blood*, 95(11):3489–3497.
147. Medzhitov R (2007). Recognition of microorganisms and activation of the immune response. *Nature*, 449(7164):819–826.
148. Medzhitov R, Preston-Hurlburt P, Janeway CA (1997). A human homologue of the Drosophila Toll protein signals activation of adaptive immunity. *Nature*, 388(6640):394–397.
149. Mempel TR, Henrickson SE, von Andrian UH (2004). T-cell priming by dendritic cells in lymph nodes occurs in three distinct phases. *Nature*, 427(6970):154–159.
150. Mercier BC et al. (2009). TLR2 Engagement on $CD8^+$ T Cells Enables Generation of Functional Memory Cells in Response to a Suboptimal TCR Signal. *The Journal of Immunology*, 182(4):1860–1867.
151. Michie CA et al. (1992). Lifespan of human lymphocyte subsets defined by CD45 isoforms. *Nature*, 360(6401):264–265.
152. Miles RH et al. (1994). Interferon-gamma increases mortality following cecal ligation and puncture. *The Journal of Trauma: Injury, Infection, and Critical Care*, 36(5):607–611.
153. Mittrücker H-W, Visekruna A, Huber M (2014). Heterogeneity in the Differentiation and Function of $CD8^+$ T Cells. *Archivum Immunologiae et Therapiae Experimentalis*, 62(6):449–458.
154. Monserrat J et al. (2009). Clinical relevance of the severe abnormalities of the T cell compartment in septic shock patients. *Critical Care*, 13(1):R26.
155. Munford RS, Pugin J (2001). Normal Responses to Injury Prevent Systemic Inflammation and Can Be Immunosuppressive. *American Journal of Respiratory and Critical Care Medicine*, 163(2):316–321.
156. Murphey ED et al. (2004). Diminished bacterial clearance is associated with decreased IL-12 and interferon-gamma production but a sustained proinflammatory response in a murine model of postseptic immunosuppression. *Shock (Augusta, Ga.)*, 21(5):415–25.
157. Murphy K, Weaver C (2018). *Janeway Immunologie. [Janeway Immunology]* Berlin, Heidelberg, Springer Berlin Heidelberg.
158. Naik SH et al. (2007). Development of plasmacytoid and conventional dendritic cell subtypes from single precursor cells derived *in vitro* and *in vivo*. *Nature Immunology*, 8(11):1217–1226.
159. Netea M (2003). Proinflammatory cytokines and sepsis syndrome: not enough, or too much

of a good thing? *Trends in Immunology*, 24(5):254–258.

160. Nussenzweig MC et al. (1980). Dendritic cells are accessory cells for the development of anti-trinitrophenyl cytotoxic T lymphocytes. *Journal of Experimental Medicine*, 152(4):1070–1084.
161. Ogura Y et al. (2001). Nod2, a Nod1/Apaf-1 Family Member That Is Restricted to Monocytes and Activates NF-κB. *Journal of Biological Chemistry*, 276(7):4812–4818.
162. Oh M-H et al. (2020). Targeting glutamine metabolism enhances tumor-specific immunity by modulating suppressive myeloid cells. *Journal of Clinical Investigation*, 130(7):3865–3884.
163. Okhrimenko A et al. (2014). Human memory T cells from the bone marrow are resting and maintain long-lasting systemic memory. *Proceedings of the National Academy of Sciences*, 111(25):9229–9234.
164. Oliveira GP et al. (2009). Intravenous glutamine decreases lung and distal organ injury in an experimental model of abdominal sepsis. *Critical Care*, 13(3):R74.
165. Onai N et al. (2007). Identification of clonogenic common $Flt3^{+}M\text{-}CSFR^{+}$ plasmacytoid and conventional dendritic cell progenitors in mouse bone marrow. *Nature Immunology*, 8(11):1207–1216.
166. Ozinsky A et al. (2000). The repertoire for pattern recognition of pathogens by the innate immune system is defined by cooperation between Toll-like receptors. *Proceedings of the National Academy of Sciences*, 97(25):13766–13771.
167. Pasquevich KA et al. (2015). Innate immune system favors emergency monopoiesis at the expense of DC-differentiation to control systemic bacterial infection in mice. *European Journal of Immunology*, 45(10):2821–2833.
168. Pastille E et al. (2011). Modulation of dendritic cell differentiation in the bone marrow mediates sustained immunosuppression after polymicrobial sepsis. *Journal of immunology*, 186(2):977–86.
169. Pastille E et al. (2015). A disturbed interaction with accessory cells upon opportunistic infection with Pseudomonas aeruginosa contributes to an impaired IFN-γ production of NK cells in the lung during sepsis-induced immunosuppression. *Innate Immunity*, 21(2):115–126.
170. Payen D et al. (2019). Multicentric experience with interferon gamma therapy in sepsis induced immunosuppression. A case series. *BMC Infectious Diseases*, 19(1):931.
171. Pearce EJ, Everts B (2015). Dendritic cell metabolism. *Nature Reviews Immunology*, 15(1):18–29.
172. Pène F et al. (2009). Toll-Like Receptors 2 and 4 Contribute to Sepsis-Induced Depletion of Spleen Dendritic Cells. *Infection and Immunity*, 77(12):5651–5658.

173. Pène F et al. (2012). Toll-Like Receptor 2 Deficiency Increases Resistance to Pseudomonas aeruginosa Pneumonia in the Setting of Sepsis-Induced Immune Dysfunction. *The Journal of Infectious Diseases*, 206(6):932–942.
174. Peng S et al. (2017). PPAR- γ Activation Prevents Septic Cardiac Dysfunction via Inhibition of Apoptosis and Necroptosis. *Oxidative Medicine and Cellular Longevity*, 2017:1–11.
175. Perrin-Cocon L et al. (2018). Toll-like Receptor 4–Induced Glycolytic Burst in Human Monocyte-Derived Dendritic Cells Results from p38-Dependent Stabilization of HIF-1α and Increased Hexokinase II Expression. *The Journal of Immunology*, 201(5):1510–1521.
176. Pihlgren M et al. (1999). Memory $CD44^{int}$ $CD8^{+}$ T cells show increased proliferative responses and IFN-γ production following antigenic challenge *in vitro*. *International Immunology*, 11(5):699–706.
177. Poehlmann H et al. (2009). Phenotype changes and impaired function of dendritic cell subsets in patients with sepsis: a prospective observational analysis. *Critical Care*, 13(4):R119.
178. Pohlmann S (2014). Mechanismen der Akkumulation von $CD4^{+}$ dendritischen Zellen im Knochenmark und deren Auswirkung auf die Differenzierung dendritischer Zellen während der polymikrobiellen Sepsis. [Mechanisms of $CD4^{+}$ dendritic cell accumulation in bone marrow and their impact on dendritic cell differentiation during polymicrobial sepsis.] *Essen University Hospital, Dissertation*:1–119.
179. van der Poll T et al. (1994). Elimination of interleukin 6 attenuates coagulation activation in experimental endotoxemia in chimpanzees. *Journal of Experimental Medicine*, 179(4):1253–1259.
180. Prescott HC et al. (2014). Increased 1-Year Healthcare Use in Survivors of Severe Sepsis. *American Journal of Respiratory and Critical Care Medicine*, 190(1):62–69.
181. Prescott HC et al. (2016). Late mortality after sepsis: propensity matched cohort study. *BMJ*, 353:i2375.
182. Prins JM et al. (1995). Release of tumor necrosis factor alpha and interleukin 6 during antibiotic killing of Escherichia coli in whole blood: influence of antibiotic class, antibiotic concentration, and presence of septic serum. *Infection and immunity*, 63(6):2236–2242.
183. Qin Y, Zhang C (2017). The Regulatory Role of IFN-γ on the Proliferation and Differentiation of Hematopoietic Stem and Progenitor Cells. *Stem Cell Reviews and Reports*, 13(6):705–712.
184. Rahman AH, Taylor DK, Turka LA (2009). The contribution of direct TLR signaling to T cell responses. *Immunologic Research*, 45(1):25–36.

185. Randolph GJ et al. (1999). Differentiation of Phagocytic Monocytes into Lymph Node Dendritic Cells *In Vivo*. *Immunity*, 11(6):753–761.
186. Riedemann NC et al. (2003). Regulation by C5a of neutrophil activation during sepsis. *Immunity*, 19(2):193–202.
187. Riedemann NC et al. (2003). Protective Effects of IL-6 Blockade in Sepsis Are Linked to Reduced C5a Receptor Expression. *The Journal of Immunology*, 170(1):503–507.
188. Rittirsch D, Flierl MA, Ward PA (2008). Harmful molecular mechanisms in sepsis. *Nature Reviews Immunology*, 8(10):776–787.
189. Rolot M et al. (2018). Helminth-induced IL-4 expands bystander memory $CD8^+$ T cells for early control of viral infection. *Nature Communications*, 9(1):4516.
190. Di Rosa F, Gebhardt T (2016). Bone Marrow T Cells and the Integrated Functions of Recirculating and Tissue-Resident Memory T Cells. *Frontiers in Immunology*, 7(FEB):1–13.
191. Rudd KE et al. (2020). Global, regional, and national sepsis incidence and mortality, 1990–2017: analysis for the Global Burden of Disease Study. *The Lancet*, 395(10219):200–211.
192. Santos I et al. (2020). CXCL5-mediated recruitment of neutrophils into the peritoneal cavity of Gdf15-deficient mice protects against abdominal sepsis. *Proceedings of the National Academy of Sciences*, 117(22):12281–12287.
193. Saunders MJ, Kane MD, Todd MK (2004). Effects of a carbohydrate-protein beverage on cycling endurance and muscle damage. *Medicine and science in sports and exercise*, 36(7):1233–8.
194. Schenkel JM et al. (2013). Sensing and alarm function of resident memory $CD8^+$ T cells. *Nature Immunology*, 14(5):509–513.
195. Schindler R et al. (1990). Correlations and interactions in the production of interleukin-6 (IL-6), IL-1, and tumor necrosis factor (TNF) in human blood mononuclear cells: IL-6 suppresses IL-1 and TNF. *Blood*, 75(1):40–47.
196. Schlitzer A et al. (2015). Identification of cDC1- and cDC2-committed DC progenitors reveals early lineage priming at the common DC progenitor stage in the bone marrow. *Nature Immunology*, 16(7):718–728.
197. Schlitzer A, Ginhoux F (2014). Organization of the mouse and human DC network. *Current Opinion in Immunology*, 26(1):90–99.
198. Schraml BU et al. (2013). Genetic Tracing via DNGR-1 Expression History Defines Dendritic Cells as a Hematopoietic Lineage. *Cell*, 154(4):843–858.
199. Schwalbe RA et al. (1992). Pentraxin family of proteins interact specifically with phosphorylcholine and/or phosphorylethanolamine. *Biochemistry*, 31(20):4907–4915.

200. Scott NM et al. (2014). Prostaglandin E 2 imprints a long-lasting effect on dendritic cell progenitors in the bone marrow. *Journal of Leukocyte Biology*, 95(2):225–232.
201. See P et al. (2017). Mapping the human DC lineage through the integration of high-dimensional techniques. *Science*, 356(6342):eaag3009.
202. Serbina N V. et al. (2003). TNF/iNOS-Producing Dendritic Cells Mediate Innate Immune Defense against Bacterial Infection. *Immunity*, 19(1):59–70.
203. Sercan Alp Ö et al. (2015). Memory $CD8^+$ T cells colocalize with IL-7^+ stromal cells in bone marrow and rest in terms of proliferation and transcription. *European Journal of Immunology*, 45(4):975–987.
204. Shankaran V et al. (2001). IFNgamma and lympohcytes prevent primary tomour development and shape tomour immunogenicity. *Nature*, 410(6832):1107–1111.
205. Shiow LR et al. (2006). CD69 acts downstream of interferon-α/β to inhibit S1P 1 and lymphocyte egress from lymphoid organs. *Nature*, 440(7083):540–544.
206. Shreedhar V et al. (1999). Dendritic Cells Require T Cells for Functional Maturation In Vivo. *Immunity*, 11(5):625–636.
207. Shrikant PA et al. (2010). Regulating functional cell fates in $CD8^+$ T cells. *Immunologic Research*, 46(1–3):12–22.
208. Singer M et al. (2016). The Third International Consensus Definitions for Sepsis and Septic Shock (Sepsis-3). *JAMA*, 315(8):801.
209. de Smedt T et al. (1997). Effect of interleukin-10 on dendritic cell maturation and function. *European Journal of Immunology*, 27(5):1229–1235.
210. Smirnov A et al. (2017). Sphingosine 1-phosphate- and C-C chemokine receptor 2-dependent activation of CD4+ plasmacytoid dendritic cells in the Bone marrow contributes to signs of sepsis-induced immunosuppression. *Frontiers in Immunology*, 8(Nov):1–15.
211. Smirnov A (2017). Aktivierung von plasmazytoiden dendritischen Zellen im Knochenmark während der polymikrobiellen Sepsis. [Activation of plasmacytoid dendritic cells in bone marrow during polymicrobial sepsis.] *Essen University Hospital, Dissertation*:1–100.
212. Steensberg A et al. (2003). IL-6 enhances plasma IL-1ra, IL-10, and cortisol in humans. *American Journal of Physiology-Endocrinology and Metabolism*, 285(2):E433–E437.
213. Steinman RM, Cohn ZA (1973). Identification of a novel cell type in peripheral lymphoid organs of mice. *The Journal of Experimental Medicine*, 137(5):1142–1162.
214. Steinman RM, Witmer MD (1978). Lymphoid dendritic cells are potent stimulators of the primary mixed leukocyte reaction in mice. *Proceedings of the National Academy of Sciences*, 75(10):5132–5136.

215. Stonoga ETS et al. (2019). Effects of intraperitoneal glutamine in the treatment of experimental sepsis. *ABCD. Arquivos Brasileiros de Cirurgia Digestiva (São Paulo)*, 32(2):2–5.

216. Strobl H et al. (1997). flt3 Ligand in Cooperation With Transforming Growth Factor-β1 Potentiates *In Vitro* Development of Langerhans-Type Dendritic Cells and Allows Single-Cell Dendritic Cell Cluster Formation Under Serum-Free Conditions. *Blood*, 90(4):1425–1434.

217. Sundquist M, Wick MJ (2009). Salmonella induces death of $CD8^+$ dendritic cells but not $CD11c^{int}CD11b^+$ inflammatory cells *in vivo* via MyD88 and TNFR1. *Journal of Leukocyte Biology*, 85(2):225–234.

218. Surh CD, Sprent J (2008). Homeostasis of Naive and Memory T Cells. *Immunity*, 29(6):848–862.

219. Takeuchi O et al. (2001). Discrimination of bacterial lipoproteins by Toll-like receptor 6. *International Immunology*, 13(7):933–940.

220. Talay O et al. (2009). B7-H1 (PD-L1) on T cells is required for T-cell-mediated conditioning of dendritic cell maturation. *Proceedings of the National Academy of Sciences*, 106(8):2741–2746.

221. Tang Y et al. (2012). Antigen-specific effector $CD8^+$ T cells regulate allergic responses via IFN-γ and dendritic cell function. *Journal of Allergy and Clinical Immunology*, 129(6):1611-1620.e4.

222. Tao K-M et al. (2014). Glutamine supplementation for critically ill adults. *Cochrane Database of Systematic Reviews*, 2014(9).

223. Taylor MD et al. (2020). $CD4^+$ and $CD8^+$ T Cell Memory Interactions Alter Innate Immunity and Organ Injury in the CLP Sepsis Model. *Frontiers in Immunology*, 11(November):1–12.

224. Testi R, Phillips JH, Lanier LL (1989). Leu 23 induction as an early marker of functional CD3/T cell antigen receptor triggering. Requirement for receptor cross-linking, prolonged elevation of intracellular [Ca++] and stimulation of protein kinase C. *Journal of immunology*, 142(6):1854–60.

225. Thimme R et al. (2003). $CD8^+$ T cells mediate viral clearance and disease pathogenesis during acute hepatitis B virus infection. *Journal of virology*, 77(1):68–76.

226. Tinsley KW et al. (2003). Sepsis Induces Apoptosis and Profound Depletion of Splenic Interdigitating and Follicular Dendritic Cells. *The Journal of Immunology*, 171(2):909–914.

227. De Trez C et al. (2005). TLR4 and Toll-IL-1 Receptor Domain-Containing Adapter-Inducing IFN-β, but Not MyD88, Regulate *Escherichia coli*-Induced Dendritic Cell Maturation and Apoptosis *In Vivo*. *The Journal of Immunology*, 175(2):839–846.

228. Tsuda Y et al. (2004). CCL2, a product of mice early after systemic inflammatory response syndrome (SIRS), induces alternatively activated macrophages capable of impairing antibacterial resistance of SIRS mice. *Journal of Leukocyte Biology*, 76(2):368–373.
229. Ueki IF et al. (2013). Respiratory virus–induced EGFR activation suppresses IRF1-dependent interferon λ and antiviral defense in airway epithelium. *Journal of Experimental Medicine*, 210(10):1929–1936.
230. Vénéreau E, Ceriotti C, Bianchi ME (2015). DAMPs from Cell Death to New Life. *Frontiers in Immunology*, 6(AUG):1–11.
231. Venet F et al. (2009). Increased circulating regulatory T cells ($CD4^+CD25^+CD127^-$) contribute to lymphocyte anergy in septic shock patients. *Intensive Care Medicine*, 35(4):678–686.
232. Vincent J-L et al. (2019). Frequency and mortality of septic shock in Europe and North America: a systematic review and meta-analysis. *Critical Care*, 23(1):196.
233. Vincent JL et al. (1996). The SOFA (Sepsis-related Organ Failure Assessment) score to describe organ dysfunction/failure. *Intensive Care Medicine*, 22(7):707–710.
234. Vincent WR, Rapaport E (1965). Serum creatine phosphokinase in the diagnosis of acute myocardial infarction. *The American Journal of Cardiology*, 15(1):17–26.
235. Volk HD, Reinke P, Döcke WD (2000). Clinical aspects: from systemic inflammation to 'immunoparalysis'. *Chemical immunology*, 74:162–77.
236. Vrisekoop N et al. (2008). Sparse production but preferential incorporation of recently produced naïve T cells in the human peripheral pool. *Proceedings of the National Academy of Sciences*, 105(16):6115–6120.
237. Waisman A et al. (2017). Dendritic cells as gatekeepers of tolerance. *Seminars in Immunopathology*, 39(2):153–163.
238. Wakkach A et al. (2003). Characterization of dendritic cells that induce tolerance and T regulatory 1 cell differentiation *in vivo*. *Immunity*, 18(5):605–17.
239. Wang F et al. (2018). Glycolytic Stimulation Is Not a Requirement for M2 Macrophage Differentiation. *Cell Metabolism*, 28(3):463-475.e4.
240. Wang J, Zhou J, Bai S (2020). Combination of Glutamine and Ulinastatin Treatments Greatly Improves Sepsis Outcomes. *Journal of Inflammation Research*, Volume 13:109–115.
241. Wang ZE et al. (1994). $CD4^+$ effector cells default to the Th2 pathway in interferon gamma-deficient mice infected with Leishmania major. *The Journal of experimental medicine*, 179(4):1367–71.
242. Warburg O, Wind F, Negelein E (1927). The metabolism of tumors in the body. *Journal of General Physiology*, 8(6):519–530.

243. Ward PA (2004). The dark side of C5a in sepsis. *Nature Reviews Immunology*, 4(2):133–142.
244. Wculek SK et al. (2019). Metabolic Control of Dendritic Cell Functions: Digesting Information. *Frontiers in Immunology*, 10(April):775.
245. Weil MH, Shubin H, Biddle M (1964). Shock Caused by Gram-negative Microorganisms. *Annals of Internal Medicine*, 60(3):384.
246. Wen H et al. (2006). Severe Sepsis Exacerbates Cell-Mediated Immunity in the Lung Due to an Altered Dendritic Cell Cytokine Profile. *The American Journal of Pathology*, 168(6):1940–1950.
247. Westera L et al. (2013). Closing the gap between T-cell life span estimates from stable isotope-labeling studies in mice and humans. *Blood*, 122(13):2205–2212.
248. White JT et al. (2016). Virtual memory T cells develop and mediate bystander protective immunity in an IL-15-dependent manner. *Nature Communications*, 7(1):11291.
249. Wichterman KA, Baue AE, Chaudry IH (1980). Sepsis and septic shock—A review of laboratory models and a proposal. *Journal of Surgical Research*, 29(2):189–201.
250. Winter DR, Amit I (2015). DCs are ready to commit. *Nature Immunology*, 16(7):683–685.
251. Wolk K et al. (1999). Comparison of Monocyte Functions after LPS- or IL-10-Induced Reorientation: Importance in Clinical Immunoparalysis. *Pathobiology*, 67(5–6):253–256.
252. Wu L et al. (1997). Cell-Autonomous Defects in Dendritic Cell Populations of Ikaros Mutant Mice Point to a Developmental Relationship with the Lymphoid Lineage. *Immunity*, 7(4):483–492.
253. Wu L et al. (1998). RelB Is Essential for the Development of Myeloid-Related CD8α$^-$ Dendritic Cells but Not of Lymphoid-Related CD8α$^+$ Dendritic Cells. *Immunity*, 9(6):839–847.
254. Wu L, Li CL, Shortman K (1996). Thymic dendritic cell precursors: relationship to the T lymphocyte lineage and phenotype of the dendritic cell progeny. *Journal of Experimental Medicine*, 184(3):903–911.
255. Wu X et al. (2006). Novel Function of IFN-γ: Negative Regulation of Dendritic Cell Migration and T Cell Priming. *The Journal of Immunology*, 177(2):934–943.
256. Xander N et al. (2019). Rhinovirus-Induced SIRT-1 via TLR2 Regulates Subsequent Type I and Type III IFN Responses in Airway Epithelial Cells. *The Journal of Immunology*, 203(9):2508–2519.
257. Yokoyama WM et al. (1988). Characterization of a cell surface-expressed disulfide-linked dimer involved in murine T cell activation. *Journal of immunology*, 141(2):369–76.
258. Zarember KA, Godowski PJ (2002). Tissue Expression of Human Toll-Like Receptors and

Differential Regulation of Toll-Like Receptor mRNAs in Leukocytes in Response to Microbes, Their Products, and Cytokines. *The Journal of Immunology*, 168(2):554–561.

259. Zeerleder S et al. (2006). TAFI and PAI-1 levels in human sepsis. *Thrombosis Research*, 118(2):205–212.
260. Zha Z et al. (2017). Interferon-γ is a master checkpoint regulator of cytokine-induced differentiation. *Proceedings of the National Academy of Sciences*, 114(33):E6867–E6874.
261. Zhang E et al. (2019). TLR2 Stimulation Increases Cellular Metabolism in CD8 + T Cells and Thereby Enhances CD8 + T Cell Activation, Function, and Antiviral Activity. *The Journal of Immunology*, 203(11):2872–2886.
262. Ziegler SF, Ramsdell F, Alderson MR (1994). The activation antigen CD69. *Stem Cells*, 12(5):456–465.

6. Annex

6.1 Supplemental data

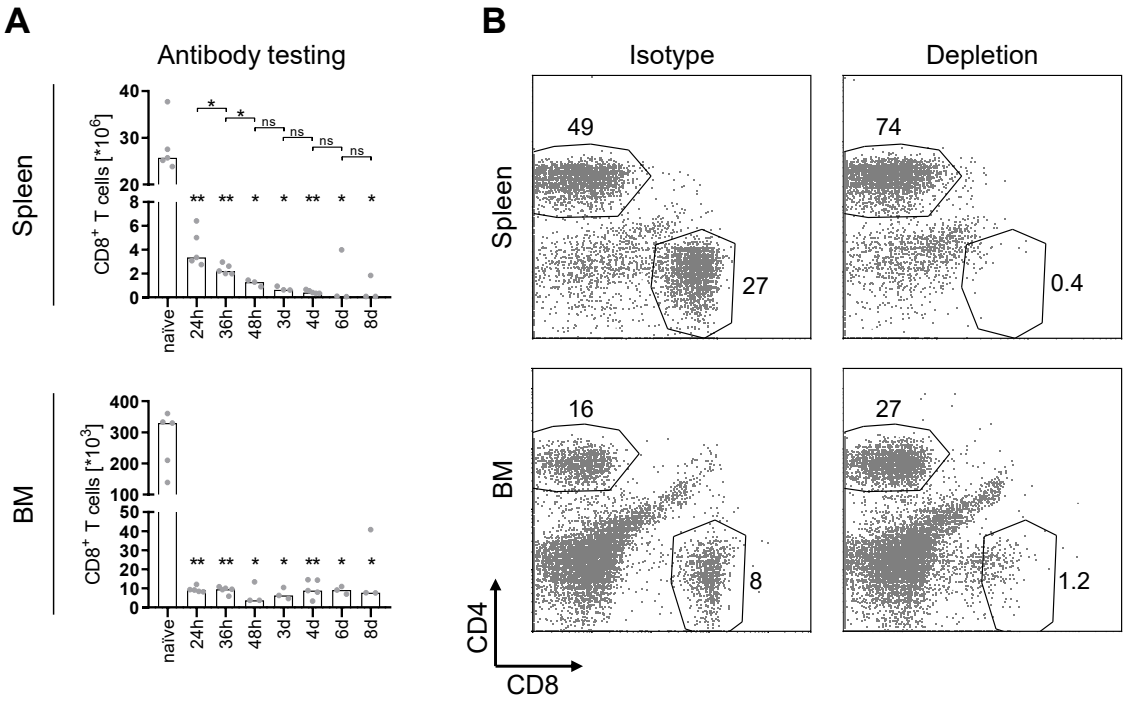

Figure 23 Duration and efficiency of CD8⁺ T cell depletion in bone marrow and spleen with and without CLP. Several time points were measured during antibody testing regarding efficiency and duration of CD8⁺ T cell depletion in bone marrow (BM) and spleen (A). The data is depicted as the median and individual values from n = 3-5 mice per group. Non-parametric *Mann-Whitney U*-test was performed for statistical analysis comparing the value to the naïve value or as indicated. Further, anti-mouse CD8β antibody or HRPN as isotype control was injected in wild-type mice three days prior CLP operation (B). The dot plots show the composition of CD4⁺ and CD8⁺ T cells in bone marrow and spleen four days after CLP. Numbers describe the percentage share after gating for CD3⁺ cells. Significant results are indicated as $p \leq 0.05$ (*) and $p \leq 0.01$ (**).

6.2 List of abbreviations

%	Percent
°C	Degree Celsius
µg	Microgram
µl	Microliter
µm	Micrometer
µM	Micromolar
2-DG	2-Deoxy-D-glucose
2-NBDG	2-NBD glucose
acetyl-CoA	Acetyl coenzyme A
AF	Alexa Fluor
APC	Allophycocyanin
APC	Antigen-presenting cell
ATP	Adenosine triphosphate
B cell	B lymphocyte
BMC	Bone marrow cells
BMDC	Bone marrow-derived dendritic cell
BMDM	Bone marrow-derived macrophages
BUN	Blood urea nitrogen
BV	Brilliant Violet
CARS	Compensatory anti-inflammatory response syndrome
CCL	CC-motif ligand
CCR	CC-motif receptor
CD	Cluster of Differentiation
cDC	Conventional dendritic cell
CDP	Common dendritic cell progenitor
CLP	Cecal ligation and puncture
CM	Culture medium
cm	Centimeter
CO_2	Carbon dioxide
CpG	CpG oligodeoxynucleotides
CPK	Creatine phosphokinase
d	Days
DAMP	Damage-associated molecular pattern
DC	Dendritic cell
DIC	Disseminated intravascular coagulopathy
dN	Double negative
DON	6-Diazo-5-oxo-L-norleucine
dP	Double positive
ECAR	Extracellular acidification rate
EDTA	Ethylenediaminetetraacetic acid
ELISA	Enzyme-linked Immunosorbent Assay

FACS	Fluorescence-activated cell sorting
FAO	Fatty acid oxidation
FCCP	Carbonyl cyanide-4 (trifluoromethoxy) phenylhydrazone
FCS	Fetal calf serum
FITC	Fluorescein isothyocyanate
FL	Flt3 ligand
FSC	Forward scattering
FvD	Fixable viability dye
g	Gravitational field strength
GLS2	Glutaminase 2
Glut1	Glucose transporter 1
GM-CSF	Granulocyte-macrophage colony-stimulating factor
GRA	Granulocytes
h	Hours
H_2O_2	Hydrogen peroxide
H_2SO_4	Sulfuric acid
HIV	Human immunodeficiency viruse
HK2	Hexokinase 2
i.m.	Intramuscular
i.p.	Intraperitoneal
i.v.	Intravenous
IFN	Interferon
IgG	Immunoglobulin G
IL	Interleukin
IRAK-1	Interleukin receptor associated kinase – 1
IRF8	Interferon regulatory factor 8
kg	Kilogram
ko	Knockout
LPS	Lipopolysaccharides
LYM	lymphocytes
MACS	Magnetic-activated cell sorting
mdDCs	Monocyte-derived bone marrow-derived dendritic cell
MDP	Monocyte-dendritic cell progenitor
mg	Milligram
MHC	Major Histocompatibility Complex
ml	Milliliter
MMR	Macrophage mannose receptor
MO	Monocytes
mRNA	Messenger ribonucleic acid
NaCl	Sodium chloride
NAD	Nicotinamide adenine dinucleotide
NFkB	Nuclear factor kappa-light-chain-enhancer of activated B cells
ng	Nanogram

NK cell	Natural killer cell
NOD	Nucleotide-binding oligomerization domain
OCR	Oxygen consumption rate
OD	Optical density
ova	Ovalbumin
OXPHOS	Oxidative phosphorylation
P_3CSK_4	$Pam_3CysSerLys_4$; triacylated lipopeptide ; TLR2 ligand
PAI-1	Plasminogen activator inhibitor type-1
PAMP	Pathogen-associated molecular pattern
PB	Pacific blue
PBS	Phosphate-buffered Saline
PCR	Polymerase chain reaction
pDC	Plasmacytoid dendritic cells
PE	Phycoerythrin
PerCP-Cy5.5	Peridinin chlorophyll protein-Cyanine5.5
PMA	Phorbol-12-myristat-13-acetat
preDC	Dendritic progenitor cell
PRR	Pattern recognition receptor
s.c.	Subcutaneous
S1P	Sphingosine 1-phosphate
S1PR1	Sphingosine 1-phosphate receptor-1
sDC	Splenic dendritic cell
SIRS	Systemic inflammatory response syndrome
SOFA	Sequential Organ Failure Assessment
SSC	Side scattering
T cell	T lymphocyte
TCA	Tricarboxylic acid
T_{CM}	Central memory T cells
TCR	T cell receptor
$T_{E/EM}$	Effector/effector memory T cells
TGFβ	Transforming growth factor-β
Th	T helper cell
TLR	Toll-like receptor
TMB	Tetramethylbenzidine
T_N	Naïve T cells
TNFα	Tumor Necrosis Factor-α
TSC	Total spleen cells
T_{VM}	Virtual memory T cells
WBC	White blood cells
ZTL	Central Animal Laboratory / *Zentrales Tierlaboratorium*

6.3 List of figures

6.4 List of tables

6.5 Acknowledgment

Zu Beginn möchte ich mich bei Stefanie Flohé für die Möglichkeit der Verfassung meiner Doktorarbeit in ihrer Arbeitsgruppe bedanken. Ein großes Dankeschön für die sehr gute Betreuung und Unterstützung während der experimentellen sowie schreibenden Tätigkeiten. Ein weiterer Dank gilt meiner Zweitbetreuerin Kathrin Sutter, welche neben neuen Ideen auch mit verschiedenen Materialen aushalf. Dankbar bin ich auch, Teil der RTG1949 gewesen zu sein, wodurch ich mit vielen interessanten Menschen in Kontakt und in den wissenschaftlichen Austausch kommen durfte.

Was wäre diese anstrengende und ereignisreiche Zeit nur ohne diese tollen Menschen in der Arbeitsgruppe gewesen. Ich hatte immer viel Freude bei euch und konnte in jeglicher emotionalen Lage auf euch zählen. Auch ein gelegentliches und stets (un)erwartetes Singen konnte euch nicht abschrecken. Für die Hilfe bei zahlreichen Experimenten danke ich insbesondere Michaela Bak, Marion Frisch, Lisa Wienhöfer und Alina Kuschick. Hierbei möchte ich Michaela die „sDCs“ und Marion die „BMDCs“ widmen. ;-) Für die Hilfe im Labor und jegliche Unterstützung danke ich auch Monika Hepner, Andrea Sowislok, Heike Rekasi, Lea Boller und Nadine Gausmann. Für die Einarbeitung und einen guten Start in meine Doktorarbeitszeit möchte ich außerdem Anna Smirnov und Melanie Nehring danken.

Andrea Engler möchte ich für die Durchführung und Analyse der Seahorse Experimente danken. Außerdem ein Dank an Thekla Kemper für die Durchführung sowie Mengji Lu für die Möglichkeit der PCR Analysen. Qian Li auch ein Dank für die methodische Unterweisung in die 2-NBDG Färbung. Ein weiterer Dank gilt Mechthild Hemmler-Roloff für die Durchführung sowie Astrid Westendorf für die Möglichkeit der Luminex Analysen. Außerdem möchte ich mich bei Jadwiga Jablonska, Ekatarina Pylaeva, Elena Siakaeva und Ilona Spyra für die Kooperation und Zusammenarbeit bei verschiedenen Experimenten bedanken.

Ein besonderes Dankeschön an Andreas Schnietz, Carlotta Büth, Denis Hessel, Eva Brosch, Laura Berkemeyer und Lea Boller, die Teile meiner schriftlichen Arbeit auf Herz und Nieren geprüft habe. Dank auch an alle Freunde, die mich darüber hinaus während dieser Zeit unterstützt haben. Ein herzliches und besonderes Dankeschön an Carlotta, die mich nahezu unermüdlich unterstützt und motiviert hat. :) Zu guter Letzt gilt mein Dank meiner Familie, insbesondere meinen Eltern, welche mich bis hierhin begleitet haben.

Ohne euch wäre das alles nicht möglich gewesen!

6.6 Curriculum Vitae

Der Lebenslauf ist in der Online-Version aus Gründen des Datenschutzes nicht enthalten.

Der Lebenslauf ist in der Online-Version aus Gründen des Datenschutzes nicht enthalten.

6.7 Statutory declarations

In accordance with § 6 (para. 2, clause g) of the Regulations Governing the Doctoral Proceedings of the Faculty of Biology for awarding the doctoral degree Dr. rer. nat., I hereby declare that I represent the field to which the topic "$CD8^+$ T cells in the bone marrow and their impact on the differentiation of dendritic cells during polymicrobial sepsis" is assigned in research and teaching and that I support the application of Anne-Charlotte Antoni.

Essen, date _____ _____ _____

Name of the scientific supervisor/member of the University of Duisburg-Essen

Signature of the supervisor/member of the University of Duisburg-Essen

In accordance with § 7 (para. 2, clause d and f) of the Regulations Governing the Doctoral Proceedings of the Faculty of Biology for awarding the doctoral degree Dr. rer. nat., I hereby declare that I have written the herewith submitted dissertation independently using only the materials listed and have cited all sources taken over verbatim or in content as such.

Münster, date _____ _____

Signature of the doctoral candidate

In accordance with § 7 (para. 2, clause e and g) of the Regulations Governing the Doctoral Proceedings of the Faculty of Biology for awarding the doctoral degree Dr. rer. nat., I hereby declare that I have undertaken no previous attempts to attain a doctoral degree, that the current work has not been rejected by any other faculty, and that I am submitting the dissertation only in this procedure.

Münster, date _____ _____

Signature of the doctoral candidate